NASA
TT
F-432
c.1

A.G. TEMKIN, AND OTHERS

NON-STATIONARY HEAT AND MASS TRANSFER

TECH LIBRARY KAFB, NM
0068787

Edited by I.G. Gurevich, I.P. Zhuk, and N.G. Kondrashov

TRANSLATED FROM RUSSIAN

Published for the National Aeronautics and Space Administration, U.S.A.
and the National Science Foundation, Washington, D.C.
by the Israel Program for Scientific Translations

TECH LIBRARY KAFB, NM
0068787

AKADEMIYA NAUK BELORUSSKOI SSR
INSTITUT TEPLO- I MASSOOBMENA

Academy of Sciences of the Belorussian SSR
Institute of Heat and Mass Transfer

A. G. Temkin, and others

Non-stationary Heat and Mass Transfer

(Voprosy nestatsionarnogo perenosa tepla i massy)

Edited by I. G. Gurevich, I. P. Zhuk, and N. G. Kondrashov

Nauka i Tekhnika
Minsk 1965

Translated from Russian

Israel Program for Scientific Translations
Jerusalem 1967

NASA TT F-432
TT 67-51368

Published Pursuant to an Agreement with
THE NATIONAL AERONAUTICS AND SPACE ADMINISTRATION, U.S.A.
and
THE NATIONAL SCIENCE FOUNDATION, WASHINGTON, D.C.

Copyright © 1967
Israel Program for Scientific Translations Ltd.
IPST Cat. No. 1817

Translated by Abraham Aladjem

Printed in Jerusalem by S. Monson

Price: $4.00

Available from the
U.S. DEPARTMENT OF COMMERCE
Clearinghouse for Federal Scientific and Technical Information
Springfield, Va. 22151

TABLE OF CONTENTS

	Page
List of Abbreviations	v
Temkin, A.G. Thermal Conductivity of Exothermic Bodies	1
Tsoi, P.V. and O.B. Kianovskii. A Contact Problem for a Generalized System of Differential Equations of Heat and Mass Transfer	11
Parnas, A.L. On the Unsteady Convective Heat Exchange with an Oscillating Body	18
Parnas, A.L. Experimental Study of Heat Exchange in the Case of a Cylinder in a Transverse Air Stream	22
Sovkin, V.F. and M.P. Shatunov. Thermal Relations During the Grinding of Metals, and a Practical Method for Their Calculation	27
Temkin, A.G. Reconstruction of the Heat and Mass Content Fields of a Colloidal Body	59
Bobrova, G.I. and G.D. Rabinovich. Determination of the Soret Coefficients and the Concentration Diffusion Coefficients by an Unsteady-State Method	67
Bobrova, G.I. and G.D. Rabinovich. Intensification of the Thermal Diffusion Separation Process in a Clusius-Dickel Column	75
Novikov, P.A. Effect of the Vibration Rate of a Body on Heat and Mass Transfer Under the Conditions of Vacuum Sublimation	81
Novikov, P.A. and B.M. Smol'skii. The Mechanisms of Heat and Mass Transfer During the Vibrations of a Body Undergoing Sublimation in a Rarified Gaseous Medium Under the Conditions of Free Convection	86
Nikitina, L.M. The Mass Transfer Coefficient of Air	92
Nikitina, L.M. The Specific Isothermal Mass Capacity of Humid Air	96
Pikus, I.F. Some Problems of the Fluidized-Bed Drying of Heat-Sensitive Materials in a Cyclic Regime	98
Lyuboshits, A.I. Experimental Determination of the Mass Transfer Coefficient in the Cooling of Moist Grain After Drying in Multisectional Packed Heat Exchangers	106

Page

Lyuboshits, A.I. Determination of the Optimum Thickness of Layers in Multisectional Packed Heat Exchangers 109

Finaev, Yu.A. Dependence of the Combustion Rate of Coke Particles on the Flow Rate Round the Particles, in a Generalized Dimensionless Form 112

Avakov, A.I., K.E. Garyainov, and L.T. Yakovlev. Thermal Stresses in Cellular Concretes During Hydrothermal Processing 115

Vinokurov, E.F. The Iteration Method of Solving the Plane Elastic-Plastic Problem of Soil Mechanics 121

Berkovskii, B. and Z. Shul'man. Exact Solution of the Equations for the Boundary Layer of Pseudoplastic Fluids on a Permeable Flat Plate and in the Vicinity of the Critical Point 126

EXPLANATORY LIST OF ABBREVIATIONS OF USSR INSTITUTIONS AND JOURNALS APPEARING IN THIS TEXT

Abbreviation	Full name (transliterated)	Translation
AN BelSSR	Akademiya Nauk Belorusskoi SSR	Academy of Sciences of the Belorussian SSR
AN SSSR	Akademiya Nauk SSSR	Academy of Sciences of the USSR
AN UkrSSR	Akademiya Nauk Ukrainskoi SSR	Academy of Sciences of the Ukrainian SSR
IFZh	Inzhenerno-Fizicheskii Zhurnal	Engineering-Physics Journal
NKTP	Narodnyi Komissariat Tyazheloi Promyshlennosti	People's Commissariat of Heavy Industry
PMM	Prikladnaya Matematika i Mekhanika	Journal of Applied Mathematics and Mechanics
Trudy MIPP	Trudy Moskovskogo Tekhnologicheskogo Instituta Pishchevoi Promyshlennosti	Proceedings of the Moscow Institute for Food Industry
Trudy NIKFI	Trudy Vsesoyuznogo Nauchno-issledovatel'skogo Kinofotoinstituta	All-Union Research Institute for Cinematography and Photography
ZhFKh	Zhurnal Fizicheskoi Khimii	Journal of Physical Chemistry
ZhTF	Zhurnal Tekhnicheskoi Fiziki	Journal of Technical Physics

This is a collection of papers most of which deal with the problems of non-stationary (unsteady-state) heat and mass transfer, encountered in various branches of science and technology. Several of the papers are strictly analytical and are related to the solution of the unsteady-state heat and mass transfer equations, as applied to definite practical problems. Other papers correlate data obtained in experimental investigations of heat and mass transfer processes under unsteady-state conditions, accompanied by the vibration of solid bodies, flux pulsations, etc.

This book is intended for the use of scientists, university staff, and engineers.

Editorial Board:
I. G. Gurevich, I. Z. Zhuk, and
I. G. Kondrashov

A.G. Temkin

THERMAL CONDUCTIVITY OF EXOTHERMIC BODIES

THE THERMAL CONDUCTIVITY EQUATION. INITIAL AND BOUNDARY CONDITIONS.

The temperature field of a k-dimensional body, whose shape differs only slightly from the classical, is described by the equation

$$\frac{\partial t}{\partial H} = \frac{\partial^2 t}{\partial N^2} + \frac{k-1}{N}\frac{\partial t}{\partial N} + W(N, H), \tag{1}$$

where N is a dimensionless coordinate /1, 2/, and H is the homochronicity complex /2, 3/ equal to the product of the Fourier and Lobachevskii numbers. The dimensionless intensity of heat sources is proportional to the absolute /4, 5/

$$W(N, H) = \frac{R^2}{\lambda \mathrm{Lo} t_0} W(n, \tau), \tag{2}$$

and is a sum of partial intensities

$$W(N, H) = \sum_{\nu} Q_{\nu}(N) U_{\nu}(H) = \sum_{\nu} W_{\nu}(N, H). \tag{3}$$

The initial temperature distribution is nonhomogeneous:

$$t(N, 0) = t_0(N). \tag{4}$$

On the surface of the body convective heat exchange occurs with the surroundings

$$\frac{\partial t(1, H)}{\partial N} = B[t_e(H) - t(1, H)], \tag{5}$$

whose temperature is a function of time. The body contains no cavities and its temperature field is symmetrical

$$\frac{\partial}{\partial N} t(0, H) = 0. \tag{6}$$

The above condition is satisfied by the function $Q_{\nu}(N)$ and $t_0(N)$.

THE TEMPERATURE FIELD COMPONENTS

The temperature field of an exothermic body is shaped under the effect of the internal evolution of heat, convective heat exchange with the

surroundings, and the nonhomogeneous initial temperature distribution:

$$t(N, H) = t_w(N, H) + t_e(N, H) + t_i(N, H). \quad (7)$$

The temperature field component arising because of heat exchange by the Newton rule comprises the external-action and after-effect fields /2/:

$$t_e(N, H) = t_{ea}(N, H) + t_{er}(N, H). \quad (8)$$

The main contribution is made by the external-action field /2/

$$t_{ea}(N, H) = \sum_{n=0}^{\infty} t_e^{(n)}(H) L_{2n}(N, B, k) \quad (9)$$

which is a series whose terms are the derivatives of the temperature of the surroundings $t_e^{(n)}(H)$ and the radial polynomials computed by a recursion formula

$$L_{2n}(N, B, k) = \nabla^{-2} L_{2n-2}(N, B, k) - \underline{\nabla^{-2} L_{2n-2}}(N, B, k) - \frac{1}{kB} \overline{\underline{L_{2n-2}}}(N, B, k). \quad (10)$$

Here, as in /5, 6/ the symbol ∇^{-2} is a double integral

$$\nabla^{-2} F(N) = \int_0^N \eta^{1-k} d\eta \int_0^{\eta} \xi^{k-1} L_{2n-2}(\xi, B, k) d\xi, \quad (11)$$

whose value at the point $N = 1$ is denoted by underlining:

$$\underline{\nabla^{-2} F(N)} = \nabla^{-2} F(1) = \int_0^1 \eta_1^{1-k} d\eta_1 \int_0^{\eta_1} \xi^{k-1} F(\xi) d\xi; \quad (12)$$

the mean value of the preceding polynomial is

$$\overline{\underline{L_{2n-2}}}(N, B, k) = k \int_0^1 \xi^{k-1} L_{2n-2}(\xi, B, k) d\xi. \quad (13)$$

The remainder of the field (8) is the external after-effect field

$$t_{er}(N, H) = \sum_{n=0}^{\infty} t_e^{(n)}(0)(-1)^n \sum_{p=1}^{\infty} \times \frac{2r(\mu_p N, k) \exp(-\mu_p^2 H)}{\left[1 + \frac{2-k}{B} + \frac{\mu_p^2}{B^2}\right] r'(\mu_p, k) \mu_p^{2n}}, \quad (14)$$

where the values of μ_p are the roots of the characteristic equation

$$\left[\frac{d}{dN} \ln r(\mu N, k)\right]_{N=1} = -B. \quad (15)$$

The external field satisfies the thermal conductivity equation

$$\frac{\partial t}{\partial H} = \frac{\partial^2 t}{\partial N^2} + \frac{k-1}{N} \frac{\partial t}{\partial N}, \quad (16)$$

the symmetry condition (6) at the center of the body, the boundary condition of the third kind (5) and the homogeneous initial temperature-distribution equation

$$t_e(N, 0) = 0. \quad (17)$$

The temperature field component existing because of a nonhomogeneous initial temperature distribution

$$t_i(N, H) = \sum_{p=1}^{\infty} c_p r(\mu_p, k) \exp(-\mu_p^2 H), \quad (18)$$

is residual by nature and becomes negligibly small with time. The expansion coefficients of $t_0(N)$ into a Dini series in terms of $r(\mu_p N, k)$ may be expressed in two equivalent forms:

$$c_p = \frac{2\int_0^1 f(N)\, N^{k-1} r(\mu_p N, k)\, dN}{\frac{k-2}{\mu_p^2} r(\mu_p, k) r'(\mu_p, k) + r'^2(\mu_p, k) + r^2(\mu_p, k)}; \tag{19}$$

or

$$c_p = \frac{2\int_0^1 f(N)\, N^{k-1} r(\mu_p N, k)\, dN}{\left[1 + \frac{2-k}{B} + \frac{\mu_p^2}{B^2}\right] r'^2(\mu_p)}, \tag{20}$$

or as the functions $r(\mu N, k)$ orthogonal in the interval [0; 1] with a weight N^{k-1} or simply orthogonal on the volume of the k-dimensional body:

$$\int_0^1 N^{k-1} r(\mu_p N, k)\, r(\mu_q N, k)\, dN = \begin{cases} 0; & p \neq q, \\ \frac{1}{2}\left[\frac{k-2}{\mu_p^2} r(\mu_p, k) r'(\mu_p, k) + r'^2(\mu_p, k) + r^2(\mu_p, k,)\right]; & p = q, \end{cases} \tag{21}$$

where μ_p and μ_q are the roots of the characteristic equation (15).

The above initial field $t_i(N, H)$ satisfies the same convective heat exchange equation (16)

$$\frac{\partial t_i(1; H)}{\partial N} + B t_i(1; H) = 0, \tag{22}$$

the initial condition

$$t_i(N; 0) = t_0(N), \tag{23}$$

and the symmetry condition (6)

The internal heat source field t_w must satisfy the thermal conductivity equation (1), the uniform initial temperature-distribution equation (17), the symmetry condition (6) and the convective heat-exchange equation (22). For the sake of convenience, we shall consider at first the field of a simpler partial heat source.

FIELD OF ACTION OF A PARTIAL HEAT SOURCE

A partial heat source is defined as a multiplicative function of the coordinates and time

$$W_v(N, H) = Q_v(N) U_v(H), \tag{24}$$

where $Q_v(N)$ is the source distribution function, and $U_v(H)$ is a function of its intensity. Evidently, in rather generalized terms, any heat source may be regarded as a sum of partial sources (3). Except where stated otherwise, we shall assume that

$$Q_v(N) U_v(H) = Q(N) U(H). \tag{25}$$

By analogy with /2, 3, 5—7/ it can be assumed that the field of action of a partial heat source may be represented as a series in terms of its intensity derivatives

$$t_{wa}(N, H) = \sum_{n=-1}^{\infty} P_n(N) U^{(n)}(H). \tag{26}$$

The thermal conductivity equation for a partial source

$$\frac{\partial t}{\partial H} = \nabla^2 t + Q(N) U(H) \tag{27}$$

indicates that the radial quasipolynomials of the field of action satisfy the system

$$\nabla^2 P_{-1} = 0; \tag{28}$$

$$\nabla^2 P_0 + Q = P_{-1}; \tag{29}$$

$$\nabla^2 P_1 = P_0; \tag{30}$$

$$\nabla^2 P_{n+1} = P_n. \tag{31}$$

The radial quasipolynomials must satisfy the symmetry condition in the center of the body

$$P_n'(0) = 0 \tag{32}$$

and the boundary conditions of the third kind for the surface

$$P_n'(1) + BP_n(1) = 0 \tag{33}$$

since the action field of heat sources has at its center a zero gradient (6) while condition (22) is satisfied on the surface of the body.

Integration of the system yields the following expressions for the first radial quasipolynomials:

$$P_{-1}(N) = 0; \tag{34}$$

$$P_0(N) = \underline{\nabla^{-2} Q} - \frac{1}{kB} \overline{Q} - \nabla^{-2} Q; \tag{35}$$

$$P_1(N) = \left[\underline{\nabla^{-2} Q} + \frac{1}{kB} \overline{Q}\right] L_2(N, B, k) + \left[\underline{\nabla^{-4} Q} + \frac{1}{kB} \overline{\nabla^{-2} Q}\right] - \nabla^{-4} Q(N), \tag{36}$$

and since a deductive relationship exists between successive radial quasipolynomials,

$$P_n(N) = \nabla^{-2} P_{n-1} - \underline{\nabla^{-2} P_{n-1}} - \frac{1}{kB} \overline{P_{n-1}}, \tag{37}$$

we obtain the following sum for the n-th quasipolynomial

$$P_n(N) = \sum_{p=0}^{n} \left[\underline{\nabla^{-2p-2} Q} + \frac{1}{kB} \overline{\nabla^{-2p} Q}\right] \times L_{2n-2p}(N, B, k) - \nabla^{-2n-2} Q(N). \tag{38}$$

THE AFTER-EFFECT FIELD OF A PARTIAL HEAT SOURCE

The after-effect field of a partial heat source must satisfy the thermal conductivity equation (16), the conditions (6) and (22), and, at the initial

moment of time, the equation

$$t_{wa\nu}(N, 0) + t_{wr\nu}(N, 0) = 0, \tag{39}$$

whose value is of the opposite sign to the value of the action field. It is evident that

$$t_{wr\nu}(N, H) = \sum_{n=0}^{\infty} U_{\nu}^{(n)}(0) \left[\sum_{p=0}^{n} \left(\underline{\nabla^{-2p-2} Q_{\nu}} + \frac{1}{kB} \overline{\nabla^{-2n} Q_{\nu}} \right) \times \right.$$

$$\left. \times L_{2n-2p}(N, H, B, k) + \sum_{p=1}^{\infty} c_{p\nu} r(\mu_p N, k) \exp(-\mu_p^2 H) \right]. \tag{40}$$

The generalized radial functions

$$L_{2n}(N, H, B, k) = (-1)^n \sum_{p=1}^{\infty} \times \frac{2r(\mu_p N, k) \exp(-\mu_p^2 H)}{[1 + (2-k)B^{-1} + \mu_p^2 B^{-2}] \mu_p^{2n+1} r'(\mu_p, k)} \tag{41}$$

are series that form the residual field (14), while the Dini series coefficients are

$$c_{p\nu} = \frac{2 \int_0^1 \nabla^{-2p-2} Q_{\nu}(N) N^{k-1} r(\mu_p N, k) dN}{[1 + (2-k)B^{-1} + \mu_p^2 B^{-2}] r'^2(\mu_p, k)} \tag{42}$$

The heat source field

$$t_{w\nu}(N, H) = t_{wa\nu}(N, H) + t_{wr\nu}(N, H) \tag{43}$$

satisfies the thermal conductivity equation (27) for a simple heat source, and the conditions of symmetry (6), convective heat exchange (5), and homogeneous initial temperature distribution (39).

THE FIELD OF A COMPLEX HEAT SOURCE

The temperature field created by a complex heat source (3) is the sum of similar field components of simple heat sources (26) and (40):

$$t_w(N, H) = t_{wa} + t_{wr} = \sum_{\nu} t_{wa\nu}(N, H) + t_{wr\nu}(N, H). \tag{44}$$

Each product of the integral operator (as applied to the distribution function of the simple source) and its intensity function may be presented as follows:

$$\nabla^{-2p} Q_{\nu}(N) U_{\nu}^{(q)}(H) = \frac{\partial^q}{\partial H^q} \nabla^{-2p} W_{\nu}(N, H), \tag{45}$$

or, more simply,

$$\nabla^{-2p} W_{\nu}^{(q)}(N, H). \tag{46}$$

However, a sum of simple heat sources creates a complex source; hence

$$\sum_{\nu} \nabla^{-2p} W_{\nu}^{(q)}(N, H) = \nabla^{-2p} W^{(q)}(N, H). \tag{47}$$

In this way, the action of an internal heat source (dispersed within a body which exchanges heat with its surroundings by convection) has the form

$$t_{wa}(N, H) = \sum_{n=0}^{\infty} \left\{ \sum_{p=0}^{n} \left[\overline{\nabla^{-2p-2} W^{(n)}(N, H)} + \right.\right.$$

$$\left. + \frac{1}{kB} \overline{\nabla^{-2p} W^{(n)}(N, H)} \right] L_{2n-2p}(N, B, k) -$$

$$\left. - \nabla^{-2n-2} W^{(n)}(N, H) \right\}, \qquad (48)$$

and its after-effect field may be obtained by summation of the respective fields of the simple source

$$t_{wr}(N, H) = \sum_{n=0}^{\infty} \left\{ \sum_{p=0}^{n} \left[\overline{\nabla^{-2p-2} W^{(n)}(N, 0)} + \right.\right.$$

$$\left. + \frac{1}{kB} \overline{\nabla^{-2p} W^{(n)}(N, 0)} \right] L_{2n-2p}(N, H, B, k) + \sum_{p=1}^{\infty} \times$$

$$\left. \times \frac{2 \int_0^1 \nabla^{-2n-2} W^{(n)}(\nu, 0) \nu^{k-1} r(\mu_p \nu, k) d\nu r(\mu_p N, k) \exp(-\mu_p^2 H)}{[1 + (2-k) B^{-1} + \mu_p^2 B^{-2}] r'^2(\mu_p, k)} \right\}. \qquad (49)$$

Expression (44) is the integral (1) satisfying the boundary conditions (6) and (22) and the initial condition

$$t_w(N, 0) = t_{wa}(N, 0) + t_{wr}(N, 0) = 0. \qquad (50)$$

Thus, the temperature field of an exothermic body containing a complex heat source is described by a sum of three components

$$t(N, H) = t_e(N, H) + t_w(N, H) + t_i(N, H), \qquad (51)$$

which satisfies the thermal-conductivity equation for an exothermic body (1), the nonhomogeneous initial temperature-distribution equation (4), the condition of convective heat exchange (5) on its surface, and the condition of symmetry (6) at the center of the body. The main component of the above temperature field would be the sum of action field t_{ea} of the surroundings and the internal heat sources, and thus we obtain the following expression for prolonged periods:

$$\lim_{H \to \infty} [t(N, H) - t_{ea}(N, H) - t_{wr}(N, H)] = 0. \qquad (52)$$

The after-effect fields of the surroundings and the sources, and the initial distribution may be neglected.

NATURE OF THE CHANGES IN THE SURROUNDINGS TEMPERATURE AND THE INTENSITY OF THE INTERNAL HEAT SOURCES

The main component of the temperature field of a body consists of a sum of the action field of the surroundings (9) and the internal heat sources (48).

The action field of the surroundings

$$t_{ea}(N, H)=\sum_{n=0}^{\infty} t_e^{(n)}(H)\, L_{2n}(N, B, k) \tag{53}$$

is a convergent series if (according to the Cauchy convergence test) the inequality

$$\lim_{n\to\infty} \sqrt[n]{|t_e^{(n)}(H)|}\ \sqrt[n]{|L_{2n}(N, B, k)|}=\omega<1 \tag{54}$$

is satisfied at any $H \in [0, \infty]$ and $N \in [0, 1]$.

The radial polynomials of the third kind decrease as their exponent is increased /1/:

$$\left(\frac{1}{kB}\right)^n \leqslant |L_{2n}(N, B, k)| \leqslant \left(\frac{1}{2k}+\frac{1}{kB}\right)^n, \tag{55}$$

and for this reason the series (53) is uniformly convergent for any H and N when the surroundings temperature derivatives are, at any moment of time H, restricted by

$$\lim_{n\to\infty} \sqrt[n]{|t_e^{(n)}(H)|}\ \left(\frac{2+B}{2kB}\right)=\omega<1. \tag{56}$$

The above condition is satisfied by the exponential surroundings temperature

$$t_e(H)=t_0[1-\exp(-PH)];\ t_e(H)=t_0\exp(-PH), \tag{57}$$

when the Predvoditelev number

$$|P| \leqslant \frac{2kB}{2+B}\,\omega, \quad \omega<1. \tag{58}$$

Since the radial polynomials are related by the expression

$$\nabla^2 L_{2n}(N, B, k)=L_{2n-2}(N, B, k), \tag{59}$$

the series would be uniformly convergent if there were a change in $t_e(H)$ (56):

$$\sum_{n=1}^{\infty} t_e^{(n)}(H)\, L_{2n-2}(N, B, k)=\frac{\partial}{\partial H}\, t_{ea}(N, H), \tag{60}$$

$$\sum_{n=1}^{\infty} t_e^{(n)}(H)\, \nabla^2 L_{2n}(N, B, k)=\nabla^2 t_{ea}(N, H) \tag{61}$$

and hence they would coincide with the right-hand term of the above equations, they could be differentiated over time, and the ∇^2 differential operator could be applied to the series (53), which describes the effect of the external temperature.

The limitations that apply to the changes in the intensity of internal heat sources W with time are a consequence of the uniform convergence of the series (54) whose form is:

$$\begin{aligned} t_{wa}(N, H)=&\left\{\left[\underbrace{\nabla^{-2}W}+\frac{1}{kB}\,\overline{\nabla^{-2}W}\right]\times\right.\\ &\left.\times L_0(N, B, k)-\nabla^{-2}W(N, H)\right\}+\\ +&\left\{\left[\underbrace{\nabla^{-2}W^{(1)}}+\frac{1}{kB}\,\overline{\nabla^{-2}W^{(1)}}\right] L_2(N, B, k)+\right. \end{aligned} \tag{62}$$

$$+\left[\underbrace{\nabla^{-4}W^{(1)}}+\frac{1}{kB}\overbrace{\nabla^{-4}W^{(1)}}\right]L_0(N,B,k)-\nabla^{-4}W^{(1)}(N,H)\Big\}+\cdots$$

$$\cdots+\left\{\left[\underbrace{\nabla^{-2}W^{(n)}}+\frac{1}{kB}\overbrace{\nabla^{-2}W^{(n)}}\right]L_{2n}(N,B,k)+\right.$$

$$+\left[\underbrace{\nabla^{-4}W^{(n)}}+\frac{1}{kB}\overbrace{\nabla^{-4}W^{(n)}}\right]L_{2n-2}(N,B,k)+$$

$$+\left[\underbrace{\nabla^{-2q}W^{(n)}}+\frac{1}{kB}\overbrace{\nabla^{-2q}W^{(n)}}\right]L_{2n-2q}(N,B,k)+\cdots \tag{62}$$

$$\cdots+\left[\underbrace{\nabla^{-2n}W^{(n)}}+\frac{1}{kB}\overbrace{\nabla^{-2n}W^{(n)}}\right]L_0(N,B,k)-$$

$$\left.-\nabla^{-2n}W^{(n)}(N,H)\right\}+\cdots$$

Let us evaluate the general term of such an expansion. Since in each case $L_0(N,B,k)=1$, the last difference may be written as

$$\underbrace{\nabla^{-2n}W^{(n)}}-\nabla^{-2n}W^{(n)}(N,H)=$$

$$=\int_N^1\eta_1^{1-k}\,d\eta_1\int_0^{\eta_1}\xi^{k-1}\,\frac{\partial^n}{\partial H^n}\,\nabla^{-2n+2}W(\xi,H)\,d\xi. \tag{63}$$

Naturally, it may be assumed that the distribution of internal heat sources and their derivatives are not impulse functions, and that the relationship

$$\sup_{\substack{N\in[0,1]\\H\in[0,\infty]}}\left|\frac{\partial^n}{\partial H^n}\,W(N,H)\right|=[W^{(n)}] \tag{64}$$

is always valid. Hence, from the integral (63) we obtain the following evaluation /2/:

$$\left|\int_1^N\eta^{1-k}\,d\eta\int_0^{\eta_1}\xi^{k-1}\,\nabla^{-2n+2}W^{(n)}(\xi,H)\,d\xi\right|\leqslant$$

$$\leqslant[W^{(n)}]\underbrace{\nabla^{-2n}1}=[W^{(n)}]\,\frac{1}{(2n)!!\,k(k+2)\ldots(k+2n-2)}\,. \tag{65}$$

By analogy, the mean value of the integral operator exponent also has an upper limit

$$\left|\overbrace{\nabla^{-2n}W^{(n)}}\right|\leqslant[W^{(n)}]\overbrace{\nabla^{-2n}1}=[W^{(n)}]\times\frac{1}{(2n)!!\,k(k+2)\ldots(k+2n)}\,, \tag{66}$$

and, hence the three leading terms of the symbol ∇^{-2} do not exceed

$$\left|\underbrace{\nabla^{-2n}W^{(n)}}+\frac{1}{kB}\overbrace{\nabla^{-2n}W^{(n)}}-\nabla^{-2n}W^{(n)}(N,H)\right|<[W^{(n)}]\times$$

$$\times\frac{1+\dfrac{1}{(k+2n)B}}{(2n)!!\,k\ldots(k+2n-2)}\,. \tag{67}$$

With respect to the general term of the sum (62), an evaluation of the radial polynomial (55) and the exponent of the integral operator /2/,

$$\nabla^{-2q}1=\frac{N^{2q}}{(2q)!!\,k(k+2)\ldots(k+2q-2)}\,, \tag{68}$$

leads to the conclusion that the inequality

$$\left|\left[\underline{\nabla^{-2q}W^{(n)}} + \frac{1}{kB}\overline{\nabla^{-2q}W^{(n)}}\right]L_{2n-2q}(N, B, k)\right| \leqslant$$

$$\leqslant \left(\frac{1}{2k} + \frac{1}{kB}\right)^{2n-2q}|W^{(n)}|\left|\underline{\nabla^{-2q}1} + \overline{\nabla^{-2q}1}\,\frac{1}{kB}\right| \tag{69}$$

is always valid.

It is evident that

$$\left|\underline{\nabla^{-2q}1} + \frac{1}{kB}\overline{\nabla^{-2q}1}\right| = \frac{\left(1 + \frac{1}{(k+2q)B}\right)}{(2q)!!k\ldots(k+2q-2)} <$$

$$< \left(\frac{1}{(2k)^q} + \frac{q}{kB}\,\frac{1}{(2k)^{q-1}}\right) < \left(\frac{1}{2k} + \frac{1}{kB}\right)^q \tag{70}$$

and even more evident that:

$$\left|\left[\underline{\nabla^{-2q}W^{(n)}} + \frac{1}{kB}\overline{\nabla^{-2q}W^{(n)}}\right]L_{2n-2q}(N, B, k)\right| <$$

$$< |W^{(n)}|\left(\frac{1}{2k} + \frac{1}{kB}\right)^n. \tag{71}$$

Thus, the sum comprised in the series (62) and related to the n-th derivative of the source intensity with respect to time has a value smaller than $n\left(\frac{1}{2k} + \frac{1}{kB}\right)^n |W^{(n)}|$

$$\left|\sum_{p=0}^{n}\left[\underline{\nabla^{-2p-2}W^{(n)}} + \frac{1}{kB}\overline{\nabla^{-2p-2}W^{(n)}}\right]L_{2n-2p}(N, B, k) - \nabla^{-2n}W^{(n)}(N, H)\right| < n|W^{(n)}|\left(\frac{1}{2k} + \frac{1}{kB}\right)^n \tag{72}$$

and the absolute magnitude of the action field of internal heat sources — the series (48) or, which is exactly the same, (62), is limited by the sum of the series

$$|t_{wa}(N, H)| < \sum_{n=1}^{\infty} n\left(\frac{2+B}{2kB}\right)^n \sup|W^{(n)}(N, H)|, \tag{73}$$

comprising only nonnegative terms.

The numerical series formed by the nonnegative terms is convergent if, in accordance with Cauchy's test for convergence,

$$\lim_{n\to\infty} \sqrt[n]{\sup|W^{(n)}(\overline{N, H})|}\,\frac{2+B}{2kB} < 1. \tag{74}$$

In this way, the series (62) would be uniformly convergent if the derivatives (with respect to time) of the intensities of internal heat sources were limited by a value depending on the number of finite body dimensions and the Biot number:

$$\lim_{n\to\infty}\left[\sup\left|\frac{\partial^n}{\partial H^n}W(N, H)\right|\right]^{\frac{1}{n}} < \frac{2kB}{2+B}. \tag{75}$$

The uniform convergence of the series

$$\frac{\partial t_{wa}}{\partial H} = \sum_{n=0}^{\infty} \left\{ \sum_{p=0}^{n} \left[\nabla^{-2p-2} W^{(n+1)}(N, H) + \right.\right.$$

$$\left. + \frac{1}{kB} \sqrt{\nabla^{-2p-2} W^{(n+1)}(N, H)} \right] \times$$

$$\left. \times L_{2n-2p}(N, B, k) - \nabla^{-2n-2} W^{(n+1)}(N, H) \right\}; \qquad (76)$$

$$\nabla^2 t_{wa} = \sum_{n=0}^{\infty} \left\{ \sum_{p=0}^{n} \left[\sqrt{\nabla^{-2p-2} W^{(n)}(N, H)} + \right.\right.$$

$$\left. + \frac{1}{kB} \sqrt{\nabla^{-2p-2} W^{(n)}(N, H)} \right] \times$$

$$\left. \times \nabla^2 L_{2n-2p}(N, B, k) - \nabla^{-2n} W^{(n)}(N, H) \right\} \qquad (77)$$

and their coincidence with the right-hand term of the above equations is proved in a similar way.

The condition (75) is satisfied in the case of exponentially changing heat sources

$$W(N, H) = \sum_{\mu=1}^{m} Q_{\mu}(N) \exp(-P_{\nu} H), \qquad (78)$$

when the number P_{ν} is lower than the same value as in evaluation (59)

$$0 \leqslant P_{\nu} < \frac{2kB}{2 + B}. \qquad (79)$$

Bibliography

1. Temkin, A.G. — Vsesoyuznoe nauchno-tekhnicheskoe soveshchanie po intensifikatsii protsessov sushki. Energeticheskaya sektsiya, Profizdat. 1958.
2. Temkin, A.G. — IFZh, No. 1. 1959.
3. Temkin, A.G. — IFZh, No. 4. 1962.
4. Lykov, A.V. Teplo- i massoobmen v protsessakh sushki (Heat and Mass Transfer in Drying Processes). — Gosenergoizdat. 1956. [Translated by IPST, No. 2145.]
5. Temkin, A.G. Teplo- i massoperenos (Heat and Mass Transfer), 5. — Minsk, Izdatel'stvo AN BSSR. 1961.
6. Temkin, A.G. — IFZh, No. 10. 1962.
7. Carslaw, H.S. and J.C. Jaeger. Conduction of Heat in Solids, Second edition. 1959.
8. Lykov, A.V. Teoriya teploprovodnosti (The Theory of Thermal Conductivity). — GITTL. 1952.
9. Temkin, A.G. — Izvestiya Vuzov, Energetika, No. 8. 1961.

P. V. Tsoi and O. B. Kianovskii

A CONTACT PROBLEM FOR A GENERALIZED SYSTEM OF DIFFERENTIAL EQUATIONS OF HEAT AND MASS TRANSFER

The potential fields of generalized charges and their fluxes change continuously at the contact surface between two bodies.

The above problem may be mathematically stated as follows.

It is necessary to determine the functions $u_1(x, t)$ and $u_2(x, t)$ that satisfy the system

$$\left.\begin{aligned} \frac{\partial u_1}{\partial t} &= a_{11}^2 \frac{\partial^2 u_1}{\partial x^2} + a_{12}^2 \frac{\partial^2 u_2}{\partial x^2} \\ \frac{\partial u_2}{\partial t} &= a_{21}^2 \frac{\partial^2 u_1}{\partial x^2} + a_{22}^2 \frac{\partial^2 u_2}{\partial x^2} \end{aligned}\right\} \tag{1}$$

and the initial condition

$$u_k(x, 0) = f_k(x); \ (k = 1. 2) \tag{2}$$

in a semiinfinite space $\Omega\{0 < x < +\infty, \ t > 0\}$.

For another medium $\Omega^{(-)}\{-\infty < x < 0, \ t > 0\}$ it is necessary to find the functions $u_1^{(-)}(x, t)$ and $u_2^{(-)}(x, t)$ that satisfy the system

$$\left.\begin{aligned} \frac{\partial u_1^{(-)}}{\partial t} &= b_{11}^2 \frac{\partial^2 u_1^{(-)}}{\partial x^2} + b_{12}^2 \frac{\partial^2 u_2^{(-)}}{\partial x^2} \\ \frac{\partial u_2^{(-)}}{\partial t} &= b_{21}^2 \frac{\partial^2 u_1^{(-)}}{\partial x^2} + b_{22}^2 \frac{\partial^2 u_2^{(-)}}{\partial x^2} \end{aligned}\right\} \tag{3}$$

and the initial condition

$$u_k^{(-)}(x, 0) = f_k^{(-)}(x); (k = 1, 2). \tag{4}$$

At the contact boundary between two media ($x = 0$) the functions $u_k(x, t)$ and $u_k^{(-)}(x, t)$ must satisfy the following continuity conditions:

$$u_k(+0, t) = u_k^{(-)}(-0, t), \tag{5}$$

$$\lambda_k \frac{\partial u_k}{\partial x}\Big|_{x=+0} = \lambda_k^{(-)} \frac{\partial u_k^{(-)}}{\partial x}\Big|_{x=-0} \tag{6}$$

Let

$$\lambda_k \frac{\partial u_k}{\partial x}\Big|_{x=+0} = \lambda_k^{(-)} \frac{\partial u_k^{(-)}}{\partial x}\Big|_{x=-0} = \varphi_k(t), \tag{7}$$

where $\varphi_k(t)$ is a function of the specific flux of the k-th generalized charge (heat or mass of the bound matter) at the contact boundary between the two media.

Let us assume that the functions $\varphi_1(t)$ and $\varphi_2(t)$ are known to us. In that case the contact problem of heat and mass transfer (1) — (6) is broken down into two independent boundary problems of the second kind for semiinfinite media.

Let us apply to system (1) the Fourier cosine transform by the variable x and the Laplace transform by t. In that case, taking into account conditions (2) and (7) we obtain

$$\left.\begin{aligned}
&(p + a_{11}^2 \xi^2)\,\bar{u}_1^* + a_{12}^2 \xi^2 \bar{u}_2^* = -\sqrt{\frac{2}{\pi}} \times \\
&\times \left[\frac{a_{11}^2}{\lambda_1}\,\varphi_1(p) + \frac{a_{12}^2}{\lambda_2}\,\varphi_2(p)\right] + f_1^* \\
&a_{21}^2 \xi^2 \bar{u}_1^* + (p + a_{22}^2 \xi^2)\,\bar{u}_2^* = -\sqrt{\frac{2}{\pi}} \times \\
&\times \left[\frac{a_{21}^2}{\lambda_1}\,\bar{\varphi}_1(p) + \frac{a_{22}^2}{\lambda_2}\,\bar{\varphi}_2(p)\right] + f_2^*
\end{aligned}\right\}, \tag{8}$$

and, from there

$$\begin{aligned}
\bar{u}_1^*(\xi, p) = \frac{1}{D(\xi, p)} \Bigg\{ &-\sqrt{\frac{2}{\pi}} \left[\frac{a_{11}^2}{\lambda_1}\,\bar{\varphi}_1(p) + \right. \\
&\left. + \frac{a_{12}^2}{\lambda_2}\,\bar{\varphi}_2(p)\right](p + a_{22}^2 \xi^2) + \sqrt{\frac{2}{\pi}} \left[\frac{a_{21}^2}{\lambda_1}\,\varphi_1(p) + \right. \\
&\left. + \frac{a_{22}^2}{\lambda_2}\,\bar{\varphi}_2(p)\right] a_{12}^2 \xi^2 + [(p + a_{22}^2 \xi^2) f_1^*(\xi) - a_{12}^2 f_2^*(\xi) \xi^2] \Bigg\},
\end{aligned} \tag{9}$$

$$\begin{aligned}
\bar{u}_2^*(\xi, p) = \frac{1}{D(\xi, p)} \Bigg\{ &-\sqrt{\frac{2}{\pi}} \left[\sum_{k=1}^{2} \frac{a_{2k}^2}{\lambda_k}\,\bar{\varphi}_k(p)\right](p + a_{11}^2 \xi^2) + \\
&+ a_{21}^2 \xi^2 \sqrt{\frac{2}{\pi}} \sum \frac{a_{1k}^2}{\lambda_k}\,\bar{\varphi}_k(p) + (p + a_{11}^2 \xi^2) f_2^*(\xi) - a_{21}^2 \xi^2 f_1^*(\xi),
\end{aligned} \tag{10}$$

where

$$D(\xi, p) = \begin{vmatrix} p + a_{11}^2 \xi^2 & a_{12}^2 \xi^2 \\ a_{21}^2 \xi^2 & p + a_{22}^2 \xi^2 \end{vmatrix}.$$

When the corresponding inverse integral transform is applied to $\bar{u}_1^*(\xi, p)$, we obtain

$$\begin{aligned}
u_1(x, t) = &\sum_{k=1}^{2} \frac{1}{2c_k \sqrt{\pi}} \times \\
\times \Bigg\{ &-\int_0^t \frac{m_{1k}\,\varphi_{11}(\tau) - n_{1k}\,\varphi_{12}(\tau)}{\sqrt{t - \tau}} \exp\left[-\frac{x^2}{4c_k^2 (t - \tau)}\right] d\tau + \\
&+ \frac{1}{\sqrt{t}} \int_0^\infty [m_{1k} f_1(\sigma) - n_{1k} f_2(\alpha)] \left\{ \exp\left(-\frac{(x - \alpha)^2}{4c_k^2 t}\right) + \right. \\
&\left. + \exp\left(-\frac{(x + \alpha)^2}{4c_k^2 t}\right)\right] d\alpha \Bigg\},
\end{aligned} \tag{11}$$

where

$$\left.\begin{aligned} \varphi_{1k}(\tau) &= \frac{a_{11}^2}{\lambda_1}\,\varphi_1(\tau) + \frac{a_{12}^2}{\lambda_2}\,\varphi_2(\tau) \\ m_{1k} &= (a_{22}^2 - c_k^2)(a_{11}^2 + a_{22}^2 - 2c_k^2)^{-1} \\ n_{1k} &= a_{12}^2(a_{11}^2 + a_{22}^2 - 2c_k^2)^{-1} \\ c_k^2 &= \frac{(a_{11}^2 + a_{22}^2) + (-1)^{k+1}\sqrt{(a_{11}^2 - a_{22}^2) + 4a_{12}^2 a_{21}^2}}{2} \end{aligned}\right\} \tag{12}$$

The function $u_2(x, t)$ is determined in a similar way:

$$u_2(x, t) = \sum_{k=1}^{2} \frac{1}{2c_k\sqrt{\pi}} \times$$

$$\times \left\{ -\int_0^t \frac{m_{2k}\varphi_{12}(\tau) - n_{2k}\varphi_{11}(\tau)}{\sqrt{t-\tau}} \exp\left[-\frac{x^2}{4c_k^2(t-\tau)}\right] d\tau + \right.$$

$$+ \frac{1}{\sqrt{t}} \int_0^{\infty} [m_{2k} f_2(\alpha) - n_{2k} f_1(\alpha)] \left[\exp\left(-\frac{(x-\alpha)^2}{4c_k^2 t}\right) + \right.$$

$$\left. \left. + \exp\left(-\frac{(x+\alpha)^2}{4c_k^2 t}\right)\right] d\tau \right\}, \tag{13}$$

where

$$m_{2k} = (a_{11}^2 - c_k^2)(a_{11}^2 + a_{22}^2 - 2c_k^2)^{-1};$$
$$n_{2k} = a_{21}^2(a_{11}^2 + a_{22}^2 - 2c_k^2)^{-1}.$$

In order to determine the functions $u_1^{(-)}(x, t)$ and $u_2^{(-)}(x, t)$ let us transform the range $\Omega^{(-)}\{-\infty < x < 0,\ t > 0\}$ by replacing the variable $z = -x$ in the range $\Omega\{0 < z < +\infty,\ t > 0\}$. In that case the system (3) and the boundary conditions (7) assume the form

$$\left\{ \frac{\partial u_j^{(-)}}{\partial t} = b_{j1}\frac{\partial^2 u_1^{(-)}}{\partial z^2} + b_{j2}\frac{\partial^2 u_2^{(-)}}{\partial z^2} \right\} \quad (j = 1, 2); \tag{14}$$

$$\lambda_k^{(-)}\frac{\partial u_k^{(-)}}{\partial z}\Big|_{z=0} = \varphi_k(t). \tag{15}$$

Solving the system (14) for boundary conditions (4) and (15) we obtain

$$u_1^{(-)}(z, t) = \sum_{k=1}^{2} \frac{1}{2l_k\sqrt{\pi}} \times$$

$$\times \left\{ \int_0^t \frac{m_{1k}^{(-)}\varphi_{11}^{(-)}(\tau) - n_{1k}^{(-)}\varphi_{12}^{(-)}(\tau)}{\sqrt{t-\tau}} \exp\left[-\frac{z^2}{4l_k^2(t-\tau)}\right] d\tau + \right.$$

$$+ \frac{1}{\sqrt{t}} \int_0^{\infty} [m_{1k}^{(-)} f_1^{(-)}(-\alpha) - n_{1k}^{(-)} f_2^{(-)}(-\alpha)] \times$$

$$\left. \times \exp\left[-\frac{(z-\alpha)^2}{4l_k^2 t}\right]\left[1 + \exp\left(-\frac{\alpha z}{l_k^2 t}\right)\right] d\alpha \right\}, \tag{16}$$

where

$$\left.\begin{aligned} m_{1k}^{(-)} &= (b_{11}^2 - l_k^2)(b_{12}^2 + b_{22}^2 - 2l_k^2)^{-1} \\ n_{1k} &= b_{12}^2 (b_{11}^2 + b_{22}^2 - 2l_k^2)^{-1} \\ l_k^2 &= \frac{(b_{11}^2 + b_{22}^2) + (-1)^{k+1}\sqrt{(b_{11}^2 - b_{22}^2)^2 + 4b_{12}^2 b_{21}^2}}{2} \end{aligned}\right\}. \tag{17}$$

The function $u_2^{(-)}(z, t)$ is determined in a similar way.

The solution of $u_k(x, t)$ and $u_k^{(-)}(z, t)$ involved the use of two unknown functions $\varphi_1(t)$ and $\varphi_2(t)$ — functions of the generalized charge fluxes at the boundary between two bodies. Thus, the problem is solved completely when these functions are determined.

Let us write equations (1) and (3) and the respective boundary conditions in a matrix form

$$\frac{\partial u}{\partial t} = A \frac{\partial^2 u}{\partial x^2}; \tag{18}$$

$$\left.\begin{aligned} u(x, 0) &= f(x) \\ \frac{\partial u}{\partial x}\Big|_{x=+0} &= \varphi(t) \end{aligned}\right\}; \tag{19}$$

$$\frac{\partial u^{(-)}}{\partial t} = B \frac{\partial^2 u^{(-)}}{\partial x^2}; \tag{20}$$

$$\left.\begin{aligned} u^{(-)}(x, 0) &= f^{(-)}(x) \\ \frac{\partial u^{(-)}}{\partial x}\Big|_{x=-0} &= \varphi^{(-)}(t) \end{aligned}\right\}, \tag{21}$$

where

$$A = \left\| \begin{matrix} a_{11}^2 & a_{12}^2 \\ a_{21}^2 & a_{22}^2 \end{matrix} \right\|; \quad f(x) = \left\| \begin{matrix} f_1(x) \\ f_2(x) \end{matrix} \right\}; \quad \varphi(t) = \left\| \begin{matrix} \frac{\varphi_1(t)}{\lambda_1} \\ \frac{\varphi_2(t)}{\lambda_2} \end{matrix} \right\};$$

$$B = \left\| \begin{matrix} b_{11}^2 & b_{12}^2 \\ b_{21}^2 & b_{22}^2 \end{matrix} \right\}; \quad f^{(-)}(x) = \left\| \begin{matrix} f_1^{(-)}(x) \\ f_2^{(-)}(x) \end{matrix} \right\}; \quad \varphi^{(-)}(t) = \left\| \begin{matrix} \frac{\varphi_1(t)}{\lambda_1^{(-)}} \\ \frac{\varphi_2(t)}{\lambda_2^{(-)}} \end{matrix} \right\}.$$

The column matrix $u(x, t)$ satisfying equation (18) and condition (19) will be written as

$$u(x, t) = \frac{1}{2\sqrt{\pi t}} \int_0^\infty \frac{1}{\sqrt{A}} \exp\left[-\frac{(x-\alpha)^2}{4At}\right] \times$$

$$\times \left[1 + \exp\left(-\frac{\alpha x}{At}\right)\right] f(\alpha)\, d\alpha -$$

$$- \frac{1}{\sqrt{\pi}} \int_0^t \frac{\sqrt{A}}{\sqrt{t-\tau}} \exp\left[-\frac{x^2}{4A(t-\tau)}\right] \varphi(\tau)\, d\tau. \tag{22}$$

The matrix $u^{(-)}(z, t)(z = -x)$ satisfying equation (20) and condition (21) is determined by the equation

$$u^{(-)}(z,t) = \frac{1}{2\sqrt{\pi t}} \int_0^\infty \frac{1}{\sqrt{B}} \exp\left[-\frac{(z-\alpha)^2}{4Bt}\right] \times$$

$$\times \left[1 + \exp\left(-\frac{\alpha z}{Bt}\right)\right] f^{(-)}(-\alpha)\, d\alpha +$$

$$+ \frac{1}{\sqrt{\pi}} \int_0^t \frac{\sqrt{B}}{\sqrt{t-\tau}} \exp\left[-\frac{z^2}{4B(t-\tau)}\right] \varphi^{(-)}(\tau)\, d\tau. \qquad (23)$$

In order to determine $\varphi(t)$ and $\varphi^{(-)}(t)$ we shall use the continuity condition (5), which in a matrix form is written as

$$u(+0, t) = u^{(-)}(-0, t). \qquad (24)$$

Let us carry out the transition to boundary at $x \to 0$ $(z \to 0)$ in equations (22) and (23). By substituting these boundary values in (24), we obtain

$$\int_0^t \frac{\sqrt{B}\,\varphi^{(-)}(\tau) + \sqrt{A}\,\varphi(\tau)}{\sqrt{t-\tau}}\, d\tau =$$

$$= \frac{1}{\sqrt{t}} \int_0^\infty \left[\frac{1}{\sqrt{A}} \exp\left(-\frac{\alpha^2}{4At}\right) f(\alpha) -\right.$$

$$\left. - \frac{1}{\sqrt{B}} \exp\left(-\frac{\alpha^2}{4Bt}\right) f^{(-)}(-\alpha)\right] d\alpha$$

or

$$\int_0^t \frac{\Phi(\tau)}{\sqrt{t-\tau}} = F(t), \qquad (25)$$

where

$$\Phi(\tau) = \sqrt{B}\,\varphi^{(-)}(\tau) + \sqrt{A}\,\varphi(\tau);$$

$$F(t) = \frac{1}{\sqrt{t}} \int_0^\infty \left[\frac{1}{\sqrt{A}} \exp\left(-\frac{\alpha^2}{4At}\right) f(\alpha) -\right.$$

$$\left. - \frac{1}{\sqrt{B}} \exp\left(-\frac{\alpha^2}{4Bt}\right) f^{(-)}(-\alpha)\right] d\alpha;$$

$\Phi(\tau)$ and $F(t)$ are single-column matrices.
The Abel integral equation (25) will have the following solution /3/:

$$\Phi(t) = \frac{1}{\pi} \frac{d}{dt} \int_0^t \frac{F(\tau)}{\sqrt{t-\tau}}. \qquad (26)$$

Let

$$\gamma = \frac{1}{\lambda}, \quad F(t) = \begin{Vmatrix} F_1(t) \\ F_2(t) \end{Vmatrix},$$

then

$$\Phi(t) = \sqrt{A}\,\varphi(t) + \sqrt{B}\,\varphi^{(-)}(t) =$$

$$= \left[\sqrt{A}\begin{Vmatrix}\gamma_1 & 0\\ 0 & \gamma_2\end{Vmatrix} + \sqrt{B}\begin{Vmatrix}\gamma_1^{(-)} & 0\\ 0 & \gamma_2^{(-)}\end{Vmatrix}\right]\begin{Vmatrix}\varphi_1(t)\\ \varphi_2(t)\end{Vmatrix}$$

$$= \begin{Vmatrix}d_{11} & d_{12}\\ d_{21} & d_{22}\end{Vmatrix}\begin{Vmatrix}\varphi_1(t)\\ \varphi_2(t)\end{Vmatrix},$$

where

$$d = \begin{Vmatrix}d_{11} & d_{12}\\ d_{21} & d_{22}\end{Vmatrix} = \sqrt{A}\begin{Vmatrix}\gamma_1 & 0\\ 0 & \gamma_2\end{Vmatrix} - \sqrt{B}\begin{Vmatrix}\gamma_1^{(-)} & 0\\ 0 & \gamma_2^{(-)}\end{Vmatrix}.$$

The matrix elements d are determined by a simple method. For instance, if the roots of the characteristic matrix determinants A and B are real and different we have

$$d = \left\{\frac{1}{c_1^2 - c_2^2}\sum_{k=1}^{2}(-1)^{k+1}c_k\begin{Vmatrix}(c_k^2 - a_{22}^2)a_{12}^2\\ a_{21}^2(c_k^2 - a_{11}^2)\end{Vmatrix}\right\}\begin{Vmatrix}\gamma_1 & 0\\ 0 & \gamma_2\end{Vmatrix} +$$

$$+\left\{\frac{1}{l_1^2 - l_2^2}\sum_{k=1}^{2}(-1)^{k+1}l_k\begin{Vmatrix}(l_k^2 - b_{22}^2)b_{12}^2\\ b_{21}^2(l_k^2 - b_{11}^2)\end{Vmatrix}\right\}\begin{Vmatrix}\gamma_1^{(-)} & 0\\ 0 & \gamma_2^{(-)}\end{Vmatrix},$$

where C_k^2 and l_k^2 are the roots of the characteristic matrix determinants A and B as determined by equations (12) and (17)

Copying equation (26) row by row we obtain

$$\left.\begin{aligned} d_{11}\varphi_1(t) + d_{12}\varphi_2(t) &= F_1(t)\\ d_{21}\varphi_1(t) + d_{22}\varphi_2(t) &= F_2(t)\end{aligned}\right\}. \tag{27}$$

where

$$F_k(t) = \frac{1}{\pi}\frac{d}{dt}\int_0^t \frac{F_k(\tau)}{\sqrt{t-\tau}}\,d\tau. \tag{28}$$

By solving the algebraic system (27) we obtain

$$\left.\begin{aligned}\varphi_1(t) &= \frac{F_1(t)d_{22} - F_2(t)d_{12}}{d_{11}d_{22} - d_{12}d_{21}};\\ \varphi_2(t) &= \frac{F_2(t)d_{11} - F_1(t)d_{21}}{d_{11}d_{22} - d_{12}d_{21}}.\end{aligned}\right\} \tag{29}$$

The functions $\varphi_1(t)$ and $\varphi_2(t)$ in equation (29) describe the unsteady specific fluxes of generalized charges at the contact boundary between two bodies, for nonhomogeneous initial conditions.

Let us assume the existence of a constant distribution field of generalized charges at the initial moment (prior to the contact), i.e.,

$$f_k(x) = u_k^0 = \text{const}, \quad f_k^{(-)}(x) = v_k^0 = \text{const};$$

then

$$F(t) = \frac{1}{\sqrt{t}}\int_0^\infty\left[\frac{1}{\sqrt{A}}\exp\left(-\frac{\alpha^2}{4At}\right)f(\alpha) -\right.$$

$$\left. - \frac{1}{\sqrt{B}}\exp\left(-\frac{\alpha^2}{4Bt}\right)f^{(-)}(\alpha)\right]d\alpha = \frac{\sqrt{\pi}}{2}(u^0 - v^0).$$

Hence

$$F_k(t) = \frac{1}{\pi} \frac{d}{dt} \int_0^t \frac{F_k(\tau)\, d\tau}{\sqrt{t-\tau}} =$$

$$= \frac{\Delta u_k}{2\sqrt{\pi}} \frac{d}{dt} \int_0^t \frac{d\tau}{\sqrt{t-\tau}}. \qquad (30)$$

where

$$\Delta u_k = u_k^0 - v_k^0 \quad (k = 1, 2).$$

Substitution of (30) into (29) yields

$$\varphi_1(t) = \frac{d_{22}\Delta u_1 - d_{12}\Delta u_2}{(d_{11}d_{22} - d_{12}d_{21})\sqrt{\pi t}};$$

$$\varphi_2(t) = \frac{d_{11}\Delta u_2 - d_{21}\Delta u_1}{(d_{11}d_{22} - d_{12}d_{21})\sqrt{\pi t}}. \qquad (31)$$

For $a_{12} = b_{12} = 0$ we obtain (after some simplifications)

$$\varphi_1(t) = \frac{u_1^0 - v_1^0}{(a_{11}\gamma_1 + b_{11}\gamma_1^{(-)})\sqrt{\pi t}}. \qquad (32)$$

Equation (32) has been derived in /4/, in the solution of an analogous contact problem for free transfer.

Bibliography

1. Lykov, A.V. and Yu.A. Mikhailov. Teoriya teplo- i massoperenosa (The Theory of Heat and Mass Transfer). — Gosenergizdat. 1963.
2. Kim, E.I. Ob odnoi zadachi teploobmena sistemy tel (One Problem in the Heat Transfer in a System of Bodies). — PMM, Vol. 21, No. 3. 1957.
3. Mikhlin, S.G. Lektsii po lineinym integral'nym uravneniyam (Lectures on Linear Integral Equations). — Fizmatgiz. 1959.
4. Tsoi, P.V. — IFZh, No. 1. 1961.

A. L. Parnas

ON THE UNSTEADY CONVECTIVE HEAT EXCHANGE WITH AN OSCILLATING BODY

It is well known /1, 4, and others/ that heat exchange with a body in a pulsating gas stream is quasisteady if the pulse amplitude and frequency are low.* It can be proved easily that in such a case the effect of the pulsation is accounted for in the dimensionless equation by means of a single additional complex comprising the amplitude of the oscillation velocity, e.g., v/V_0 or $\mathrm{Re}_v = vd/\nu$.

The specific features of the unsteady state appear as the oscillation amplitude and frequency are increased, and the quasisteady state is disturbed. By using the dimensionality methods /2/, it can be shown that two, rather than one, complexes — $\mathrm{Sh} = fd/V_0$ and a/d** — must be introduced into the dimensionless equation in order to correct it for the effect of pulsations.

It is a common assumption /1, 3, etc./ that in order to have a quasisteady state the term in the Navier-Stokes equation expressing local acceleration should be small with respect to the term for convective acceleration; the above condition may be written in the following form:

$$\frac{\partial V}{\partial \tau} \ll V \frac{\partial V}{\partial l}. \qquad (1)$$

By assuming that $\partial V/\partial \tau \sim V/T$ and $\partial V/\partial l \sim V/d$, inequality (1) is transformed into

$$\mathrm{Sh} = \frac{d}{VT} \ll 1. \qquad (2)$$

Expression (2) makes it possible to evaluate to a rough approximation only the order of magnitude of Sh. At the same time it is very important (for the solution of many research and practical problems) to have more or less accurate numerical values of the parameters separating the quasisteady from the truly unsteady-state regions. At present, collection of such data (especially in the case of nonstreamlined bodies) is apparently possible only by experiment.

We carried out experimental work on the heat exchange with a cylinder in a transverse air stream, which oscillated either in the same direction or in a direction normal to the air flow; the experimental apparatus and

* Quasisteady means that the instantaneous value of the heat exchange coefficient may be determined from the relationships established under steady-state conditions.

** Apparently, those terms are equivalent to a certain other pair of independent dimensionless parameters formed by combing Sh and a/d either with one another or with some other important dimensionless number, e.g., Sh with Re_v, Sh with v/V_0, etc.

the main experimental results have been reported in /5/. Some of the results obtained in experiments in which the cylinder oscillated in the direction of the air flow are shown in the figure. Sections a and b show that processing of the results on the basis of Re_v or Sh alone is not sufficient.

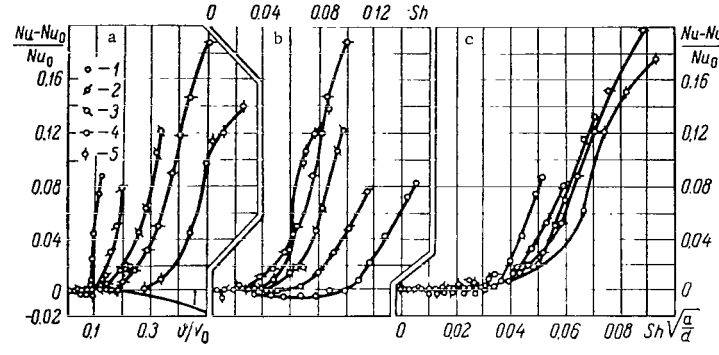

Processing of experimental data on heat exchange with a cylinder in a transverse air stream and oscillating in the direction of the air flow – in the form of the following functions: $(Nu-Nu_0)/Nu_0$ as a function of v/V_0 (a); $(Nu-Nu_0)/Nu_0$ as a function of Sh (b); and $(Nu-Nu_0)/Nu_0$ as a function of $Sh\sqrt{a/d}$ (c) (Re = 1450, ϵ = 2.6%, d = 8.4 mm, V_0 = 2.6 m/sec).

1) a/d = 0.11; 2) 0.27; 3) 0.52; 4) 0.78; 5) 1.14. I) quasisteady values.

Section b of the figure shows in particular that a marked increase in Nu (which within the range studied is a measure also of the deviations from a quasisteady state) begins at different values of Sh, depending on the a/d ratio. This becomes clear when we take into account the fact that the commonly accepted estimation that $\partial V/\partial\tau \sim V/T$ is only approximate. Since in the above case the air velocity with respect to the cylinder equals $V_0 + v \sin \omega\tau$, it is evident that $\partial V/\partial\tau \sim v/T$ and that the following equation should be used (instead of (2)):

$$\mathrm{Sh}\,\frac{v}{V_0} \ll 1. \tag{3}$$

In this case, the use of a/d is more convenient than the use of the v/V_0 ratio. Then, from the equation $v = 2\pi af$ and from (3) it is possible to describe the condition of the quasisteady state as

$$\mathrm{Sh}\sqrt{a/d} \ll 1. \tag{4}$$

In this way, in the case studied the validity of the quasisteady approximation should be determined not by the Sh number, but by a certain value of the complex $Sh\sqrt{a/d}$ or by $Sh(v/V_0)$. The processing of the experimental points is shown in section c of the figure, where the values of Nu_c were determined by means of the following equation /5/:

$$\mathrm{Nu_c}/\mathrm{Nu_0} = \frac{1}{2\pi}\int_0^{2\pi}\left|1 + \frac{v}{V_0}\sin x\right|^{1/2} dx. \tag{5}$$

The figure shows that the correlation of experimental points in section c is better than in sections a and b of the figure, while the deviation from

a quasisteady state is, indeed, characterized by a certain definite value of the complex $\mathrm{Sh}\sqrt{a/d}$. Let us use the index k to denote a value of the above complex for which $(\mathrm{Nu}-\mathrm{Nu}_c)/\mathrm{Nu}_0 = 1\%$. In that case the data in section c of the figure correspond to $(\mathrm{Sh}\sqrt{a/d})_k \approx 0.04$. A rapid increase in the value of $\mathrm{Nu}-\mathrm{Nu}_c$ takes place in the range in which $\mathrm{Sh}\sqrt{a/d} > (\mathrm{Sh}\sqrt{a/d})_k$. A similar treatment of the experimental data obtained at other values of V_0 and with a cylinder of a diameter $d = 2.8$ mm shows that at $\mathrm{Re}_f = 200-3000$, $\mathrm{Sh} < 0.12$, $v/V_0 <$ and $\varepsilon = 2-6\%$ the value of $(\mathrm{Sh}\sqrt{a/d})_k$ varies within the range

$$(\mathrm{Sh}\sqrt{a/d})_k = 0{,}03 \div 0.055\,^{*} \tag{6}$$

or, in a different form

$$\left(\mathrm{Sh}\frac{v}{V_0}\right)_k = 0.008 \div 0.019\,. \tag{7}$$

In the range studied, the value of the Re number had little effect on $(\mathrm{Sh}\sqrt{a/d})_k$. Hence, it is natural to assume that the values determined by equations (6) and (7) could be used within a wide range of values of Re. The above assumption is supported, in particular, by a comparison between our data and experimental results /6, 7/ obtained at $\mathrm{Re} < 200$.

In the case of oscillations normal to the stream velocity, the relative velocity modulus is

$$V = \sqrt{V_0^2 + v^2 \sin^2 \omega\tau}. \tag{8}$$

If, at first approximation, the oscillations parallel to the stream are neglected, and if we take into account the fact that at low v/V_0 we have $\partial V/\partial\tau \sim v^2/V_0 T$, the condition of the quasisteady state for transverse oscillations assumes the form

$$\mathrm{Sh}\left(\frac{v}{V_0}\right)^2 \ll 1 \tag{9}$$

or

$$\mathrm{Sh}\left(\frac{a}{d}\right)^{1/4} \ll 1. \tag{10}$$

However, in our experiments we were unable to determine the value of $[\mathrm{Sh}\,v/V_0{}^2]_k$. This is attributed to the fact that the experiments were carried out at Sh values close to 0.19. At such values of Sh there was a maximum in the value of $\mathrm{Nu}-\mathrm{Nu}_c$, which is apparently associated with the interaction between the flow disturbances caused by the cylinder oscillations and the disturbances caused by eddying from the cylinder /5/. At the same time the experiments showed that if we neglect the "resonance" phenomenon at $\mathrm{Sh} = 0.19$ the quasisteady state in the case of transverse vibrations is observed at higher values of the parameters a and f (all other conditions being equal). This is in good agreement with the fact that the acceleration in the case of transverse oscillations is, as a rule, much less pronounced than in the case of longitudinal oscillations. In particular, it can be proved with ease that the ratio of these values is approximately $\frac{1}{2}\frac{v}{V_0}$.

* Smaller values of $(\mathrm{Sh}\sqrt{a/d})_k$ correspond to lower degrees of turbulence of the stream. This may be explained as follows: the lower the value of ϵ (i. e., the pulsations "background" of the main stream), the greater is the effect of the additional disturbances caused by the cylinder oscillations.

SYMBOLS

a and f — oscillation amplitude and frequency; d — characteristic parameter (cylinder diameter); l — length; Re_v — the "vibration" Reynolds number; T — characteristic time (oscillation period); V and V_0 — relative and absolute air velocity with respect to the oscillating cylinder; v — amplitude of the velocity fluctuations; ε — degree of turbulence; ν — kinematic viscosity; τ — time; w — angular frequency.

Subscripts: c — average (with respect to time) value calculated by assuming that the oscillations are quasisteady; f — calculated at the stream temperature; k — value corresponding to $(Nu - Nu_c)/Nu_0 = 1\%$; 0 — value under stationary conditions (in the absence of pulsations).

Bibliography

1. Loitsyanskii, L.G. Laminarnyi pogranichnyi sloi (The Laminary Boundary Layer). — Fizmatgiz. 1962.
2. Sedov, L.I. Metody podobiya i razmernosti v mekhanike (The Similarity and Dimensionality Methods in Mechanics). — Gostekhizdat. 1957.
3. Eckert, E.R. and R.M. Drake. The Theory of Heat and Mass Transfer [Russian translation. 1961.]
4. Lemlich, R. — Chemical Engineering, No. 10. 1961.
5. Parnas, A.L. — IFZh, No. 10. 1964.
6. Pelepeichenko, I.P. and D.F. Simbirskii. — Teploenergetika, No. 3. 1963.
7. Shteinberg, A.S. — Teploenergetika, No. 8. 1962.

A. L. Parnas

EXPERIMENTAL STUDY OF HEAT EXCHANGE IN THE CASE OF A CYLINDER IN A TRANSVERSE AIR STREAM

The study of various unsteady effects during forced flow round solid bodies is of interest for the solution of a number of scientific and technological problems. In particular, we should mention the determination of the time needed for the establishment of a steady-state heat exchange process after a sudden (jumplike) change in the velocity and temperature of a stream round a cylinder.

Data obtained in theoretical analyses /1—6/, as well as simple calculations of the unsteady heating of the air "film" (boundary layer) adjacent to the body show that in the uninterrupted flow region the time needed for the establishment of a steady-state heat exchange process is determined (as is well known) by the value Ho $\approx 1 \div 2$.

We know of no published paper in which a determination has been made of the time of establishment of a steady-state heat exchange during shedding of eddies in the rear-end section of the cylinder. However, an approximate evaluation of the characteristic time, based on an examination of the formation and detachment of eddies behind the cylinder, indicates a value of the order of Ho ≈ 5 for the region of shedding of eddies (i.e., for the heat exchange from the cylinder as a whole). The above evaluation is only approximate and requires experimental proof. We know of only one paper /7/ reporting such an experimental study.* The characteristic times reported in that paper were much greater than Ho = 5. It appears that the results of /7/ could be affected by some inadequacies in the measurement methods used, in particular by the time lag in the measuring circuit and the flow of heat over the cylinder body. As shown in /8/, such heat flow may substantially distort the results of experimental studies of unsteady-state heat exchange involving temperature recording at any point of the thin-walled model.

In our experiments we used a procedure that eliminated the above fault. The cylinder to be investigated was prepared in the form of a dense (winding-to-winding) coil of thin insulated wire on a material having a low thermal conductivity (paper or the like). As is well known, cylinders of such constructions are widely used for steady-state measurements. The

* A paper /9/ reports the results of an experimental study of the unsteady-state diffusion from the surface of a sphere to a fluid (with sufficient liquid to cause drop formation) flowing round the sphere. However, the data collected in those experiments, as well as the suggestions based on them /10/, should not be applied without a special check to the case of heat exchange involving a cylinder in a transverse air flow. Such a check must be carried out in view of the substantial difference in the body shapes and the values of Pr in /9/ and in the case discussed here.

coil of wire (which in our experiments served as a resistance thermometer) was a part of a bridge circuit coupled through a strain-gage amplifier to the circuit of an oscillograph. The natural frequency of the circuit was $(2-4)\times10^3$ cps. In this way, we record the average (over the cylinder circumference) temperature in the form of an oscillogram, which was then used to calculate the average (over the circumference) heat exchange coefficient for a consecutive series of adequately small time intervals. It can be shown that in the case of a very small change in the cylinder temperature (as compared with the initial temperature gradient between the cylinder and the air stream) the average (over the surface) heat exchange determined by the above method is independent of the heat flow along the surface. In our experiments the above condition was satisfied with a fair degree of accuracy: in the initial time interval studied by us the cylinder temperature rose by only 0.5°C while the temperature gradient was 40—50°C. The corrections for heat escape to the base of the model were calculated by the method described in /11/ and for the initial moment of time they were quite small.

The experiments were carried out as follows. Air preheated to 70—80°C was fed in through a nozzle pointed in a vertical (downward) direction, and the cylinder to be studied was placed in front of the nozzle (Figure 1). A ribbon blocking the air path was placed between the cylinder and the nozzle. The experiment was started by removing the barrier, as a result of which the heated air came into contact with the cylinder and the heat exchange started. The time of removal of the barrier did not exceed 0.002 sec. The distance between the barrier and the nozzle was sufficiently large not to increase markedly the resistance of the air path. For this reason the air flow rate did not change as a result of the removal of the ribbon. The measuring circuit made it possible to record without distortion processes with a duration of 0.001 sec or more. In our experiments the air velocity ranged from 1 to 8 m/sec and the cylinders used had diameters of 8.4 and 2.6 mm. Those values corresponded to Re_f values between 400 and 3700.

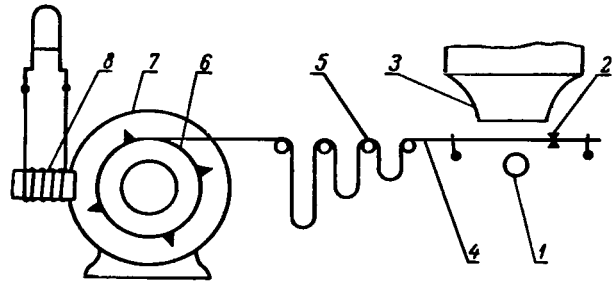

FIGURE 1. Experimental apparatus.

1 – cylinder to be studied; 2 – marker for the removal of the barrier; 3 – nozzle; 4 – ribbon serving as barrier; 5 – tube; 6 – gear wheel; 7 – electric motor; 8 – inductive revolutions recorder.

In accordance with the theories of similarity and dimensionality, and taking into account the fact that for air Pr ≈ const, the experimental data were processed by using the expressions

$$Nu/Nu_0 = f_1 (Ho, Re_f) \quad (1)$$

or

$$Nu/Nu_0 = f_2 (Ho)_{Re_f = const}. \quad (2)$$

The maximum error in the determination of Nu/Nu_0 did not exceed 13%. The maximum error in the determination of Ho depended on the duration of the process, and at Ho = 10 it was equal to 15%. The error decreased at Ho > 10 and increased at Ho < 10. The value of Re_f was determined with an error not exceeding 3%. The value of Nu_0 was taken from the results obtained in the processing of the respective oscillograms at Ho > 30—40 and in all cases did not differ by more than 10% (on the average by 5—6%) from the value of Nu obtained in the same apparatus in steady-state experiments.

The results obtained in the processing of typical oscillograms are shown in Figure 2. The figure shows that the shape of the experimental curves is in agreement with the physical concepts advanced in /9, 10/. In fact, when the ribbon is removed the air starts to move downwards from the nozzle, the cold air surrounding the cylinder forms a hydrodynamic boundary layer, and an eddy is created in the rear-end zone of the cylinder. In the starting moment a heat flow naturally did not exist (Nu = 0). Subsequently, hot air flows from the nozzle, a thermal boundary layer is formed in the front part, and the air in the rear-end zone of the cylinder is heated. A heat flow, which gradually reaches a steady value, is created in the pickup. Let us assume that the time needed for the establishment of steady-state conditions corresponds to the attainment of $Nu = 0.9\ Nu_0$. In such a case it is evident from Figure 2a that this corresponds to Ho = 10—12. This is much lower than the value reported in /7/ and is only slightly higher than Ho ≈ 5.

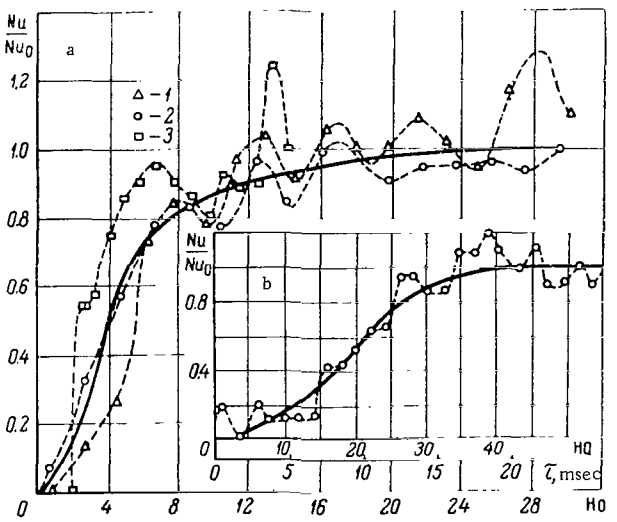

FIGURE 2. Heat exchange in the case of a sudden surge of a flow and of a temperature gradient between the flow and a cylinder with a diameter of 8.4 mm (a) or 2.6 mm (b).

a) 1—Re_f = 2900; 2—1600; 3—760; b) Re_f = 790. The continuous lines are averaged curves.

Such a higher value is satisfactorily explained by accepting that after the removal of the ribbon the velocities field in the space between the nozzle and the cylinder is rearranged from one steady-state value to another. The time required for such a rearrangement is approximately equal to the time during which the flow travels the distance from the exit of the nozzle to the rear end of the cylinder. In our experiments that distance was about 42 mm or 5d for the cylinder with a diameter of 8.4 mm; in that case the time of rearrangement of the velocities field was $\tau = 5\,d/V$, which corresponded to Ho = 5.

Thus, it may be assumed that in the above case the time of transition to steady-state heat exchange conditions is determined not only by the time expended for heating of the air in the vicinity of the cylinder but also by the time of rearrangement of the velocities field. To check the validity of the above assumption and to study the unsteady-state heat transfer at lower Re numbers we carried out similar experiments with a pickup of an analogous construction and a diameter of 2.6 mm. The distance between the pickup and the nozzle was the same as in the case of the pickup with a diameter of 8.4 mm. For this reason the value of Ho corresponding to the time of establishment of the velocities field was greater (by a factor of about 3) than the respective value for the larger cylinder. One of the curves showing the variations in the heat transfer coefficient, which was obtained in the processing of the experimental data, is shown in Figure 2b. In spite of the fact that the value of Re_f for the above curve (Re_f = 790) is practically the same as the respective value for one of the curves in Figure 2a, the transition to steady-state conditions indeed took place at substantially larger values of Ho (Ho $\approx$ 30).

Thus, the time of establishment of steady-state heat transfer during a really instantaneous change in the velocities field must be determined by Ho $<$ 10 — a value that was obtained by processing experimental data for a cylinder 8.4 mm in diameter. Hence, it may be assumed that the experiments with the cylinder 2.6 mm in diameter express mainly the rearrangement of the velocities field in front of the cylinder and are not characteristic. Thus, the processing of the other oscillograms obtained with the 2.6 mm cylinder is not reported in this paper.

The curves shown in Figure 2a indicate a peculiar feature of the heat transfer process. Fluctuations with a period approximately equal to Ho = 5 and an amplitude equal to 10—20% of the average value of Nu/Nu_0 are superposed on the monotonous change in Nu/Nu_0. At the same time, data from the literature show that the time of shedding of eddies from a cylinder in a transverse flow is also determined by Ho = 5. Hence, it may be assumed that the pulsations in the heat transfer coefficient are caused by the periodical fluctuations in the flow on the rear-end part of the cylinder, associated with the shedding of eddies. At the same time, it should be remembered that the error in the measurement of Nu/Nu_0 in the above experiments was of the order of 10%. Hence, additional experiments are required to establish the nature of the pulsations in Nu/Nu_0 and especially of their amplitude*.

* In the heat transfer studies with a pickup element 2.6 mm in diameter (Figure 2b) the sensitivity of the measuring circuit was lower than for the pickup element 8.4 mm in diameter. For this reason, the current fluctuations at the "out" end of the circuit (converted to fluctuations in the heat transfer coefficient) may be distorted by external electrical disturbances and are less specific than in Figure 2a.

SYMBOLS

$Nu = \alpha d/\lambda$ — Nusselt number; $Re = Vd/\nu$ — Reynolds number; $Ho = V\tau/d$ — the homochronicity number [Strouhal number]; $Pr = \nu/a$ — Prandtl number; d — cylinder diameter; V — air velocity; α, λ, ν, a — the heat-transfer, thermal-conductivity, kinematic-viscosity and thermal-diffusivity coefficients of air; τ — time.

Subscripts: f — calculated at a flow temperature at some distance from the body; 0 — steady-state conditions.

Bibliography

1. Loitsyanskii, L.G. Laminarnyi pogranichnyi sloi (The Laminary Boundary Layer). — Fizmatgiz. 1962.
2. Sovremennoe sostoyanie gidroaerodinamiki vyazkoi zhidkosti (Present State of the Hydroaerodynamics of Viscous Liquids). Edited by S. Gold'shtein. Vols. I, II. [Russian translation. 1948.]
3. Stuartson, K. Problems of Mechanics. [Russian translation. 1963.]
4. Targ, S.M. Osnovnye zadachi teorii laminarnykh techenii (Fundamental Problems of the Theory of Laminary Flow). — Gostekhizdat. 1951.
5. Cess, R.D. — Trans. ASME, Vol. C83, No. 3. 1961.
6. Goodman, T.R. — Trans. ASME, Vol. C84, No. 4. 1962.
7. Kudryashev, L.I. and A.A. Smirnova. — Trudy Kuibyshevskogo aviatsionnogo instituta, No. 12. 1961; No. 15. 1962; IFZh, No. 10. 1962.
8. Nicoll, K.M. — AIAA Journal, Vol. 1, No. 4. 1963.
9. Katsnel'son, B.D. and F.A. Timofeeva. Teploperedacha i gidrodinamika (Heat Transfer and Hydrodynamics), Vol. 12. — Mashgiz. 1949; Kotloturbostroenie, No. 5. 1948.
10. Kutateladze, S.S. and V.M. Borishanskii. Spravochnik po teploperedache (Handbook of Heat Transfer). — Gosenergoizdat. 1959.
11. Kozlov, L.V. — Izvestiya AN SSSR, OTN; Mekhanika i mashinostroenie, No. 6. 1961.

V. F. Sovkin and M. P. Shatunov

THERMAL RELATIONS DURING THE GRINDING OF METALS, AND A PRACTICAL METHOD FOR THEIR CALCULATION

THE CONTACT METHOD FOR THE DETERMINATION OF TEMPERATURES AND HEAT FLUXES DURING GRINDING

The temperature field during grinding has been determined /7, 8/ by solving the contact thermal problem for a natural boundary condition of the fourth kind, describing the heat distribution between all interacting bodies. The equations derived in /7, 8/ may be converted into a more convenient form for calculations.

It is found that the temperature and heat fluxes during the contact and noncontact periods are expressed by three simple parameters ϑ, ξ, η by means of a single tabulated function $K(\xi, \eta)$.

For the contact period $0 \leqslant \tau \leqslant \tau_0$ /7/ presents two analytical expressions for the temperature which are different in form but equivalent:

$$T(y, \tau) = \frac{q_0}{A}\sqrt{\tau}\frac{1}{\eta}[\operatorname{erfc}\xi - \exp(\eta^2 + 2\xi\eta_1)\operatorname{erfc}(\xi+\eta_1)] \tag{1}$$

or

$$T(y, \tau) = \frac{q_0}{A}\sqrt{\tau}\cdot 2\sum_{n=0}^{\infty}(-2\eta)^n i^{n+1}\operatorname{erfc}\xi, \tag{2}$$

where q_0 is the heat evolved in unit time from a unit contact surface area

$$A = \sqrt{(\lambda c\gamma)_\vartheta} = \sqrt{(\lambda c\gamma)_\kappa};\quad \xi = \frac{|y|}{\sqrt{4a\tau}};\quad \eta_1 = \frac{m_0 c_\vartheta + a}{A}\sqrt{\tau};$$
$$\operatorname{erfc} x = \frac{2}{\sqrt{\pi}}\int_x^\infty l^{-u^2}du;\quad i^{n+1}\operatorname{erfc} x = \int_x^\infty i^n \operatorname{erfc} u\,du. \tag{3}$$

Expression (2) is more adequate for calculations in the case of small values, for which the series converges very rapidly. By assuming in (2) that $\xi = 0$ and $\eta_1 = 0$ we obtain

$$T(0, \tau) = \frac{q_0}{A}\sqrt{\tau}\,2i\operatorname{erfc}0 = \frac{q_0}{A}\sqrt{\tau}\,\frac{2}{\sqrt{\pi}}. \tag{4}$$

We shall use the notation $\vartheta = \frac{2}{\sqrt{\pi}}\frac{q_0}{A}\sqrt{\tau}$.

At $0 \leqslant \tau \leqslant \tau_0$ the value of ϑ corresponds to the temperature of the contact area of the surface without taking into account the heat removed with the

chips and the coolant. By isolating ϑ as a factor, the temperature functions (1) and (2) assume the form

$$T(y, \tau) = \vartheta K(\xi, \eta_1) \quad (0 \leqslant \tau \leqslant \tau_0), \tag{5}$$

where

$$K(\xi, \eta_1) = \frac{1}{2}\sqrt{\frac{\pi}{\eta_1}}\left[\operatorname{erfc}\xi - \exp(\eta_1^2 + 2\xi\eta)\operatorname{erfc}(\xi + \eta_1)\right] \tag{6}$$

or

$$K(\xi, \eta_1) = \sqrt{\pi}\sum_{n=0}^{\infty}(-2\eta_1)^n i^{n+1}\operatorname{erfc}\xi. \tag{7}$$

The two last expressions are different analytical descriptions of the same function. At $\xi = 0$ and $\eta_1 = 0$ we have $K(0, 0) = 1$, but for other values of ξ and η $K(\xi, \eta) < 1$.

For the noncontact period $\tau_0 < \tau \leqslant \tau_1$ the temparature function derived in /7/ may be written

$$T(y, \tau) = [\vartheta K(\xi, \eta_1^f)]_{\tau-\tau}^{\tau} \quad (\tau_0 < \tau \leqslant \tau_1), \tag{8}$$

where $[F(x)]_{x_1}^{x_2} = F(x_2) - F(x_1)$ is a double substitution from x_1 to x_2; τ_1 is the time of one turn of the workpiece, and

$$\eta_1^f = \begin{cases} \dfrac{\alpha}{A}\sqrt{\tau} & (0 \leqslant \tau \leqslant \tau_0), \\ \dfrac{\alpha}{A_\partial}\sqrt{\tau} & (\tau_0 < \tau \leqslant \tau_1), \quad A_\partial = \sqrt{(\lambda c\gamma)_\partial}. \end{cases} \tag{9}$$

In this way, the temperatures during the two periods (5) and (8) are expressed through the three parameters ϑ, ξ and η by the same function $K(\xi, \eta)$. Let us describe the above parameters as the "basic" parameters. They have a simple physical meaning and are expressed by means of the starting data: $\vartheta = \frac{2}{\sqrt{\pi}}\frac{q_0}{A}\sqrt{\tau}$ is the temperature of the workpiece surface without accounting for cooling and chips; $\xi = \frac{|y|}{\sqrt{4a\tau}} = \frac{1}{\sqrt{4\mathrm{Fo}}}$ is a dimensionless parameter accounting for the depth (from the surface) of the observation point; $\eta = \eta^c + \eta_1^f$ is a dimensionless parameter accounting for the heat removed with the cooling fluid η^f and the chips;

$$\eta^c = \begin{cases} \dfrac{m_0 c_\partial}{A}\sqrt{\tau} & (0 \leqslant \tau \leqslant \tau_0), \\ 0 & (\tau_0 < \tau \leqslant \tau_1). \end{cases} \tag{10}$$

In equations (5) and (8) the function $K(\xi, \eta)$ serves as a correction factor for the effects of depth, cooling, and chips. The two equations have the same structure, which makes it possible to use the same program for the calculation of the temperature during both periods.

It is of importance to note that in the above equations the time τ serves at the same time as the second spatial coordinate describing the position of the observed element with respect to the contact zone. The temperature determined with its aid depends in fact on two spatial coordinates, although one of them is not present in an explicit form.

Let us determine the distribution of the contact heat between the interacting bodies, first for the contact period τ_0.

Differentiation of (2) with respect to y gives (assuming that $y = 0$)

$$\left|\frac{\partial T}{\partial y}\right|_{y=0} = \vartheta\left[\sqrt{\pi} - 2\eta K(0, \eta)\right]\frac{1}{\sqrt{4a\tau}}. \tag{11}$$

The heat transferred to the workpiece and the wheel is found on the basis of the Fourier law

$$\begin{aligned} q_\partial &= \lambda_\partial\left|\frac{\partial T_\partial}{\partial y}\right|_{y=0} = q_0\left[1 - \frac{2}{\sqrt{\pi}}K(0, \eta)\right]\frac{A_\partial}{A}; \\ q_\kappa &= \lambda_\kappa\left|\frac{\partial T_\kappa}{\partial y}\right|_{y=0} = q_0\left[1 - \frac{2}{\sqrt{\pi}}K(0, \eta_1)\right]\frac{A_\kappa}{A}, \end{aligned} \tag{12}$$

while the heat removed with the chips and the coolant is determined from the equations

$$\begin{aligned} q_c &= m_0 c_\partial T_\partial(0, \tau) = q_0\frac{2}{\sqrt{\pi}}\eta^c K(0, \eta); \\ q_f &= \alpha T_\partial(0, \tau) = q_0\frac{2}{\sqrt{\pi}}\eta^f K(0, \eta). \end{aligned} \tag{13}$$

The parameters q_∂, q_κ, q_c, and q_f represent the distribution of the contact heat through a unit contact area during unit time. In order to find the heat distribution over the whole contact time, these parameters should be integrated with respect to time $0 \leqslant \tau \leqslant \tau_0$.

Let us use the following notations: $Q_0 = \int_0^{\tau_0} q_0 d\tau = q_0\tau_0$ (the total quantity of contact heat, over the whole contact time);

$$Q_w = \int_0^{\tau_0} q_w d\tau; \quad Q_\kappa = \int_0^{\tau_0} q_\kappa d\tau; \quad Q_c = \int_0^{\tau_0} q_c d\tau; \quad Q_f = \int_0^{\tau_0} q_f d\tau.$$

Since τ_0 is very small, it may be calculated by some approximate equation, e.g., by the Simpson rule

$$\int_0^{\tau_0} f(\tau) d\tau = f(\tau_0)\tau_0.$$

As a result, we obtain the following equations:

$$\begin{aligned} \frac{Q_\partial}{Q_0} &= \frac{A_\partial}{A}\left[1 - \frac{2}{\sqrt{\pi}}K(0, \eta_0)\right]; \\ \frac{Q_\kappa}{Q_0} &= \frac{A_\kappa}{A}\left[1 - \frac{2}{\sqrt{\pi}}K(0, \eta_0)\right]; \\ \frac{Q_c}{Q_0} &= \frac{2}{\sqrt{\pi}}\eta_0^c K(0, \eta_0); \quad \frac{Q_f}{Q_0} = \frac{2}{\sqrt{\pi}}\eta_0^f K(0, \eta_0). \end{aligned} \tag{14}$$

where

$$\eta_0^c = \frac{m_0 c_\partial}{A}\sqrt{\tau_0}; \quad \eta_0^f = \frac{\alpha}{A}\sqrt{\tau_0}; \quad \eta_0 = \eta_0^c + \eta_0^f. \tag{15}$$

Equations (14) show the heat distribution between the interacting bodies over the whole contact period. Redistribution of the heat between the workpiece and the cooling fluid takes place during the noncontact period $\tau_0 < \tau < \tau_1$. A fraction of the heat from the part is removed by the coolant; this fraction is determined in the form of an integral

$$Q_f^{(1)} = \int_{\tau_0}^{\tau_1} \alpha T_\partial(0, \tau) d\tau.$$

Since τ_0 is very small, a differential may be substituted for (8):

$$Q_f^{(1)} = \int_{\tau_0}^{\tau_1} \alpha [\vartheta K(0, \eta_l^f)] \tau_0 d\tau = \alpha \tau_0 [\vartheta K(0, \eta^f)]_{\tau_0}^{\tau_1}.$$

From here we obtain

$$\frac{Q_f^{(1)}}{Q} = \frac{2}{\sqrt{\pi}} [\eta^f K(0, \eta^f)]_{\tau_0}^{\tau_1}. \quad (16)$$

This is the fraction of contact heat passing from the workpiece to the cooling fluid over the time $\tau_0 < \tau < \tau_1$. Subtraction of (16) from the first equation (14) yields the residual heat in the part after one full turn:

$$\left[\frac{Q_w}{Q_0}\right]_{res} = \frac{A_\partial}{A}\left[1 - \frac{2}{\sqrt{\pi}} \eta_{l0} K(0, \eta_{l0})\right] - \frac{2}{\sqrt{\pi}} [\eta^f K(0, \eta_l^f)]_{\tau_0}^{\tau_1},$$
$$\left[\frac{Q_\partial}{Q_0}\right]_{res} = \frac{A_\partial}{A}\left[1 - \frac{2}{\sqrt{\pi}} \eta_{l0} K(0, \eta_{l0})\right] - \frac{2}{\sqrt{\pi}} [\eta^f K(0, \eta^f)]_{\tau_0}^{\tau_1}, \quad (17)$$

The derived thermal relations (14) and (17) have been expressed through the "basic" parameters with the aid of the function $K(\xi, \eta)$ at $\xi = 0$.

To simplify the practical calculations the function $K(\xi, \eta)$ has been tabulated for the ranges $0 \leqslant \xi \leqslant 2$, $0 \leqslant \eta_l \leqslant 2$ with increment of 0.01 for both variables. Part of the table is presented in Appendix II. It may be used to determine the temperature and the heat fluxes on the surface of the workpiece.

The basic parameters ϑ, ξ, and η may be determined for various grinding conditions by means of nomographs with adjusted linear scales. Samples of such nomographs are shown in Appendix I. The values of the starting data that were taken as constant are as follows:

1) thermal-physical parameters /4/: $\lambda_\partial = 0.6 \frac{\text{kcal}}{\text{m·min·deg}}$; $\lambda_\kappa = 0.016 \frac{\text{kcal}}{\text{m·min·deg}}$; $c_\partial = 0.14 \frac{\text{kcal}}{\text{kg·deg}}$; $c_\kappa = 0.294 \frac{\text{kcal}}{\text{kg·deg}}$; $\gamma_\partial = 7800 \frac{\text{kg}}{\text{m}^3}$; $\gamma_\kappa = 2025 \frac{\text{kg}}{\text{m}^3}$; $\alpha = 0$; 200; and $500 \frac{\text{kcal}}{\text{m}^2\text{·min·deg}}$.

2) dimensions: wheel diameter $D = 0.5$ m; workpiece diameter $d = 0.1$ m; wheel width $B = 0.04$ m; workpiece length $L = 0.05$ m; run-out of the wheel with respect to the workpiece (at the ends) $b = 0.06$ m.

3) velocities: $v_\kappa = 1800$ m/min; $v_\partial = 50$ m/min; $S = 30$ mm/turn, $t = 0.05$ mm

The term q_0 in parameter ϑ_0 has a value $q_0 = \frac{P_z v_\kappa}{427Bl}$, where P_z is the tangential component of the cutting force, determined by means of the empirical equation of Maslov /3/; $P_z = 2.1 \cdot t^{0.8} S^{0.7} v_\partial^{0.7}$; l is the length of the contact arc as calculated by the equation $l = \sqrt{\frac{D\alpha}{D+\alpha}}$; t is the cross feed; v_∂ is the rotation speed of the part. The term $m_0 = \frac{\gamma_\partial S \cdot t \cdot v_\partial}{2\left(1 + \frac{b}{L}\right) Bl}$ in the expression for the parameter η_0^c represents the weight of the chips removed from unit area during unit time. For the parameter $\xi = \frac{|y|}{\sqrt{4a_\partial \tau_0}}$ we assumed that $|y_0| = 0.1$ mm and $a_\partial = \frac{\lambda_\partial}{(c\gamma)_\partial}$.

TABLE 1

Dependence of the temperature on the time and the depth

$$T(y,\tau)=\begin{cases}\vartheta K(\xi,\eta) & (0\leqslant\tau\leqslant\tau_0),\\ [\vartheta K(\xi,\eta)]\Big|_{\tau-\tau_0}^{\tau} & (\tau_0<\tau\leqslant\tau_1)\end{cases}$$

τ, min	$K(\xi,\tau_i)$						$\vartheta K(\xi,\tau_i)$						$T(y,\tau)$, °C					
	$y=0$	$y=0.1$	$y=0.2$	$y=0.3$	$y=0.5$	$y=1$	$y=0$	$y=0.1$	$y=0.2$	$y=0.3$	$y=0.5$	$y=1$	$y=0$	$y=0.1$	$y=0.2$	$y=0.3$	$y=0.5$	$y=1$
	mm						mm						mm					
$0.25\ \tau_0$	0.956	0.232	0.030	0.002	0.000	0.000	352	85	11	0	0	0	352	85	11	0	0	0
$0.5\ \tau_0$	0.949	0.365	0.104	0.020	0.000	0.000	490	188	54	10	0	0	490	188	54	10	0	0
$1.0\ \tau_0$	0.925	0.490	0.224	0.088	0.008	0.000	675	558	164	64	6	0	675	358	164	64	6	0
$2.0\ \tau_0$	0.941	0.613	0.373	0.210	0.053	0.000	971	633	385	217	55	0	296	275	221	153	49	0
$3.0\ \tau_0$	0.925	0.653	0.439	0.281	0.100	0.003	1169	825	555	355	126	4	198	192	170	138	71	4
$4.0\ \tau_0$	0.917	0.685	0.497	0.347	0.153	0.010	1339	1000	726	507	223	15	170	175	171	152	97	11
$5.0\ \tau_0$	0.909	0.694	0.517	0.370	0.174	0.014	1483	1133	837	604	284	23	144	133	111	97	61	8
$6.0\ \tau_0$	0.902	0.714	0.555	0.421	0.226	0.031	1613	1277	992	753	404	55	130	144	155	149	120	32
$7.0\ \tau_0$	0.895	0.722	0.574	0.448	0.254	0.042	1729	1395	1109	866	491	81	116	118	117	113	87	26
$8.0\ \tau_0$	0.888	0.717	0.570	0.445	0.253	0.042	1833	1480	1176	918	522	87	104	85	67	52	31	6
$9.0\ \tau_0$	0.881	0.724	0.588	0.468	0.284	0.061	1929	1586	1288	1025	622	134	96	106	112	107	100	47
$10\tau_0$	0.873	0.732	0.605	0.494	0.316	0.082	2015	1689	1396	1140	729	189	86	103	108	115	107	55
$11\tau_0$	0.866	0.726	0.601	0.491	0.315	0.082	2097	1758	1455	1189	763	199	82	69	59	49	34	10
$12\tau_0$	0.866	0.726	0.601	0.491	0.315	0.082	2190	1836	1520	1242	797	207	93	78	65	53	34	8
$\tau_1-\tau_0$	0.630	0.602	0.572	0.554	0.508	0.371	5744	5489	5215	5051	4632	3383						
$\tau_1=157\tau_0$	0.630	0.602	0.572	0.554	0.508	0.371	5763	5506	5232	5067	4647	3394	19	17	17	16	16	11

TABLE 2

Effect of the velocity v_∂ and the method of cooling on the contact temperature:

$T_0 = \vartheta_0 K(0, \tau_{l0})$

v_∂, m/min	$\vartheta_0 = \frac{2}{\sqrt{\pi}} \frac{q_0 \sqrt{\tau_0}}{\lambda}$	$\eta_{l0} = \frac{cm_0 + \alpha}{\lambda} \sqrt{\tau_0}$			$K(0, \eta_{l0})$			T_0, °C		
		$\alpha=0$	$\alpha=200$	$\alpha=500$	$\alpha=0$	$\alpha=200$	$\alpha=500$	$\alpha=0$	$\alpha=200$	$\alpha=500$
20	610	0.03	0.09	0.20	0.973	0.925	0.845	594	564	515
40	700	0.04	0.09	0.17	0.965	0.925	0.866	675	647	606
60	756	0.05	0.09	0.15	0.957	0.925	0.881	723	700	666
80	790	0.06	0.09	0.15	0.949	0.925	0.881	750	730	696
100	830	0.07	0.10	0.15	0.941	0.917	0.881	781	760	731
200	955	0.10	0.12	0.15	0 917	0.902	0 881	876	860	840
300	1040	0.12	0.14	0.16	0.902	0.888	0 873	938	923	908

TABLE 3

Heat distribution in the contact period as a function of the cross feed and the method of cooling

l, mm	$\eta_0^c = \frac{cm_0}{\lambda} \sqrt{\tau_0}$	$\eta_0 f = \frac{\alpha}{\lambda} \sqrt{\tau_0}$			$\frac{Q_f}{Q_0} = \frac{2}{\sqrt{\pi}} \times \eta_0 f K(0, \eta_0)$			$\frac{Q_c}{Q_0} = \frac{2}{\sqrt{\pi}} \times \eta_0^c K(0, \eta_0)$			$\frac{Q_K}{Q_0} = \frac{A}{\lambda} K [1 - \frac{2}{\sqrt{\pi}} \tau_0 K(0, \eta_0)]$			$\frac{Q_\partial}{Q_0} \frac{A_\partial}{\lambda} [1 - \frac{2}{\sqrt{\pi}} \tau_0 K(0, \eta_0)]$		
		$\alpha=0$	$\alpha=200$	$\alpha=500$	$\alpha=0$	$\alpha=200$	$\alpha=500$	$\alpha=0$	$\alpha=200$	$\alpha=500$	$\alpha=0$	$\alpha=200$	$\alpha=500$	$\alpha=0$	$\alpha=200$	$\alpha=500$
0.01	0.02	0	0.03	0.07	0	0 03	0.07	0 02	0 02	0 03	0.13	0.12	0.12	0.85	0 83	0.78
0.02	0.03	0	0.04	0.09	0	0.04	0.09	0.03	0.03	0 03	0.13	0.12	0.12	0.84	0.81	0.76
0.04	0.04	0	0.04	0.10	0	0.04	0.10	0.04	0.04	0.04	0.13	0 12	0 11	0.83	0.80	0.75
0.06	0.06	0	0.05	0.11	0	0 05	0.11	0.06	0.06	0.06	0.12	0.12	0.11	0 82	0.77	0.72
0.08	0.07	0	0.05	0.12	0	0.05	0.11	0.07	0.07	0.07	0.12	0.12	0.11	0.81	0.76	0.71
0 10	0.08	0	0 05	0.13	0	0.05	0.12	0.08	0 08	0.08	0.12	0 11	0.10	0.80	0.75	0.70
0.20	0.14	0	0.06	0.15	0	0 06	0.13	0.14	0.13	0.12	0.11	0.11	0.10	0.75	0.70	0 65
0 30	0.20	0	0.07	0.17	0	0.06	0.14	0.19	0_18	0,17	0,11	0.10	0.10	0.70	0.66	0.60

In order to determine the values of ϑ, ξ and η for other time intervals $\tau \neq \tau_0 = \frac{l}{v_\partial}$ it is necessary to multiply the values obtained from the nomographs by some correction factors depending only on the $\frac{\tau}{\tau_0}$ ratio. The same must be done for the determination of ξ at $y \neq y_0$, etc.

These tables and nomographs make it possible to reduce the calculation of the temperature and heat fluxes to a small number of arithmetic operations.

The calculations are shown schematically in tables of the temperature and the thermal relationships which were derived above (Tables 1 — 4, Figures 1 — 3). The values of the starting parameters remain constant in any of these tables. For those data, the values of the basic parameters are as follows:

$$\vartheta_0 = 730^\circ\,\text{C}, \quad \xi_0 = 0.33, \quad \eta_0^c = 0.05, \quad \eta_0^f = 0{,}04.$$

TABLE 4

Calculation of the residual heat in the workpiece after one turn:

$$\frac{Q_\partial}{Q_0} = \frac{A_\partial}{A}\left[1 - \frac{2}{\sqrt{\pi}}\eta_{i0} K(0, \tau_{i0})\right] - \frac{2}{\sqrt{\pi}}\left[\eta_{i1} f K(0, \eta_{i1} f)\right]\Big|_{\tau_0}^{t_1}$$

t, mm	$\eta_0 f = \frac{\alpha}{A_\partial}\sqrt{\tau_0}$			$\eta_1 f = \frac{\alpha}{A_\partial}\sqrt{\tau_1}$			$\frac{2}{\sqrt{\pi}}\eta_{i0} f \times K(0, \eta_{i0} f)$			$\frac{2}{\sqrt{\pi}}\eta_{i1} f \times K(0, \eta_{i1} f)$			$\frac{Q_\partial}{Q_0}$, %		
	$\alpha=0$	$\alpha=200$	$\alpha=500$	$\alpha=0$	$\alpha=200$	$\alpha=500$	$\alpha=0$	$\alpha=200$	$\alpha=500$	$\alpha=0$	$\alpha=200$	$\alpha=500$	$\alpha=0$	$\alpha=200$	$\alpha=500$
0.01	0	0.03	0.08	0	0.64	1.60	0	0.03	0.08	0	0.45	0.69	85	41	17
0.02	0	0.04	0.10	0	0.64	1.60	0	0.04	0.10	0	0.45	0.69	84	40	17
0.04	0	0.05	0.11	0	0.64	1.60	0	0.05	0.11	0	0.45	0.69	83	40	17
0.06	0	0.06	0.12	0	0.64	1.60	0	0.06	0.12	0	0.45	0.69	82	38	16
0.08	0	0.06	0.13	0	0.64	1.60	0	0.06	0.13	0	0.45	0.69	81	37	15
0.10	0	0.06	0.14	0	0.64	1.60	0	0.06	0.14	0	0.45	0.69	80	36	15
0.20	0	0.07	0.17	0	0.64	1.60	0	0.07	0.17	0	0.45	0.69	75	32	13
0.30	0	0.08	0.20	0	0.64	1.60	0	0.08	0.19	0	0.45	0.69	70	29	10

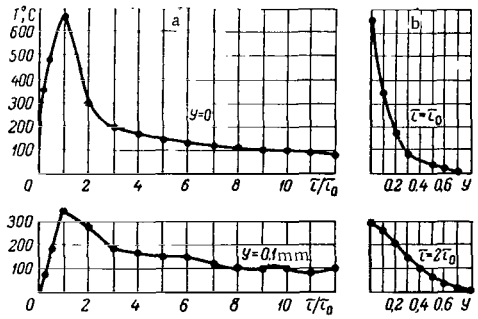

FIGURE 1. Dependence of the temperature T on the time τ and the depth y

a – at constant α; b – at constant speed.

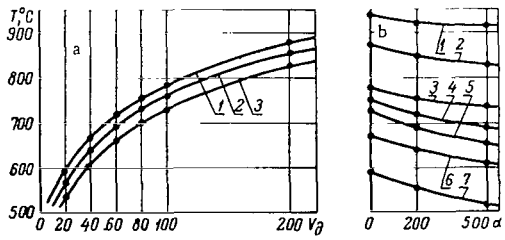

FIGURE 2. Dependence of the contact temperature T on the rotation speed of the workpiece and the cooling method.

a – at constant α (1 : α = 0, 2 : α = 200, 3 : α = 500);
b – at constant speed (1 : v_∂ = 300, 2 : v_∂ = 200, 3 : v_∂ = 100, 4 : v_∂ = 80, 5 : v_∂ = 60, 6 : v_∂ = 40, 7 : v_∂ = 20).

The nature of the temperature field during grinding, its properties, and some conclusions have been reported in /7, 8/. To this we shall add only our conclusions concerning the effect of cooling on the heat distribution. In the contact period, according to Table 3 the fraction of heat removed with the cooling fluid is relatively small. For instance, for $t = 0.04$ mm it is only 4% in regular cooling ($\alpha = 200$) and 10% in jet cooling ($\alpha = 500$).

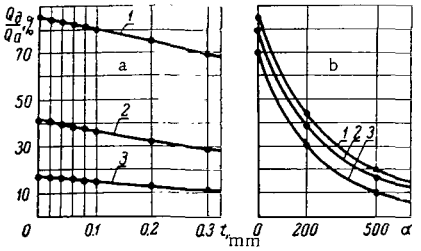

FIGURE 3. Dependence of the residual heat in the part (for one turn) on the cross feed and the cooling method.

a – at constant α (1 : $\alpha = 0$, 2 : $\alpha = 200$, 3 : $\alpha = 500$); b : at constant feed (1 : t = 0.01 mm, 2 : t = 0.1, 3 : t = 0.3).

Most of the evolved heat (about 80%) accumulates immediately in the workpiece, and is gradually transferred to the cooling fluid during the noncontact period. The fraction of heat remaining in the workpiece at the end of the turn depends to a great extent on the cooling method. For instance, for $t = 0.04$ mm it is 83% in dry grinding, 40% in regular cooling, and only 17% in jet cooling.

HEATING OF WORKPIECES DURING MULTIPASS GRINDING WITH AN IRREGULAR RIBBON SOURCE

Let us examine a rapidly moving ribbon source which is one of the main thermal models in fast cutting and grinding. The temperature field of such a source is expressed by the same function $K(\xi, \eta)$ and in the same form as (5), but the parameters ϑ and η differ from those in (5). In addition, the function $K(\xi, \eta)$ has been used to derive equations for the temperature of an arbitrary nonhomogeneous ribbon source, as well as for multipass working.

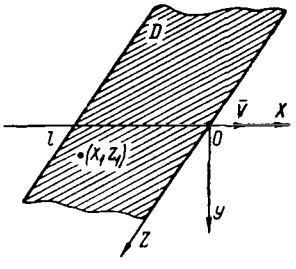

FIGURE 4. Schematic presentation of a moving heat source.

Let us assume that a heat source occupying the region D and evolving an amount of heat equal to $q(x_1, z_1)$ into the half-space $y = 0$ moves with a velocity $\bar{v}\{v, 0, 0\}$ over a plane $y = 0$ (Figure 4).

The plane $y = 0$ is cooled at the same time, i.e., part of the heat is transferred to the

surroundings and the starting temperature of the half-space $y = 0$ are assumed to be zero. Under those conditions, the temperature of the half-space $y = 0$ reached by the effect of the source is determined in the form of an integral

$$T(x, y, z, \tau) = \iint_D \frac{q(x_1, z_1)}{c\gamma} dx_1 dz_1 \times \\ \times \int_0^{\tau} G(x - x_1 + v\tau_1; y; z - z_1; \tau_1) d\tau_1, \tag{18}$$

where x_1, 0 and z_1 are the coordinates of the point source with respect to a system with a moving origin of coordinates; x, y and z are the coordinates of the observation point with respect to the same system; $G(x, y, z, \tau)$ is the temperature influence function of an instantaneous point source with an output $\vartheta = c\gamma$ for the half-space $y \geqslant 0$ in the case of a boundary condition of the third kind

$$\left[-\lambda \frac{\partial G}{\partial y} + \alpha G \right]_{y=0} = 0. \tag{19}$$

It characterizes the conditions of heat transfer from the surface $y = 0$. The three-dimensional influence function may be presented as a product:

$$G(x, y, z, \tau) = G_1(x, \tau) G_2(y, \tau) G_3(z, \tau), \tag{20}$$

where $G_1(x, \tau)$ and $G_3(z, \tau)$ are one-dimensional influence functions for infinite straight lines $(-\infty < x < \infty)$, $(-\infty < z < \infty)$ while $G_2(y, \tau)$ is a one-dimensional influence function for the half-line $[0 \leqslant y < \infty]$ at the boundary condition (19). We shall assume that the region D occupied by the source is an infinite ribbon $(l \leqslant x_1 \leqslant 0, -\infty < z_1 < \infty)$ and that the output of the source is independent of the coordinate z, i.e., that $q(x_1, z_1) = q(x_1)$. By substituting (20) in (18) and integrating with respect to z_1 (taking into account the fact that $\int_{-\infty}^{\infty} G_3(z - z_1; \tau_1) dz_1 = 1$), we obtain

$$T(x, y, \tau) = \int_l^0 \frac{q(x_1)}{c\gamma} dx_1 \int_0^{\tau} G_1(x - x_1 + v\tau_1) G_2(y; \tau_1) d\tau_1. \tag{21}$$

The subsequent operations are as in /2/. Assuming that the velocity is large, we find an approximate value for the integral with respect to time

$$\int_0^{\tau} G_1(x - x_1 + v\tau_1; \tau_1) G_2(y, \tau) d\tau_1 = \\ = \begin{cases} \dfrac{1}{v} G_2\left(y; \dfrac{x_1 - x}{v}\right), & \text{if} \quad x < x_1 \\ 0, & \text{if} \quad x > x_1 \end{cases} \tag{22}$$

Then (21) is written in the form

$$T(x, y, \tau) = \int_x^0 \frac{q(x_1)}{c\gamma v} G_2\left(y; \frac{x_1 - x}{v}\right) dx_1, \quad \text{if} \quad l \leqslant x \leqslant 0,$$

and

$$T(x,\ y,\ \tau) = \int_{l}^{0} \frac{q(x_1)}{c\gamma v} G_2\left(y;\ \frac{x_1 - x}{v}\right) dx_1, \quad \text{if} \quad x < l. \tag{23}$$

Here the first integral represents the temperature at the point (x, y, z) beneath the source, and the second integral represents the temperature behind the source. The temperature in front of the source ($x > 0$) is zero.

Let us examine first a case in which the output of the source is uniformly distributed over the coordinate x_1, i.e., $q(x_1) = q = \text{const}$ over the section $[l \leqslant x_1 \leqslant 0]$.

Let us denote: $\tau_0 = \frac{|l|}{v}$ — the time of passage of the ribbon source through a fixed point (the contact period), $\tau = \frac{|x|}{v}$ — the time from the moment of passage of the front end of the source $x_1 = 0$ over the point (x, y, z) to the moment of observation. Replacement of the variable in integrals (23) $\tau = \frac{x_1 - x}{v}$ yields

$$T(x,\ y,\ \tau) = \frac{q}{c\gamma} \int_{0}^{\tau} G_2(y,\ \tau_1)\, d\tau_1, \quad \text{if} \quad 0 \leqslant \tau \leqslant \tau_0 \tag{24}$$

and

$$T(x,\ y,\ \tau) = \frac{q}{c\gamma} \int_{\tau - \tau_0}^{\tau} G_2(y,\ \tau_1)\, d\tau_1, \quad \text{if} \quad \tau > \tau_0. \tag{25}$$

The above integrals may be calculated with the aid of the Laplace transform. The representation of the function $\frac{q}{c\gamma} G_2(y,\ \tau_1)$ is known /1/; it equals $\frac{q}{A_\partial} \frac{\exp\left(-\sqrt{\frac{p}{a}}\, y\right)}{\sqrt{p} + \frac{\alpha}{A_\partial}}$.

Hence, the representation of integral (24) would be

$$\frac{q}{A_\partial} \frac{\exp\left(-\sqrt{\frac{p}{a}}\, y\right)}{p\left(\sqrt{p} + \frac{\alpha}{A_\partial}\right)}.$$

According to the tables /1/, the integral (24) has the value

$$T(x,\ y,\ \tau) = \frac{q}{A_\partial} \sqrt{\tau}\, \frac{1}{\eta_1} \left[\operatorname{erfc} \xi - \exp(\eta_1^2 + 2\xi\eta_1) \operatorname{erfc}(\xi + \eta_1)\right] \quad (0 \leqslant \tau \leqslant \tau_0), \tag{26}$$

where

$$\xi = \frac{y}{\sqrt{4a\tau}} = \frac{1}{\sqrt{4\text{Fo}}}, \quad \eta_1 = \frac{\alpha}{A_\partial} \sqrt{\tau} = \text{Ti} \tag{27}$$

are dimensionless parameters, while Fo and Ti are the Fourier and Tikhonov numbers /1/.

By isolating in (26) the factor $\vartheta = \frac{2}{\sqrt{\pi}} \frac{q}{A_\partial} \sqrt{\tau}$, (28)

the integrals (24) and (25) can be presented in the following form:

$$T(x, y, \tau) = \vartheta K(\xi, \eta) \quad (0 \leqslant \tau \leqslant \tau_0),$$
$$T(x, y, \tau) = [\vartheta K(\xi, \eta_i)]_{\tau-\tau_0}^{\tau} \quad (\tau > \tau_0), \tag{29}$$

where $K(\xi, \eta)$ is the same function as that derived above (6).

Thus, the temperature of a rapidly moving ribbon source is expressed by the same function and in the same form as the temperature during grinding as obtained by the contact method.

However, a substantial difference also exists between them. In (5) the parameter ϑ comprises all the contact heat q_0 evolved in the contact zone, while in (29) ϑ comprises only the fraction of contact heat q that is transmitted to the workpiece and the cooling fluid. In fact, the value of q is not known in advance. This is the disadvantage of the heat source model. By itself alone, it does not describe the heat distribution between all interacting bodies.

However, since we established the common structure of the temperature fields obtained by various methods, it would be possible to determine the value of q by a comparison of equations (5) and (29). In this way, the temperature field during fast working of metals may be determined by a combination of the rapidly moving ribbon source model and the contact method. Such a combined system is very flexible and may be adapted to a wider range of problems than is possible with each of the above methods.

If the function $\vartheta K(\xi, \eta)$ is assumed to be zero for negative times, equations (29) may be combined into a single equation

$$T(x, y, \tau) = [\vartheta K(\xi, \eta_i)]_{\tau-\tau_0}^{\tau}, \tag{30}$$

where $\tau = 0$ and $\tau = \tau_0$ are the moments of passage of the front and rear ends of the ribbon source over the observation point.

Let us examine (Figure 5) a nonhomogeneous ribbon source whose output $q(x_1)$ is an arbitrary continuous function in the band $[l \leqslant x_1 \leqslant 0]$. Let us divide this band into n sufficiently narrow fractional bands $[l_{i+1}, l_i]$ $(i = 1, 2, \ldots, n)$ such that for each of them the function $q(x_1)$ may be regarded as constant: $q(x_1) = q_i$ in the band $[l_{i+1} \leqslant x_1 \leqslant l_i]$.

This means that each fractional band is regarded as an uniform source.

The temperature of such a source is determined from equation (30)

$$\mathrm{Ti}(x, y, \tau) = [\vartheta_i K(\xi, \eta_{li})]_{\tau-t_{i+1}}^{\tau-t_i}, \tag{31}$$

where $t_i = \frac{|l_i|}{v}$ and $t_{i+1} = \frac{|l_{i+1}|}{v}$ are the moments of passage of the front and rear ends of the fractional band $[l_{i+1}, l_i]$ over the observation point (x, y, z).

$$\vartheta_i = \frac{2}{\sqrt{\pi}} \frac{q}{A} \sqrt{\tau},$$
$$\eta_{li} = \begin{cases} \frac{m_i c_\partial + \alpha}{A} \sqrt{\tau} & (0 \leqslant \tau \leqslant t_{i+1} - t_i), \\ \frac{\alpha}{A_\partial} \sqrt{\tau} & (\tau > t_{i+1} - t_i), \end{cases} \tag{32}$$

where m_i is the mass of the chips removed during the passage of the i-th fractional band over unit surface in unit time.

Summation of the temperatures of the fractional sources yields the temperature of the entire ribbon source in the form

$$T(x,\ y,\ \tau)=\sum_{i=1}^{n}[\vartheta_i K(\xi,\eta_i)]_{\tau-t_{i+1}}^{\tau-t_i}. \tag{33}$$

In the above sum the only terms differing from zero are those for which $t_i<\tau$, i.e., those corresponding to the fractional bands $[l_{i+1},\ l_i]$ that have passed already or are just passing over the observation point. Hence, equation (33) may be written as follows:

$$T(x,\ y,\ \tau)=\sum_{t_i<\tau}[\vartheta_i K(\xi,\ \eta_i)]_{\tau-t_{i+1}}^{\tau-t_i}, \tag{34}$$

where the summation is expanded to all $t_i<\tau$.

Equation (34) makes it possible to determine the temperature of a ribbon source when the function $q(x_1)$ is presented in any form: analytical, graphical, or tabulated. This is of especially great importance since the law of distribution of the source output $q(x_1)$ over the contact length is determined experimentally and often no analytical expression is available for it.

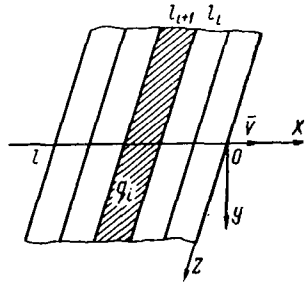

FIGURE 5. Substitution of a system of n sources of constant output for the nonhomogeneous source.

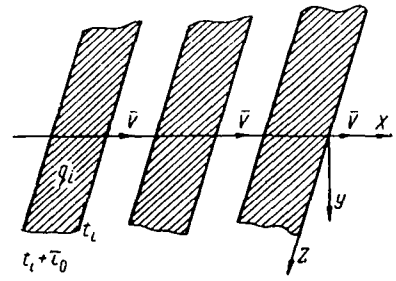

FIGURE 6. Schematic presentation of the travel of a heat source during multipass grinding.

A similar scheme may be used for temperature determination in multipass grinding, when the observed point $(x,\ y,\ z)$ passes several times over the contact surface. This is equivalent to its passage over several ribbon sources following each other at definite time intervals equal to the time of one turn of the workpiece (Figure 6).

For the sake of simplicity we shall regard such sources as uniform, i.e., their output q_i is constant. They may differ from one another. Summation of the temperatures of all the sources that have passed or are passing beneath the points of operation yields the temperature after several passages in the form

$$T(x,\ y,\ \tau)=\sum_{t_i<\tau}[\vartheta_i K(\xi,\eta_i)]_{\tau-t_i-\tau_0}^{\tau-t_i}, \tag{35}$$

where t_i and $t_i+\tau_0$ are the moments of passage of the front and the rear ends of the source q_i over the observation point; $\tau_0=\frac{|l|}{v}$ is the contact time. The

number of terms in sum (35) is determined by the number of passages (turns) up to the moment of observation.

Let us assume that all the passages took place under identical conditions. In that case the parameters ϑ_i and η_i would be the same for all passages: $\vartheta_i = \vartheta$, $\eta_i = \eta$.

The time of one passage (turn) would be denoted as $\tau_1 = t_{i+1} - t_i$, and we should assume that it is constant for all passages. In that case $t_i = (i-1)\tau_1$, $i = 1, 2\ldots$

Of greatest importance is the temperature at the end of the n-th contact period, i.e., at the moment $\tau = t_n + \tau_0$, as well as the residual temperature at the end of the n-th turn, i.e., at the moment $\tau = t_{n+1}$. Let us use for them the following notation:

$$T_n(x, y) = T(x, y, t_n + \tau_0) = \sum_{i=1}^{n} [\vartheta K(\xi, \eta)]_{(n-i)\tau_1}^{(n-i)\tau_1+\tau_0},$$
$$T_n(x, y) = T(x, y, t_{n+1}) = \sum_{i=1}^{n} [\vartheta K(\xi, \eta_i)]_{(n-i+1)\tau_1-\tau_0}^{(n-i+1)\tau_1}. \quad (36)$$

It is evident that the above sums satisfy the following recursion equations for n:

$$T_n(x, y) = T_{n-1}(x, y) + [\vartheta K(\xi, \eta_i)]_{t_n}^{t_n+\tau_0},$$
$$T'_n(x, y) = T'_{n-1}(x, y) + [\vartheta K(\xi, \eta)]_{t_{n+1}-\tau_0}^{t_{n+1}}, \text{ where } t_n = (n-1)\tau_1. \quad (37)$$

By taking the values $n = 1, 2\ldots$ we can find in a sequence the contact and residual values of the temperature for any number of turns. It is characteristic that in all cases discussed the temperature has been expressed by the three basic parameters ϑ, ξ and η with the aid of the same function $K(\xi, \eta)$.

TABLE 5

Dependence of the surface temperature on the number of passages

n	$T_n(x, y)$, °C		$T'_n(x, y)$	
	$\alpha = 0$	$\alpha = 200$	$\alpha = 0$	$\alpha = 200$
1	699	675	29	18
2	728	693	50	29
3	748	704	66	37
4	765	712	81	44
5	779	718	94	49
6	792	723	106	54
7	804	728	117	58
8	815	732	127	61
9	826	735	137	64
10	835	738	146	67
11	844	741	155	70
12	853	744	164	73
13	861	746	172	75

Table 5 shows the dependence of the temperatures $T_n(x, y)$ and $T'_n(x, y)$ of the surface $y = 0$ on the number of turns during external cylindrical grinding in the absence of cooling ($\alpha = 0$) and with regular cooling ($\alpha = 200$ kcal/m^2·min·deg). The thermal-physical parameters and the dimensions are the

same as in section one. The table shows that each passage causes a certain increment ΔT_n of the contact and residual temperature of the workpiece surface. This increment becomes smaller as the number of the passage is increased. For instance, in grinding with cooling the ΔT_n is 11°C at $n = 2$ and 3°C at $n = 10$. The value of ΔT_n is markedly affected by the cooling method. Thus, at $n = 10$ and in the case of cooling its value is three times the increment obtained in the absence of cooling.

Thus, cooling reduces considerably the rate of heating during the multipass grinding of workpieces. The determination of the temperature in multipass grinding of metals has been the subject of papers /4 and 9/. Equations (35) and (37) are more convenient for practical calculations.

THE STEADY TEMPERATURE DURING MULTIPASS GRINDING

In studies of the thermal phenomena accompanying the grinding process, we distinguish the following different temperatures: (1) local temperature, within the range of action of a single abrasive grain /5/; (2) contact temperature, averaged over the contact spot of the grinding wheel and the workpiece /6, 7/; and (3) the steady temperature during prolonged grinding.

The moving ribbon source model is the most common thermal model in grinding. The steady temperature in workpieces with flat or cylindrical surfaces is determined on the basis of the above model.

Let us consider a plate-shaped workpiece $0 \leqslant y \leqslant R_1$ (Figure 7). Ribbon sources with a width l_0 move on the workpiece surface $y = 0$ with a velocity $\bar{v}\{v, 0, 0\}$ and transfer an amount of heat $q_w \frac{\text{kcal}}{\text{m}^2 \cdot \text{min}}$ to the workpiece; the distance between two ribbons is l_1, equal to the length of one passage. The surfaces $y = 0$ and $y = R_1$ are cooled at the same time, and it is assumed that the heat transfer coefficients are α and α_1 respectively.

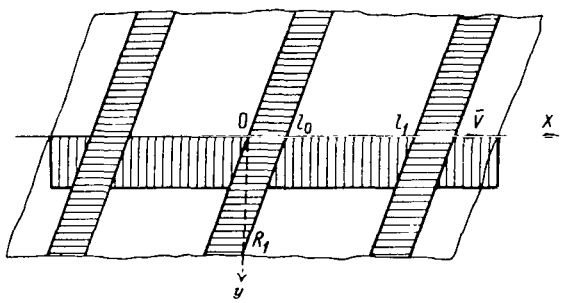

FIGURE 7. Scheme of the travel of a heat source during multipass flat grinding

The scheme of Figure 7 may serve as the thermal model in multipass flat grinding with cooling.

If the system of coordinates x, y, z, moved together with the source at a speed $\bar{v}\{v, 0, 0\}$ the thermal conductivity equation would assume the form /2/

$$\frac{1}{a}\left(\frac{\partial T}{\partial \tau} - v\frac{\partial T}{\partial x}\right) = \nabla^2 T, \qquad (38)$$

where $\nabla^2 T$ is the Laplacian operator.

The steady temperature of the system discussed here is described by the equations

$$\frac{\partial^2 T}{\partial x^2} + \frac{\partial^2 T}{\partial y^2} + \frac{v}{a}\frac{\partial T}{\partial x} = 0,$$
$$\left[-\lambda\frac{\partial T}{\partial y} + \alpha T\right]_{y=0} = Q(x), \tag{39}$$
$$\left[\lambda\frac{\partial T}{\partial y} + \alpha_1 T\right]_{y=R_1} = 0.$$

In this case the function $Q(x)$ over the section $[0 \leqslant x \leqslant l_1]$ is determined by the equations

$$Q(x) = \begin{cases} q_w [0 \leqslant x \leqslant l_0] \\ 0 \ [l_0 < x \leqslant l_1] \end{cases} \tag{40}$$

and continues over the whole numerical range $(-\infty < x < \infty)$ according to a periodic function, the period being l_1.

The steady temperature $T(x, y)$ should also be a periodic function of x with a period l_1. Hence, it may be presented as a Fourier series

$$T(x, y) = \sum_{n=-\infty}^{\infty} T_n(y)\, l^{i\,2n\pi\frac{x}{l_1}}. \tag{41}$$

where

$$T_n(y) = \frac{1}{l_1}\int_0^{l_1} T(x, y)\, l^{-i\,2n\pi\frac{x}{l_1}}\, dx \quad (n = 0;\ \pm 1;\ \pm 2\ldots). \tag{42}$$

The following equations are derived from (39) for the Fourier coefficients $T_n(y)$:

$$T_n''(y) - S_n^2 T_n(y) = 0,$$
$$-\lambda T_n'(0) + \alpha T_n(0) = Q_n, \tag{43}$$
$$\lambda T_n'(R_1) + \alpha T_n(R_1) = 0,$$

where

$$S_n^2 = \left(\frac{2n\pi}{l_1}\right)^2 - i\,\frac{2n\pi}{l_1}\,\frac{v}{a};$$
$$Q_n = \frac{1}{l_1}\int_0^{l_1} Q(x)\, l^{-i\,2n\pi\frac{x}{l_1}}\, dx. \tag{44}$$

The solution of the differential equation (44) is in the form

$$T_n(y) = A_n l^{S_n y} + B_n l^{-S_n y}, \tag{45}$$

where the constants A_n and B_n are determined from the boundary conditions.

By substitution of $T_n(y)$ in (41) we obtain an expression for the steady temperature in the form of a series. Of the greatest practical interest is the steady temperature averaged over the length of a passage, i.e., the value of

$$\overline{T}(y) = \frac{1}{l_1}\int_0^{l_1} T(x, y)\, dy. \tag{46}$$

It coincides with the Fourier coefficient (42) at $n = 0$ and, hence, satisfies equation (43) at $n = 0$:

$$\begin{aligned}&\overline{T}''(y)=0,\\&-\lambda\overline{T}'(0)+\alpha\overline{T}(0)=q_{\mathrm{w}}\frac{l_0}{l_1},\\&\lambda\overline{T}'(R)+\alpha_1\overline{T}(R)=0.\end{aligned}\qquad(47)$$

It is solved readily:

$$\overline{T}(y)=\frac{l_0}{l_1}\frac{q_{\mathrm{w}}}{\alpha}\frac{1+\dfrac{\alpha_1(R_1-y)}{\lambda_{\mathrm{w}}}}{1+\dfrac{\alpha_1}{\alpha}+\dfrac{\alpha_1 R_1}{\lambda_{\mathrm{w}}}}.$$

Substituting in the above equation the values of $q_д = q_0 \dfrac{A_{\mathrm{w}}}{A}$ where q_0 is the total quantity of heat evolved in unit time from a unit contact surface,

$$A_{\mathrm{w}}=\sqrt{(\lambda c\gamma)_{\mathrm{w}}};\quad A=\sqrt{(\lambda c\gamma)_{\mathrm{w}}}+\sqrt{(\lambda c\gamma)_{\kappa}},$$

we obtain

$$\overline{T}(y)=\frac{l_0}{l_1}\frac{A_{\mathrm{w}}}{A}\frac{q_0}{\alpha}\cdot\frac{1+\dfrac{\alpha_1(R_1-y)}{\lambda_{\mathrm{w}}}}{1+\dfrac{\alpha_1}{\alpha}+\dfrac{\alpha_1 R_1}{\lambda_{\mathrm{w}}}}.\qquad(48)$$

In the case of a thick-walled part, for which it could be assumed that $R_1\to\infty$, the steady temperature is described by a simpler equation

$$\vartheta=\frac{l_0}{l_1}\frac{A_{\mathrm{w}}}{A}\frac{q}{\alpha}.\qquad(49)$$

It is obvious that at $\alpha = 0$ equation (49) is transformed into (50). This means that under adiabatic conditions on the opposite face the average steady temperature would also equal ϑ.

Isolating the factor ϑ from equation (48), we can write the equation as

$$\overline{T}(y)=\vartheta\frac{1+\dfrac{\alpha_1(R_1-y)}{\lambda_{\mathrm{w}}}}{1+\dfrac{\alpha_1}{\alpha}+\dfrac{\alpha_1 R_1}{\lambda_{\mathrm{w}}}}.\qquad(50)$$

This is the average steady temperature of a flat workpiece during multipass grinding.

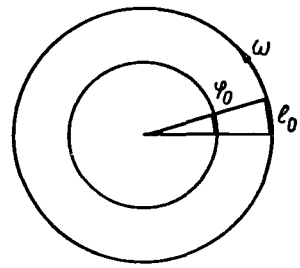

FIGURE 8. Schematic view of the travel of a heat source during cylindrical grinding.

Let us repeat a similar calculation for a ring-shaped part confined between two cylindrical planes $r=R$ and $r=R_1$.

A ribbon source moves on the $r=R$ plane with an angular velocity ω and comes into contact with the part at the arc l_0. The scheme (Figure 8) corresponds to either external or internal cylindrical grinding.

When the axis of the polar system of coordinates moves together with the source, the thermal conductivity equation for the above system has the form

$$\frac{1}{a}\left(\frac{\partial T}{\partial \tau}-\omega\frac{\partial T}{\partial \varphi}\right)=\nabla^2 T. \tag{51}$$

The steady temperature is described by the equations

$$\begin{gathered}\frac{\partial^2 T}{\partial r^2}-\frac{1}{r}\frac{\partial T}{\partial r}+\frac{1}{r^2}\frac{\partial^2 T}{\partial \varphi^2}+\frac{\omega}{a}\frac{\partial T}{\partial \varphi}=0,\\ \left[\lambda\frac{\partial T}{\partial r}+\alpha T\right]_{r=R}=Q(\varphi),\\ \left[-\lambda\frac{\partial T}{\partial r}+\alpha_1 T\right]_{r=R_1}=0.\end{gathered} \tag{52}$$

In this case the function $Q(\varphi)$ over the section $[0\leqslant\varphi\leqslant 2\pi]$ is determined by the equations

$$Q(\varphi)=\begin{cases} q_w & [0\leqslant\varphi\leqslant\varphi_0]\\ 0 & [\varphi_0<\varphi\leqslant 2\pi]\end{cases} \tag{53}$$

and $Q\varphi$ has a period of 2π.

The steady temperature $T(r, \varphi)$ is also a periodic function of φ with a period of 2π and may be represented by a Fourier series

$$T(r,\ \varphi)=\sum_{n=-\infty}^{\infty}T_n(r)\,l^{in\varphi}, \tag{54}$$

whose coefficients

$$T_n(r)=\frac{1}{2\pi}\int_0^{2\pi}T(r,\ \varphi)\,l^{-in\varphi}d\varphi \tag{55}$$

must satisfy the following equations derived from (53):

$$\begin{gathered}T_n''(r)+\frac{1}{r}T_n'(r)+\left(\frac{in\omega}{a}-\frac{n^2}{r^2}\right)T_n(r)=0,\\ \lambda T_n'(R)+\alpha T_n(R)=Q_n,\\ -\lambda T_n'(R_1)+\alpha_1 T_n(R_1)=0,\end{gathered} \tag{56}$$

where

$$Q_n=\frac{1}{2\pi}\int_0^{2\pi}Q(\varphi)\,l^{-in\varphi}d\varphi;\quad Q_0=\frac{l_0}{l_1}q_w;\quad l_1=2\pi R. \tag{57}$$

The solution of the differential equation (56) has the form

$$T_n(r)=A_nH_n^{(1)}\left(\sqrt{\frac{in\omega}{a}}\,r\right)+B_nH_n^{(2)}\left(\sqrt{\frac{in\omega}{a}}\,r\right), \tag{58}$$

where $H_n^{(1)}(z)$ and $H_n^{(2)}(z)$ are Hankel functions of the first and second kind; A_n and B_n are constants that are determined from the boundary conditions.

By substituting the value of $T_n(r)$ in (54) we obtain the steady temperature in the form of a series that is not presented here in an explicit form because of its complexity.

As above, we shall only determine the temperature averaged over the length of a passage

$$\overline{T}(r) = \frac{1}{2\pi} \int_0^{2\pi} T(r, \varphi) d\varphi = T_0(r). \tag{59}$$

It satisfies equations (56) for $n = 0$:

$$\begin{aligned} &\overline{T}''(r) + \frac{1}{r}\overline{T}'(r) = 0, \\ &\lambda \overline{T}'(R) + \alpha \overline{T}(R) = \frac{l_0}{l_1} q_w, \\ &-\lambda \overline{T}'(R_1) + \alpha_1 \overline{T}(R_1) = 0. \end{aligned} \tag{60}$$

The general solution of the differential equation (60) has the form

$$\overline{T}(r) = c_1 + c_2 l_n r. \tag{61}$$

By determining the constants c_1 and c_2 from the boundary conditions and substituting the value of $q_w = \frac{A_w}{A} q_0$, we obtain

$$\overline{T}(r) = \frac{l_0}{l_1} \frac{A_w}{A} \frac{q_0}{\alpha} \frac{1 + \frac{\alpha_1 R_1}{\lambda_w} l_n \frac{r}{R_1}}{1 + \frac{\alpha_1 R_1}{\alpha R} + \frac{\alpha_1 R_1}{\lambda_w} l_n \frac{R}{R_1}}. \tag{62}$$

Under adiabatic conditions on the nonworked surface ($\alpha_1 = 0$) the mean steady temperature is equal to

$$\vartheta = \frac{l_0}{l_1} \frac{A_w}{A} \frac{q_0}{\alpha}. \tag{63}$$

It coincides with the value of ϑ for flat grinding.

It is evident that in the case of a solid cylindrical part ($R_1 = 0$) as well as for a thick-walled ring-shaped part ($R_1 = \infty$) the equation (62) is also transformed into (63). Let us write equation (62) in the form

$$\overline{T}(r) = \vartheta \frac{1 + \frac{\alpha_1 R_1}{\lambda_w} l_n \frac{r}{R_1}}{1 + \frac{\alpha_1 R_1}{\alpha R} + \frac{\alpha_1 R_1}{\lambda_w} l_n \frac{R}{R_1}}. \tag{64}$$

This is the mean steady temperature in cylindrical grinding. The equation is valid for both external and internal grinding, provided that R and α denote the radius and the thermal conductivity coefficient of the worked surface while R_1 and α_1, are the same values for the nonworked surface.

The above equations do not contain in an explicit form the speed of the source on the workpiece surface. It is comprised indirectly, by means of the contact heat q_0.

The value of ϑ is the same for all types of grinding discussed here and it represents the mean steady temperature in the case of adiabatic conditions

on the nonworked surface or in the absence of such a surface (or when it is removed to infinity).

A calculation of the mean steady temperature (when the starting parameters have the values shown in section 1) is presented below. In the case of adiabatic conditions on the nonworked surface, the mean steady temperature is equal to

$$\vartheta = \frac{l_0}{l_1}\,\frac{A_д}{A}\,\frac{g_0}{\alpha} = 86°C.$$

When the cooling conditions of both surfaces are the same, the temperatures are as tabulated in Table 6.

TABLE 6

Temperatures of the various surfaces of a workpiece

Surface	Type of grinding		
	flat	external cylindrical	internal cylindrical
Worked	70	72	69
Intermediate . .	43	47	44
Nonworked	16	18	15

In all three cases the thickness of the workpiece was assumed to be 0.01 mm. For a ring-shaped part the diameter of the worked surface was assumed to be d = 0.1 m.

APPENDIX 1

Nomograph 1

$$\vartheta_0 = \frac{2}{\sqrt{\pi}}\,\frac{q}{A}\,\sqrt{\tau_0} =$$

$$= 84.2 S^{0.1} t^{0.45} v_w^{0.2}$$

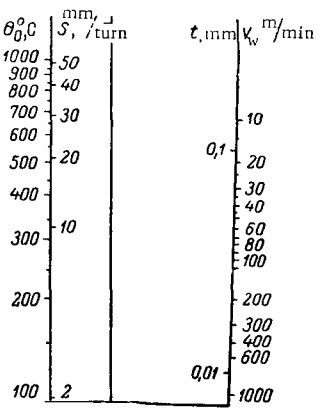

Nomograph 2

$$\xi = \frac{|y_0|}{\sqrt{4a\tau_0}} =$$

$$= 0.023 v_w^{0.5} t^{-0.25}$$

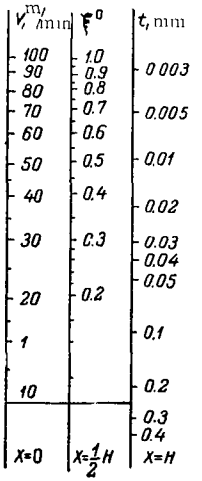

Nomograph 3

$$\eta_0^c = \frac{m_0 c_0}{A}\sqrt{\tau_0} =$$

$$= 0.066 v_w^{0.5} t^{0.75}$$

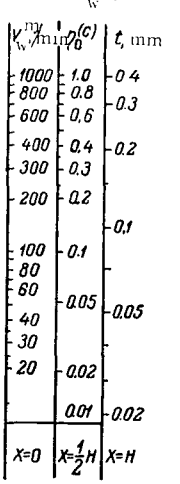

Nomograph 4

$$\tau_0^{**} = \frac{\alpha}{A}\sqrt{\tau_0} =$$

$$= 0.647 v_w^{-0.5} t^{0.25}$$

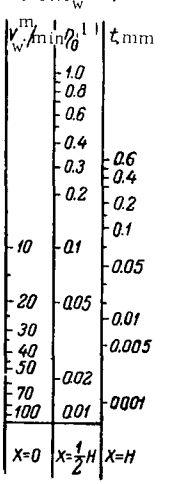

APPENDIX 2

Tabulated values of the temperature function

$$K(\xi, \eta)$$

η	$K(\xi, \eta)$	η	$K(\xi, \eta)$	η	$K(\xi, \eta)$	η	$K(\xi, \eta)$
				$\xi = 0$			
0.00	1.0000	0.51	0.6765	1.01	0.5045	1.51	0.3990
0.01	0.9909	0.52	0.6720	1.02	0.5019	1.52	0.3973
0.02	0.9823	0.53	0.6676	1.03	0.4993	1.53	0.3957
0.03	0.9737	0.54	0.6633	1.04	0.4963	1.54	0.3940
0.04	0 9653	0.55	0.6590	1.05	0.4942	1.55	0.3924
0.05	0.9571	0.56	0.6547	1.06	0.4917	1.56	0.3907
0.06	0.9489	0.57	0.6505	1.07	0.4892	1.57	0.3891
0.07	0.9408	0.58	0.6464	1.08	0.4867	1.58	0.3875
0.08	0.9329	0.59	0.6423	1.09	0.4843	1.59	0.3859
0.09	0.9251	0.60	0.6392	1.10	0.4819	1.60	0.3843
0.10	0.9174	0.61	0.6342	1.11	0.4795	1.61	0.3828
0.11	0.9098	0.62	0.6302	1.12	0.4771	1.62	0.3812
0.12	0.9023	0.63	0.6263	1.13	0.4747	1.63	0.3797
0.13	0.8949	0.64	0.6224	1.14	0.4724	1.64	0.3781
0.14	0.8876	0,65	0.6186	1.15	0.4701	1.65	0.3766
0.15	0.8805	0.66	0.6148	1.16	0.4678	1.66	0.3751
0.16	0.8734	0.67	0.6110	1.17	0.4655	1.67	0.3736
0.17	0.8664	0.68	0.6073	1.18	0.4633	1.68	0.3721
0.18	0.8595	0.69	0.6037	1.19	0.4611	1.69	0.3706
0.19	0.8527	0.70	0.6000	1.20	0.4588	1.70	0.3692
0.20	0.8460	0.71	0.5964	1.21	0.4566	1.71	0.3677
0.21	0.8394	0.72	0.5929	1.22	0.4545	1.72	0.3663
0.22	0.8329	0.73	0.5894	1.23	0.4523	1.73	0.3648
0.23	0.8265	0.74	0.5859	1.24	0.4502	1.74	0.3634
0.24	0.8201	0.75	0.5825	1.25	0.4481	1.75	0.3620
0.25	0.8139	0.76	0.5791	1.26	0.4460	1.76	0.3606
0.26	0.8077	0.77	0.5757	1.27	0.4439	1.77	0.3592
0.27	0.8016	0.78	0.5724	1.28	0.4418	1.78	0.3578
0.28	0.7956	0.79	0.5691	1.29	0.4398	1.79	0.3565
0.29	0.7897	0.80	0.5658	1.30	0.4378	1.80	0.3551
0.30	0.7838	0.81	0.5626	1.31	0.4358	1.81	0.3538
0.31	0.7780	0.82	0.5594	1.32	0.4338	1.82	0.3524
0.32	0.7723	0.83	0.5562	1.33	0.4318	1.83	0.3511
0.33	0.7667	0.84	0.5531	1.34	0.4299	1.84	0.3498
0.34	0.7611	0.85	0.5500	1.35	0.4279	1.85	0.3484
0.35	0.7556	0.86	0.5470	1.36	0.4260	1.86	0.3471
0.36	0.7502	0.87	0.5439	1.37	0.4241	1.87	0.3459
0.37	0.7449	0.88	0.5409	1.38	0.4222	1.88	0.3446
0 38	0.7396	0.89	0.5379	1.39	0.4203	1.89	0.3433
0.39	0.7344	0.90	0.5350	1.40	0.4185	1.90	0.3420
0.40	0.7292	0.91	0.5321	1.41	0.4166	1.91	0.3408
0.41	0.7241	0.92	0.5292	1.42	0.4148	1.92	0.3395
0.42	0.7191	0.93	0.5264	1.43	0.4130	1.93	0.3383
0.43	0 7141	0.94	0.5235	1.44	0.4112	1.94	0.3371
0.44	0.7092	0.95	0.5207	1.45	0.4094	1.95	0.3356
0.45	0.7044	0.96	0.5180	1.46	0.4076	1.96	0.3346
0.46	0.6996	0.97	0.5152	1.47	0.4059	1.97	0.3334
0.47	0.6948	0.98	0.5125	1.48	0.4041	1.98	0.3322
0.48	0.6902	0.99	0.5098	1.49	0.4024	1.99	0.3310
0.49	0.6855	1.00	0.5072	1.50	0.4007	2.00	0.3299
0.50	0.6810						

η	$K(\xi, \eta)$	η	$K(\xi, \eta)$	η	$K(\xi, \eta)$	η	$K(\xi, \eta)$
			$\xi = 0.01$				
0.01	0.9735	0.51	0.6657	1.01	0.4970	1.51	0.3934
0.02	0.9650	0.52	0.6613	1.02	0.4944	1.52	0.3917
0.03	0.9567	0.53	0.6570	1.03	0.4919	1.53	0.3901
0.04	0.9485	0.54	0.6528	1.04	0.4894	1.54	0.3884
0.05	0.9404	0.55	0.6485	1.05	0.4869	1.55	0.3868
0.06	0.9324	0.56	0.6444	1.06	0.4844	1.56	0.3852
0.07	0.9245	0.57	0.6403	1.07	0.4820	1.57	0.3836
0.08	0.9168	0.58	0.6362	1.08	0.4896	1.58	0.3820
0.09	0.9091	0.59	0.6322	1.09	0.4772	1.59	0.3805
0.10	0.9016	0.60	0.6282	1.10	0.4748	1.60	0.3789
0.11	0.8941	0.61	0.6242	1.11	0.4724	1.61	0.3774
0.12	0.8868	0.62	0.6204	1.12	0.4701	1.62	0.3758
0.13	0.8796	0.63	0.6165	1.13	0.4678	1.63	0.3743
0.14	0.8725	0.64	0.6127	1.14	0.4655	1.64	0.3728
0.15	0.8655	0.65	0.6089	1.15	0.4632	1.65	0.3713
0.16	0.8585	0.66	0.6052	1.16	0.4610	1.66	0.3698
0.17	0.8517	0.67	0.6015	1.17	0.4587	1.67	0.3684
0.18	0.8450	0.68	0.5979	1.18	0.4565	1.68	0.3669
0.19	0.8383	0.69	0.5943	1.19	0.4543	1.69	0.3654
0.20	0.8318	0.70	0.5907	1.20	0.4521	1.70	0.3640
0.21	0.8253	0.71	0.5872	1.21	0.4500	1.71	0.3626
0.22	0.8189	0.72	0.5837	1.22	0.4479	1.72	0.3612
0.23	0.8126	0.73	0.5803	1.23	0.4457	1.73	0.3597
0.24	0.8064	0.74	0.5769	1.24	0.4437	1.74	0.3583
0.25	0.8003	0.75	0.5735	1.25	0.4416	1.75	0.3570
0.26	0.7943	0.76	0.5702	1.26	0.4395	1.76	0.3556
0.27	0.7883	0.77	0.5669	1.27	0.4375	1.77	0.3542
0.28	0.7824	0.78	0.5636	1.28	0.4355	1.78	0.3529
0.29	0.7766	0.79	0.5604	1.29	0.4334	1.79	0.3515
0.30	0.7709	0.80	0.5572	1.30	0.4315	1.80	0.3502
0.31	0.7652	0.81	0.5540	1.31	0.4295	1.81	0.3488
0.32	0.7596	0.82	0.5509	1.32	0.4275	1.82	0.3475
0.33	0.7541	0.83	0.5478	1.33	0.4256	1.83	0.3462
0.34	0.7486	0.84	0.5447	1.34	0.4237	1.84	0.3449
0.35	0.7433	0.85	0.5417	1.35	0.4218	1.85	0.3436
0.36	0.7379	0.86	0.5387	1.36	0.4199	1.86	0.3423
0.37	0.7327	0.87	0.5357	1.37	0.4180	1.87	0.3411
0.38	0.7275	0.88	0.5327	1.38	0.4162	1.88	0.3398
0.39	0.7224	0.89	0.5298	1.39	0.4143	1.89	0.3386
0.40	0.7174	0.90	0.5269	1.40	0.4125	1.90	0.3373
0.41	0.7124	0.91	0.5241	1.41	0.4107	1.91	0.3361
0.42	0.7074	0.92	0.5213	1.42	0.4089	1.92	0.3349
0.43	0.7026	0.93	0.5185	1.43	0.4071	1.93	0.3336
0.44	0.6978	0.94	0.5157	1.44	0.4053	1.94	0.3324
0.45	0.6930	0.95	0.5129	1.45	0.4036	1.95	0.3312
0.46	0.6883	0.96	0.5102	1.46	0.4018	1.96	0.3300
0.47	0.6837	0.97	0.5075	1.47	0.4001	1.97	0.3288
0.48	0.6791	0.98	0.5049	1.48	0.3984	1.98	0.3277
0.49	0.6746	0.99	0.5022	1.49	0.3967	1.99	0.3265
0.50	0.6701	1.00	0.4996	1.50	0.3950	2.00	0.3253

Appendix 2 (continued)

η	$K(\xi, \eta)$	η	$K(\xi, \eta)$	η	$K(\xi, \eta)$	η	$K(\xi, \eta)$
			$\xi = 0.10$				
0.01	0.8255	0.51	0.5729	1.01	0.4318	1.51	0.3439
0.02	0.8187	0.52	0.5693	1.02	0.4296	1.52	0.3425
0.03	0.8119	0.53	0.5657	1.03	0.4275	1.53	0.3411
0.04	0.8052	0.54	0.5621	1.04	0.4252	1.54	0.3397
0.05	0.7986	0.55	0.5586	1.05	0.4232	1.55	0.3383
0.06	0.7921	0.56	0.5552	1.06	0.4212	1.56	0.3369
0.07	0.7857	0.57	0.5517	1.07	0.4191	1.57	0.3356
0.08	0.7794	0.58	0.5484	1.08	0.4170	1.58	0.3342
0.09	0.7731	0.59	0.5450	1.09	0.4150	1.59	0.3329
0.10	0.7670	0.60	0.5417	1.10	0.4130	1.60	0.3316
0.11	0.7609	0.61	0.5384	1.11	0.4111	1.61	0.3302
0.12	0.7549	0.62	0.5352	1.12	0.4090	1.62	0.3289
0.13	0.7490	0.63	0.5320	1.13	0.4071	1.63	0.3276
0.14	0.7432	0.64	0.5288	1.14	0.4051	1.64	0.3263
0.15	0.7375	0.65	0.5257	1.15	0.4032	1.65	0.3251
0.16	0.7318	0.66	0.5225	1.16	0.4013	1.66	0.3238
0.17	0.7262	0.67	0.5195	1.17	0.3994	1.67	0.3225
0.18	0.7207	0.68	0.5164	1.18	0.3976	1.68	0.3213
0.19	0.7153	0.69	0.5134	1.19	0.3957	1.69	0.3201
0.20	0.7099	0.70	0.5105	1.20	0.3939	1.70	0.3188
0.21	0.7046	0.71	0.5075	1.21	0.3920	1.71	0.3176
0.22	0.6994	0.72	0.5046	1.22	0.3902	1.72	0.3164
0.23	0 6942	0.73	0.5017	1.23	0.3884	1.73	0.3152
0.24	0.6891	0.74	0.4989	1.24	0.3867	1.74	0.3140
0.25	0.6841	0.75	0.4960	1.25	0.3849	1.75	0.3128
0.26	0.6791	0.76	0.4933	1.26	0.3831	1.76	0.3116
0.27	0.6742	0.77	0.4905	1.27	0.3814	1.77	0.3104
0.28	0.6693	0.78	0.4877	1.28	0.3797	1.78	0.3093
0.29	0.6646	0.79	0.4850	1.29	0.3780	1.79	0.3081
0.30	0.6598	0.80	0.4824	1.30	0.3763	1.80	0.3070
0.31	0.6552	0.81	0.4797	1.31	0.3746	1.81	0.3058
0.32	0.6506	0.82	0.4771	1.32	0.3730	1.82	0.3047
0.33	0.6460	0.83	0.4745	1.33	0.3713	1.83	0.3036
0.34	0.6415	0.84	0.4719	1.34	0.3697	1.84	0.3025
0.35	0.6371	0.85	0.4694	1.35	0.3681	1.85	0.3014
0.36	0.6327	0.86	0.4668	1.36	0.3665	1.86	0.3003
0.37	0.6284	0.87	0.4643	1.37	0.3649	1.87	0.2992
0.38	0.6241	0.88	0.4619	1.38	0.3633	1.88	0.2981
0.39	0.6199	0.89	0.4594	1 39	0.3617	1.89	0.2970
0.40	0.6157	0.90	0.4570	1.40	0 3602	1.90	0.2960
0.41	0.6116	0 91	0.4546	1.41	0.3586	1.91	0.2949
0.42	0.6075	0.92	0.4522	1.42	0.3571	1 92	0.2938
0.43	0.6035	0.93	0.4498	1.43	0.3556	1.93	0.2928
0.44	0.5995	0.94	0.4475	1.44	0.3541	1.94	0.2917
0.45	0.5956	0.95	0.4452	1.45	0.3526	1.95	0.2907
0.46	0.5917	0.96	0.4429	1.46	0.3511	1.96	0.2897
0.47	0.5878	0.97	0.4406	1.47	0.3496	1.97	0.2887
0.48	0.5840	0.98	0.4384	1 48	0.3482	1.98	0.2877
0.49	0.5803	0.99	0.4362	1.49	0.3467	1.99	0.2867
0.50	0 5766	1.00	0.4340	1.50	0.3453	2.00	0.2857

Appendix 2 (continued)

η	$K(\xi, \eta)$	η	$K(\xi, \eta)$	η	$K(\xi, \eta)$	η	$K(\xi, \eta)$
			$\xi = 0.20$				
0.01	0.6796	0.51	0.4790	1.01	0 3647	1.51	0.2924
0.02	0.6742	0.52	0.4761	1.02	0.3629	1.52	0.2912
0 03	0.6688	0.53	0.4732	1.03	0.3611	1.53	0.2901
0.04	0.6636	0.54	0.4704	1.04	0.3594	1.54	0.2889
0.05	0.6584	0.55	0.4675	1.05	0.3577	1.55	0.2878
0.06	0.6533	0.56	0.4647	1 06	0.3560	1.56	0.2866
0.07	0.6482	0.57	0.4620	1.07	0.3543	1.57	0.2856
0.08	0.6433	0.58	0.4593	1.08	0.3526	1.58	0.2844
0.09	0.6383	0.59	0.4566	1.09	0.3509	1.59	0.2834
0.10	0.6335	0.60	0.4539	1.10	0.3493	1.60	0.2822
0.11	0.6287	0.61	0.4512	1.11	0.3477	1.61	0.2811
0.12	0.6240	0.62	0.4486	1.12	0.3460	1.62	0.2801
0.13	0.6193	0.63	0.4460	1.13	0.3444	1 63	0.2789
0.14	0.6147	0.64	0.4435	1.14	0.3429	1.64	0.2780
0.15	0.6102	0.65	0.4409	1.15	0.3413	1 65	0.2769
0.16	0.6057	0.66	0.4384	1.16	0.3397	1.66	0.2758
0.17	0.6013	0.67	0.4359	1.17	0.3382	1.67	0.2748
0 18	0.5969	0.68	0.4335	1.18	0.3366	1.68	0.2737
0.19	0 5926	0 69	0.4311	1.19	0.3351	1.69	0.2727
0.20	0.5883	0.70	0.4286	1.20	0.3336	1.70	0.2716
0.21	0.5841	0.71	0.4263	1 21	0.3321	1 71	0.2705
0.22	0 5800	0.72	0 4239	1.22	0.3306	1.72	0 2696
0.23	0.5759	0.73	0.4216	1.23	0.3291	1.73	0.2686
0.24	0 5718	0.74	0.4193	1.24	0.3277	1.74	0.2676
0.25	0.5678	0.75	0.4170	1 25	0.3262	1.75	0.2666
0.26	0 5639	0 76	0.4147	1 26	0.3248	1.76	0.2658
0.27	0.5600	0.77	0.4125	1.27	0.3234	1.77	0.2646
0.28	0.5561	0.78	0.4102	1.28	0.3220	1.78	0.2638
0.29	0.5523	0.79	0.4080	1.29	0.3206	1.79	0.2626
0.30	0.5486	0.80	0.4059	1.30	0.3192	1.80	0.2618
0.31	0.5449	0.81	0.4037	1.31	0.3178	1.81	0.2606
0.32	0.5412	0.82	0.4016	1.32	0.3164	1.82	0.2601
0.33	0.5376	0.83	0.3995	1.33	0.3151	1.83	0.2592
0 34	0.5340	0.84	0.3974	1.34	0.3137	1.84	0 2578
0.35	0.5304	0.85	0.3953	1.35	0.3124	1.85	0.2570
0.36	0.5269	0.86	0.3932	1.36	0.3111	1.86	0.2565
0.37	0 5235	0.87	0.3912	1.37	0.3097	1.87	0 2555
0.38	0 5200	0.88	0.3892	1.38	0 3084	1.88	0.2545
0 39	0.5167	0.89	0.3872	1.39	0.3072	1 89	0.2533
0.40	0.5133	0.90	0.3852	1.40	0.3059	1.90	0.2528
0.41	0 5100	0.91	0.3833	1.41	0.3046	1 91	0.2519
0.42	0.5068	0.92	0 3813	1.42	0.3033	1 92	0.2510
0.43	0.5035	0.93	0.3794	1.43	0.3021	1.93	0.2496
0.44	0.5004	0.94	0.3775	1.44	0.3009	1 94	0.2497
0.45	0.4972	0.95	0.3756	1 45	0 2996	1.95	0.2483
0.46	0.4941	0.96	0.3737	1.46	0.2984	1.96	0.2483
0.47	0.4910	0.97	0.3719	1.47	0.2972	1.97	0.2462
0.48	0.4879	0.98	0.3701	1.48	0.2960	1.98	0.2460
0.49	0.4849	0.99	0.3682	1.49	0.2948	1.99	0.2447
0.50	0.4820	1.00	0.3664	1.50	0.2936	2.00	0.2441

$\xi = 0.30$

η	$K(\xi, \eta)$	η	$K(\xi, \eta)$	η	$K(\xi, \eta)$	η	$K(\xi, \eta)$
0.01	0.5525	0.51	0,3952	1.01	0.3038	1.51	0.2452
0.02	0.5483	0.52	0,3929	1.02	0.3024	1.52	0.2443
0.03	0.5442	0.53	0.3906	1.03	0.3009	1.53	0,2433
0.04	0.5401	0.54	0,3884	1.04	0.2995	1.54	0.2424
0,05	0.5361	0.55	0.3861	1.05	0.2982	1.55	0,2414
0.06	0.5321	0.56	0.3839	1.06	0.2968	1.56	0,2405
0,07	0.5282	0.57	0.3817	1.07	0,2954	1.57	0.2396
0.08	0.5243	0.58	0.3795	1.08	0.2941	1.58	0.2387
0.09	0.5205	0.59	0.3774	1.09	0.2927	1.59	0.2378
0.10	0.5167	0.60	0,3753	1.10	0.2914	1.60	0,2369
0.11	0.5130	0.61	0.3732	1.11	0.2901	1.61	0,2360
0,12	0.5093	0.62	0.3711	1.12	0.2888	1.62	0.2351
0.13	0.5056	0.63	0.3690	1.13	0,2875	1.63	0.2342
0.14	0.5021	0.64	0.3670	1.14	0.2862	1.64	0.2334
0.15	0.4985	0.65	0.3649	1.15	0.2849	1.65	0.2325
0,16	0.4950	0.66	0.3629	1.16	0.2836	1.66	0.2316
0.17	0.4915	0.67	0.3610	1.17	0.2824	1.67	0.2308
0.18	0.4881	0.68	0.3590	1.18	0.2811	1.68	0,2299
0.19	0.4848	0,69	0.3571	1.19	0.2799	1,69	0.2291
0.20	0.4814	0.70	0.3551	1.20	0,2787	1.70	0.2282
0.21	0,4781	0,71	0.3532	1.21	0.2775	1.71	0.2274
0.22	0.4749	0.72	0.3513	1.22	0.2763	1 72	0.2266
0.23	0.4717	0.73	0.3445	1.23	0.2751	1.73	0.2258
0.24	0.4685	0.74	0.3476	1.24	0.2739	1.74	0.2250
0.25	0.4653	0.75	0.3458	1.25	0.2727	1.75	0.2241
0.26	0.4622	0.76	0.3440	1.26	0.2716	1.76	0.2233
0.27	0.4592	0.77	0.3422	1.27	0,2704	1.77	0.2225
0.28	0.4561	0.78	0.3404	1.28	0.2692	1.78	0.2218
0.29	0.4532	0.79	0.3387	1.29	0.2681	1.79	0.2210
0.30	0.4502	0.80	0.3369	1.30	0.2670	1.80	0,2202
0.31	0.4473	0.81	0.3352	1.31	0.2659	1.81	0.2194
0.32	0.4444	0.82	0.3335	1.32	0.2648	1.82	0.2186
0.33	0.4415	0.83	0.3318	1.33	0.2637	1.83	0.2179
0.34	0.4387	0.84	0.3301	1.34	0.2626	1.84	0.2171
0.35	0.4359	0.85	0.3284	1.35	0.2615	1.85	0.2164
0.36	0.4331	0.86	0.3268	1.36	0.2604	1.86	0.2156
0.37	0.4227	0,87	0.3252	1.37	0.2593	1.87	0.2149
0.38	0.4227	0.88	0.3235	1.38	0.2583	1.88	0.2141
0.39	0.4250	0.89	0.3219	1.39	0.2572	1.89	0.2134
0,40	0.4224	0,90	0.3203	1.40	0.2562	1.90	0.2127
0.41	0.4198	0,91	0.3188	1.41	0.2551	1.91	0.2119
0.42	0.4172	0.92	0.3172	1.42	0,2541	1.92	0.2112
0.43	0.4147	0,93	0.3157	1.43	0.2531	1.93	0.2105
0.44	0.4121	0.94	0.3141	1.44	0.2521	1.94	0.2098
0.45	0.4097	0.95	0.3126	1.45	0.2511	1.95	0.2091
0.46	0.4072	0.96	0.3111	1.46	0.2501	1.96	0,2084
0.47	0.4047	0.97	0,3096	1.47	0.2491	1.97	0.2077
0.48	0.4023	0.98	0.3081	1.48	0.2481	1.98	0.2070
0.49	0.3999	0.99	0.3067	1.49	0.2471	1.99	0.2063
0.50	0.3976	1.00	0.3052	1 50	0.2462	2.00	0.2056

Appendix 2 (continued)

η	$K(\xi, \eta)$	η	$K(\xi, \eta)$	η	$K(\xi, \eta)$	η	$K(\xi, \eta)$
			$\xi = 0.40$				
0.01	0.4435	0.51	0.3217	1.01	0.2495	1.51	0.2019
0.02	0.4403	0.52	0.3199	1.02	0.2484	1.52	0.2012
0.03	0.4371	0.53	0.3181	1.03	0.2473	1.53	0.2004
0.04	0.4340	0.54	0.3163	1.04	0.2462	1.54	0.1997
0.05	0.4309	0.55	0.3145	1.05	0.2450	1.55	0.1989
0.06	0.4278	0.56	0.3128	1.06	0.2440	1.56	0.1982
0.07	0.4248	0.57	0.3111	1.07	0.2429	1.57	0.1975
0.08	0.4218	0.58	0.3094	1.08	0.2418	1.58	0.1967
0.09	0.4189	0.59	0.3077	1.09	0.2407	1.59	0.1960
0.10	0.4160	0.60	0.3060	1.10	0.2397	1.60	0.1953
0.11	0.4131	0.61	0.3044	1.11	0.2386	1.61	0.1946
0.12	0.4103	0.62	0.3027	1.12	0.2376	1.62	0.1939
0.13	0.4075	0.63	0.3011	1.13	0.2365	1.63	0.1932
0.14	0.4047	0.64	0.2995	1.14	0.2355	1.64	0.1925
0.15	0.4020	0.65	0.2979	1.15	0.2345	1.65	0.1918
0.16	0.3993	0.66	0.2963	1.16	0.2334	1.66	0.1911
0.17	0.3966	0.67	0.2948	1.17	0.2325	1.67	0.1904
0.18	0.3939	0.68	0.2932	1.18	0.2315	1.68	0.1897
0.19	0.3913	0.69	0.2917	1.19	0.2305	1.69	0.1890
0.20	0.3888	0.70	0.2902	1.20	0.2295	1.70	0.1884
0.21	0.3862	0.71	0.2887	1.21	0.2286	1.71	0.1877
0.22	0.3837	0.72	0.2872	1.22	0.2276	1.72	0.1870
0.23	0.3812	0.73	0.2857	1.23	0.2266	1.73	0.1864
0.24	0.3787	0.74	0.2843	1.24	0.2257	1.74	0.1857
0.25	0.3763	0.75	0.2828	1.25	0.2248	1.75	0.1851
0.26	0.3739	0.76	0.2814	1.26	0.2238	1.76	0.1844
0.27	0.3715	0.77	0.2800	1.27	0.2229	1.77	0.1838
0.28	0.3692	0.78	0.2786	1.28	0.2219	1.78	0.1832
0 29	0.3668	0.79	0.2772	1.29	0.2210	1.79	0.1825
0.30	0.3645	0.80	0.2758	1.30	0.2201	1.80	0.1819
0.31	0.3623	0.81	0.2744	1.31	0.2192	1.81	0.1813
0 32	0.3600	0.82	0.2731	1.32	0.2184	1.82	0.1807
0.33	0.3578	0.83	0.2717	1.33	0.2175	1.83	0.1800
0.34	0.3556	0.84	0.2704	1.34	0.2166	1.84	0.1794
0.35	0.3534	0.85	0.2691	1.35	0.2158	1.85	0.1788
0.36	0.3513	0.86	0.2678	1.36	0.2148	1.86	0.1782
0.37	0.3492	0.87	0.2665	1.37	0.2140	1.87	0.1776
0.38	0.3471	0.88	0.2652	1.38	0.2132	1.88	0.1770
0.39	0.3450	0.89	0.2639	1.39	0.2124	1.89	0.1764
0.40	0.3429	0.90	0.2627	1.40	0.2115	1.90	0.1758
0.41	0.3409	0.91	0.2614	1.41	0.2106	1.91	0.1753
0.42	0.3389	0.92	0.2602	1.42	0.2097	1.92	0.1747
0.43	0.3369	0.93	0.2590	1.43	0.2082	1.93	0.1741
0.44	0.3349	0.94	0.2578	1.44	0.2074	1.94	0.1735
0.45	0.3330	0.95	0.2566	1.45	0.2066	1.95	0.1730
0.46	0.3310	0.96	0.2554	1.46	0.2058	1.96	0.1724
0.47	0.3291	0.97	0.2542	1.47	0.2050	1.97	0.1718
0.48	0.3272	0.98	0.2530	1.48	0.2043	1.98	0.1713
0.49	0.3254	0.99	0.2518	1.49	0.2035	1.99	0.1707
0.50	0.3235	1.00	0.2507	1.50	0.2027	2.00	0.1700

Appendix 2 (continued)

η	$K(\xi, \eta)$	η	$K(\xi, \eta)$	η	$K(\xi, \eta)$	η	$K(\xi, \eta)$
			$\xi = 0.50$				
0.01	0.3513	0.51	0.2582	1.01	0.2029	1.51	0.1651
0.02	0.3489	0.52	0.2568	1.02	0.2011	1.52	0.1645
0.03	0.3465	0.53	0.2554	1.03	0.2003	1.53	0.1639
0.04	0.3441	0.54	0.2540	1.04	0.1994	1.54	0.1633
0.05	0.3417	0.55	0.2527	1.05	0.1985	1.55	0.1627
0.06	0.3394	0.56	0.2513	1.06	0.1977	1 56	0.1621
0.07	0.3371	0.57	0.2500	1.07	0.1968	1.57	0.1615
0.08	0.3349	0.58	0.2487	1.08	0.1960	1.58	0.1610
0.09	0.3326	0.59	0.2473	1.09	0.1951	1.59	0.1604
0.10	0.3304	0.60	0.2461	1.10	0.1943	1.60	0.1598
0.11	0.3282	0.61	0 2448	1.11	0.1935	1.61	0.1592
0.12	0.3261	0.62	0.2435	1.12	0.1926	1.62	0.1587
0.13	0.3239	0.63	0 2422	1.13	0.1918	1.63	0.1581
0.14	0.3218	0.64	0.2410	1.14	0.1910	1.64	0.1575
0.15	0.3197	0.65	0.2398	1.15	0.1902	1.65	0.1570
0.16	0.3177	0.66	0.2385	1.16	0.1894	1.66	0.1564
0.17	0.3156	0.67	0.2373	1.17	0.1886	1.67	0.1559
0.18	0.3136	0.68	0.2361	1.18	0.1879	1.68	0.1553
0.19	0.3116	0.69	0.2349	1 19	0.1871	1.69	0.1548
0.20	0.3097	0.70	0.2338	1.20	0.1863	1.70	0.1543
0.21	0.3077	0.71	0.2326	1.21	0.1855	1.71	0.1537
0.22	0.3058	0.72	0.2314	1.22	0.1848	1.72	0 1532
0.23	0.3039	0.73	0.2303	1.23	0.1840	1.73	0.1527
0.24	0.3020	0.74	0.2292	1.24	0.1833	1.74	0.1522
0.25	0.3002	0.75	0.2280	1.25	0.1826	1.75	0.1516
0.26	0.2983	0.76	0.2269	1.26	0.1818	1.76	0.1511
0.27	0.2965	0.77	0.2258	1.27	0.1811	1.77	0.1508
0.28	0.2947	0.78	0.2247	1.28	0.1804	1.78	0.1501
0.29	0.2929	0.79	0.2236	1 29	0.1796	1.79	0.1496
0.30	0.2912	0.80	0.2226	1.30	0.1789	1.80	0.1491
0.31	0.2894	0.81	0.2215	1.31	0.1782	1.81	0.1486
0.32	0.2877	0.82	0.2204	1.32	0.1775	1.82	0.1481
0.33	0.2860	0.83	0.2194	1.33	0.1768	1.83	0.1476
0.34	0.2843	0.84	0.2184	1.34	0.1761	1.84	0.1471
0.35	0.2826	0.85	0.2173	1.35	0.1755	1.85	0.1466
0.36	0.2810	0.86	0.2163	1.36	0.1748	1.86	0.1461
0.37	0.2793	0.87	0.2153	1.37	0.1741	1.87	0.1457
0.38	0.2777	0.88	0.2143	1.38	0.1734	1.88	0.1452
0.39	0.2761	0.89	0.2133	1.39	0.1728	1.89	0.1447
0.40	0.2745	0.90	0.2123	1.40	0.1721	1.90	0.1442
0.41	0.2730	0.91	0.2113	1.41	0.1714	1.91	0.1438
0.42	0.2714	0.92	0.2104	1.42	0.1708	1.92	0.1433
0.43	0.2699	0.93	0.2094	1.43	0.1701	1.93	0.1428
0.44	0.2684	0.94	0.2085	1.44	0.1695	1.94	0.1424
0.45	0.2669	0.95	0.2075	1.45	0.1689	1.95	0.1419
0.46	0.2654	0.96	0.2066	1.46	0.1682	1.96	0.1415
0.47	0.2639	0.97	0.2057	1.47	0.1676	1.97	0.1410
0.48	0.2625	0.98	0.2047	1.48	0.1670	1.98	0.1406
0.49	0.2610	0.99	0.2038	1.49	0.1663	1.99	0.1401
0.50	0.2596	1.00	0.2029	1.50	0.1657	2.00	0.1397

η	$K(\xi, \eta)$	η	$K(\xi, \eta)$	η	$K(\xi, \eta)$	η	$K(\xi, \eta)$
			$\xi = 0.60$				
0.01	0.2745	0.51	0.2042	1.01	0.1612	1.51	0.1325
0.02	0.2727	0.52	0.2032	1.02	0.1605	1.52	0.1320
0.03	0.2709	0.53	0.2021	1.03	0.1598	1.53	0.1315
0.04	0.2691	0 54	0.2011	1.04	0.1591	1.54	0.1311
0.05	0.2673	0.55	0.2000	1.05	0.1584	1.55	0.1306
0.06	0.2656	0.56	0.1990	1.06	0.1578	1.56	0.1301
0.07	0.2639	0.57	0.1980	1.07	0.1571	1.57	0.1297
0.08	0.2622	0.58	0.1970	1.08	0.1565	1.58	0.1292
0.09	0.2605	0.59	0.1960	1.09	0.1558	1.59	0.1288
0.10	0.2588	0.60	0.1950	1.10	0.1552	1.60	0.1283
0.11	0.2572	0.61	0 1940	1.11	0.1545	1.61	0.1279
0.12	0.2556	0.62	0.1930	1.12	0.1539	1.62	0.1274
0.13	0.2540	0.63	0.1921	1.13	0.1533	1.63	0.1270
0.14	0.2524	0.64	0.1911	1.14	0.1526	1 64	0.1265
0.15	0.2508	0.65	0.1902	1.15	0,1520	1.65	0.1261
0.16	0.2493	0.66	0.1892	1.16	0.1514	1.66	0.1257
0.17	0.2477	0.67	0.1883	1.17	0.1508	1.67	0.1253
0.18	0.2462	0.68	0.1874	1 18	0.1502	1.68	0.1248
0.19	0 2447	0.69	0.1865	1.19	0.1496	1.69	0.1244
0 20	0.2432	0,70	0.1856	1.20	0.1490	1.70	0.1240
0.21	0 2418	0.71	0.1847	1.21	0.1484	1.71	0.1236
0.22	0 2403	0.72	0.1838	1.22	0.1478	1.72	0.1232
0.23	0.2389	0.73	0.1829	1.23	0.1472	1.73	0.1228
0.24	0 2375	0.74	0.1820	1.24	0.1466	1.74	0.1223
0.25	0.2361	0.75	0.1812	1.25	0.1461	1.75	0.1219
0.26	0.2347	0.76	0.1803	1.26	0.1455	1.76	0.1215
0.27	0.2333	0.77	0.1795	1.27	0.1449	1.77	0.1211
0.28	0.2320	0.78	0.1786	1.28	0.1444	1.78	0.1207
0.29	0.2306	0.79	0,1778	1.29	0.1438	1.79	0.1203
0.30	0 2293	0.80	0.1770	1.30	0.1433	1.80	0.1199
0.31	0.2280	0.81	0.1762	1.31	0.1427	1.81	0.1195
0.32	0.2266	0.82	0.1754	1.32	0.1422	1.82	0.1192
0.33	0.2254	0.83	0.1745	1.33	0 1416	1.83	0.1188
0.34	0.2241	0.84	0.1738	1.34	0.1411	1.84	0.1184
0.35	0.2228	0.85	0.1730	1.35	0.1405	1.85	0.1180
0.36	0.2216	0.86	0,1722	1.36	0.1400	1.86	0.1176
0.37	0.2203	0.87	0.1714	1.37	0.1395	1.87	0.1172
0.38	0,2191	0.88	0.1706	1.38	0.1390	1.88	0.1169
0.39	0.2179	0.89	0.1699	1.39	0 1384	1.89	0.1165
0,40	0.2167	0.90	0.1691	1.40	0.1379	1.90	0 1161
0.41	0.2155	0.91	0.1683	1.41	0.1374	1.91	0.1158
0.42	0.2143	0.92	0,1676	1.42	0 1369	1.92	0.1154
0.43	0,2131	0.93	0.1669	1.43	0.1364	1.93	0.1150
0,44	0.2120	0.94	0.1661	1.34	0.1359	1.94	0,1147
0.45	0.2109	0.95	0,1654	1.45	0.1354	1.95	0.1143
0.46	0,2097	0.96	0.1647	1.46	0.1349	1.96	0.1139
0.47	0.2086	0.97	0 1640	1.47	0.1344	1.97	0.1136
0.48	0.2075	0 98	0.1633	1.48	0.1339	1.98	0.1132
0.49	0,2064	0.99	0,1626	1 49	0.1334	1.99	0.1129
0.50	0.2053	1,00	0.1619	1,50	0.1330	2.00	0.1125

η	$K(\xi, \eta)$	η	$K(\xi, \eta)$	η	$K(\xi, \eta)$	η	$K(\xi, \eta)$
			$\xi = 0.70$				
0.01	0.2115	0.51	0.1592	1.01	0.1266	1.51	0.1047
0.02	0.2101	0.52	0.1584	1.02	0.1261	1.52	0.1043
0.03	0.2088	0.53	0.1576	1.03	0.1256	1.53	0.1040
0.04	0.2075	0.54	0.1568	1.04	0.1251	1.54	0.1036
0.05	0.2062	0.55	0.1560	1.05	0.1246	1.55	0.1032
0.06	0.2049	0.56	0.1553	1.06	0.1240	1.56	0.1029
0.07	0.2036	0.57	0.1545	1.07	0.1235	1.57	0.1025
0.08	0.2024	0.58	0.1537	1.08	0.1230	1.58	0.1022
0.09	0.2011	0.59	0.1530	1.09	0.1225	1.59	0.1018
0.10	0.1999	0.60	0.1522	1.10	0.1221	1.60	0.1015
0.11	0.1987	0.61	0.1515	1.11	0.1216	1.61	0.1011
0.12	0.1975	0.62	0.1508	1.12	0.1211	1.62	0.1008
0.13	0.1963	0.63	0.1500	1.13	0.1206	1.63	0.1005
0.14	0.1951	0.64	0.1493	1.14	0.1201	1.64	0.1001
0.15	0.1940	0.65	0.1486	1.15	0.1197	1.65	0.0998
0.16	0.1928	0.66	0.1479	1.16	0.1192	1.66	0.0995
0.17	0.1917	0.67	0.1472	1.17	0.1187	1.67	0.0991
0.18	0.1906	0.68	0.1465	1.18	0.1182	1.68	0.0988
0.19	0.1894	0.69	0.1458	1.19	0.1178	1.69	0.0985
0.20	0.1883	0.70	0.1451	1.20	0.1173	1.70	0.0981
0.21	0.1872	0.71	0.1445	1.21	0.1169	1.71	0.0978
0.22	0.1862	0.72	0.1438	1.22	0.1164	1.72	0.0975
0.23	0.1851	0.73	0.1431	1.23	0.1160	1.73	0.0972
0.24	0.1840	0.74	0.1425	1.24	0.1155	1.74	0.0969
0.25	0.1830	0.75	0.1418	1.25	0.1151	1.75	0.0966
0.26	0.1820	0.76	0.1412	1.26	0.1147	1.76	0.0962
0.27	0.1809	0.77	0.1405	1.27	0.1142	1.77	0.0959
0.28	0.1799	0.78	0.1399	1.28	0.1138	1.78	0.0956
0.29	0.1789	0.79	0.1393	1.29	0.1134	1.79	0.0953
0.30	0.1779	0.80	0.1386	1.30	0.1129	1.80	0.0950
0.31	0.1769	0.81	0.1380	1.31	0.1125	1.81	0.0947
0.32	0.1760	0.82	0.1374	1.32	0.1121	1.82	0.0944
0.33	0.1750	0.83	0.1368	1.33	0.1117	1.83	0.0941
0.34	0.1741	0.84	0.1362	1.34	0.1113	1.84	0.0938
0.35	0.1731	0.85	0.1356	1.35	0.1109	1.85	0.0935
0.36	0.1722	0.86	0.1350	1.36	0.1105	1.86	0.0932
0.37	0.1713	0.87	0.1344	1.37	0.1101	1.87	0.0929
0.38	0.1703	0.88	0.1338	1.38	0.1097	1.88	0.0926
0.39	0.1694	0.89	0.1332	1.39	0.1093	1.89	0.0923
0.40	0.1685	0.90	0.1327	1.40	0.1089	1.90	0.0921
0.41	0.1676	0.91	0.1321	1.41	0.1085	1.91	0.0918
0.42	0.1668	0.92	0.1315	1.42	0.1081	1.92	0.0915
0.43	0.1659	0.93	0.1310	1.43	0.1077	1.93	0.0912
0.44	0.1650	0.94	0.1304	1.44	0.1073	1.94	0.0909
0.45	0.1642	0.95	0.1299	1.45	0.1069	1.95	0.0906
0.46	0.1633	0.96	0.1293	1.46	0.1065	1.96	0.0904
0.47	0.1625	0.97	0.1288	1.47	0.1062	1.97	0.0901
0.48	0.1616	0.98	0.1282	1.48	0.1058	1.98	0.0898
0.49	0.1608	0.99	0.1277	1.49	0.1054	1.99	0.0895
0.50	0.1600	1.00	0.1271	1.50	0.1051	2.00	0.0893

η	$K(\xi, \eta)$	η	$K(\xi, \eta)$	η	$K(\xi, \eta)$	η	$K(\xi, \eta)$
			$\xi = 0.80$				
0.01	0.1606	0.51	0.1222	1.01	0.0980	1.51	0.0814
0.02	0.1596	0.52	0.1216	1.02	0.0976	1.52	0.0811
0.03	0.1586	0.53	0.1210	1.03	0.0972	1.53	0.0809
0.04	0.1577	0.54	0.1205	1.04	0.0968	1.54	0.0806
0.05	0.1567	0.55	0.1199	1.05	0.0964	1.55	0.0803
0.06	0.1558	0.56	0.1193	1.06	0.0960	1.56	0.0801
0.07	0.1549	0.57	0.1187	1.07	0.0956	1.57	0.0798
0.08	0.1540	0.58	0.1182	1.08	0.0953	1.58	0.0795
0.09	0.1530	0.59	0.1176	1.09	0.0949	1.59	0.0793
0.10	0.1521	0.60	0.1171	1.10	0.0945	1.60	0.0790
0.11	0.1513	0.61	0.1165	1.11	0.0942	1.61	0.0787
0.12	0.1504	0.62	0.1160	1.12	0.0938	1.62	0.0785
0.13	0.1495	0.63	0.1154	1.13	0.0934	1.63	0.0782
0.14	0.1487	0.64	0.1149	1.14	0.0931	1.64	0.0780
0.15	0.1478	0.65	0.1144	1 15	0.0927	1.65	0.0777
0.16	0.1470	0.66	0.1138	1.16	0.0924	1.66	0.0775
0.17	0.1461	0.67	0.1133	1.17	0.0920	1.67	0.0772
0.18	0.1453	0.68	0.1128	1.18	0.0917	1.68	0.0770
0.19	0.1445	0.69	0.1123	1.19	0.0913	1.69	0 0767
0.20	0.1437	0.70	0.1118	1.20	0.0910	1.70	0.0765
0.21	0.1429	0.71	0.1113	1.21	0.0906	1.71	0.0762
0.22	0.1421	0.72	0.1108	1.22	0.0903	1.72	0.0760
0 23	0.1413	0.73	0.1103	1.23	0.0900	1.73	0 0757
0.24	0.1405	0.74	0.1098	1.24	0.0896	1.74	0.0755
0.25	0.1398	0.75	0.1093	1.25	0.0893	1.75	0.0752
0.26	0.1390	0.76	0.1088	1.26	0.0890	1.76	0.0750
0.27	0.1383	0.77	0.1084	1.27	0.0886	1.77	0.0748
0.28	0.1375	0.78	0.1079	1.28	0.0883	1.78	0.0745
0.29	0.1368	0.79	0.1074	1.29	0.0880	1 79	0.0743
0.30	0.1361	0.80	0 1069	1.30	0.0877	1.80	0.0741
0.31	0.1353	0.81	0.1065	1.31	0.0874	1.81	0.0738
0.32	0 1346	0.82	0.1060	1.32	0.0870	1.82	0.0736
0.33	0.1339	0.83	0.1056	1.33	0.0867	1.83	0.0734
0.34	0.1332	0.84	0.1051	1.34	0.0864	1.84	0.0732
0.35	0.1325	0.85	0.1047	1.35	0.0861	1.85	0.0729
0.36	0.1318	0.86	0.1042	1.36	0.0858	1.86	0.0727
0.37	0.1311	0.87	0.1038	1.37	0.0855	1 87	0.0725
0.38	0.1305	0.88	0.1033	1.38	0.0852	1.88	0.0723
0.39	0.1298	0.89	0.1029	1.39	0.0849	1.89	0.0720
0.40	0.1291	0.90	0.1025	1.40	0.0846	1.90	0.0718
0.41	0.1285	0.91	0.1021	1.41	0.0843	1.91	0.0716
0.42	0.1278	0.92	0.1016	1.42	0.0840	1.92	0.0714
0.43	0.1272	0.93	0.1012	1.43	0.0837	1.93	0.0712
0.44	0.1265	0.94	0.1008	1.44	0.0834	1.94	0.0709
0.45	0.1259	0.95	0.1004	1.45	0.0831	1 95	0.0707
0.46	0.1253	0.96	0.1000	1.46	0.0828	1.96	0.0705
0.47	0.1247	0.97	0.0996	1.47	0 0825	1.97	0.0703
0.48	0.1240	0.98	0.0992	1.48	0.0823	1.98	0.0701
0.49	0.1234	0.99	0.0988	1.49	0.0820	1.99	0.0699
0.50	0.1228	1.00	0.0984	1.50	0.0818	2.00	0.0697

η	$K(\xi, \eta)$	η	$K(\xi, \eta)$	η	$K(\xi, \eta)$	η	$K(\xi, \eta)$
			$\xi = 0{,}90$				
0.01	0.1201	0.51	0.0924	1.01	0.0746	1.51	0.0623
0.02	0.1194	0.52	0.0920	1.02	0.0743	1.52	0.0621
0.03	0.1187	0.53	0.0915	1.03	0.0740	1.53	0.0619
0.04	0.1181	0.54	0.0911	1.04	0.0737	1.54	0.0617
0.05	0.1174	0.55	0.0907	1.05	0.0734	1.55	0.0615
0.06	0.1167	0.56	0.0903	1.06	0.0732	1.56	0.0613
0.07	0.1160	0.57	0 0899	1.07	0.0729	1.57	0.0611
0.08	0.1154	0.58	0.0895	1.08	0.0726	1.58	0.0609
0.09	0.1147	0.59	0.0890	1 09	0.0723	1.59	0.0607
0.10	0.1141	0.60	0.0886	1.10	0.0721	1.60	0.0605
0.11	0.1135	0.61	0.0882	1.11	0.0718	1.61	0.0603
0.12	0.1128	0.62	0.0878	1.12	0.0715	1.62	0.0601
0.13	0.1122	0.63	0.0874	1.13	0.0713	1.63	0.0599
0.14	0.1116	0.64	0.0871	1.14	0.0710	1.64	0.0597
0.15	0.1110	0.65	0.0867	1.15	0.0707	1.65	0.0595
0.16	0.1104	0.66	0.0863	1.16	0.0705	1.66	0.0594
0.17	0.1098	0.67	0.0859	1.17	0.0702	1.67	0.0592
0.18	0.1092	0.68	0.0855	1.18	0.0699	1.68	0.0590
0.19	0.1086	0.69	0.0851	1.19	0.0697	1.69	0.0588
0.20	0.1080	0.70	0.0848	1.20	0.0694	1.70	0.0586
0.21	0.1074	0.71	0.0844	1.21	0.0692	1.71	0.0584
0.22	0.1068	0.72	0.0840	1.22	0.0689	1.72	0.0582
0.23	0.1063	0.73	0 0837	1.23	0.0687	1.73	0.0581
0.24	0.1057	0.74	0.0833	1.24	0.0684	1.74	0.0579
0.25	0.1052	0.75	0.0830	1.25	0.0682	1.75	0.0577
0.26	0.1046	0.76	0.0826	1.26	0.0679	1.76	0.0575
0.27	0.1041	0.77	0.0823	1.27	0.0677	1.77	0.0574
0.28	0.1035	0.78	0.0819	1.28	0.0675	1.78	0.0572
0.29	0.1030	0.79	0.0816	1.29	0.0672	1.79	0.0570
0.30	0.1025	0.80	0.0812	1.30	0.0670	1.80	0.0568
0.31	0.1019	0.81	0.0809	1.31	0.0667	1.81	0.0566
0.32	0.1014	0.82	0.0805	1.32	0.0665	1.82	0.0565
0.33	0.1009	0.83	0.0802	1.33	0.0663	1.83	0.0563
0.34	0.1004	0.84	0.0799	1.34	0.0660	1.84	0.0561
0.35	0.0999	0.85	0.0795	1.35	0.0658	1.85	0.0560
0.36	0.0994	0.86	0.0792	1.36	0.0656	1.86	0.0558
0.37	0.0989	0.87	0.0789	1.37	0.0654	1.87	0.0556
0.38	0.0984	0.88	0.0786	1.38	0.0651	1.88	0.0555
0.39	0.0979	0.89	0.0783	1.39	0.0649	1.89	0.0553
0.40	0.0974	0.90	0.0779	1.40	0.0647	1.90	0.0552
0.41	0.0970	0.91	0.0776	1.41	0.0645	1.91	0.0550
0.42	0.0965	0.92	0.0773	1.42	0.0642	1.92	0.0548
0.43	0.0960	0.93	0.0770	1.43	0.0640	1.93	0.0547
0.44	0.0955	0.94	0.0767	1.44	0.0638	1.94	0.0545
0.45	0.0951	0.95	0.0764	1.45	0.0636	1.95	0.0544
0.46	0.0946	0.96	0.0761	1.46	0.0634	1.96	0.0542
0 47	0.0942	0.97	0.0758	1.47	0.0632	1.97	0.0540
0.48	0.0937	0.98	0.0755	1.48	0.0630	1.98	0.0539
0.49	0.0933	0.99	0.0752	1.49	0.0627	1.99	0.0537
0.50	0.0928	1.00	0.0749	1.50	0.0625	2.00	0.0536

$\xi = 1.00$

η	$K(\xi, \eta)$	η	$K(\xi, \eta)$	η	$K(\xi, \eta)$	η	$K(\xi, \eta)$
0.01	0.0885	0.51	0.0688	1.01	0.0559	1.51	0.0469
0.02	0.0880	0.52	0.0685	1.02	0.0557	1.52	0.0468
0.03	0.0876	0.53	0.0682	1.03	0.0555	1.53	0.0466
0.04	0.0871	0.54	0.0679	1.04	0.0553	1.54	0.0465
0.05	0.0866	0.55	0.0675	1.05	0.0551	1.55	0.0463
0.06	0.0861	0.56	0.0672	1.06	0.0549	1.56	0.0462
0.07	0.0856	0.57	0.0669	1.07	0.0547	1.57	0.0460
0.08	0.0852	0.58	0.0667	1.08	0.0545	1.58	0.0459
0.09	0.0847	0.59	0.0664	1.09	0.0543	1.59	0.0457
0.10	0.0843	0.60	0.0661	1.10	0.0541	1.60	0.0456
0.11	0.0838	0.61	0.0658	1.11	0.0539	1.61	0.0455
0.12	0.0834	0.62	0.0655	1.12	0.0537	1.62	0.0453
0.13	0.0829	0.63	0.0652	1.13	0.0535	1.63	0.0452
0.14	0.0825	0.64	0.0649	1.14	0.0533	1.64	0.0450
0.15	0.0820	0.65	0.0646	1.15	0.0531	1.65	0.0449
0.16	0.0816	0.66	0.0644	1.16	0 0529	1.66	0.0448
0.17	0.0812	0.67	0.0641	1.17	0.0527	1.67	0.0446
0.18	0.0808	0.68	0.0638	1.18	0.0525	1.68	0.0445
0.19	0.0803	0.69	0.0635	1.19	0.0523	1.69	0.0443
0.20	0.0799	0.70	0.0633	1.20	0.0521	1.70	0.0442
0.21	0.0795	0.71	0.0630	1.21	0.0520	1.71	0.0441
0.22	0.0791	0.72	0.0627	1.22	0.0518	1.72	0.0439
0.23	0.0787	0.73	0.0625	1.23	0.0516	1.73	0.0438
0.24	0.0783	0.74	0.0622	1.24	0.0514	1.74	0.0437
0.25	0.0779	0.75	0.0620	1.25	0.0512	1.75	0.0435
0.26	0.0775	0.76	0.0617	1.26	0.0510	1.76	0.0434
0.27	0.0771	0.77	0.0615	1.27	0.0509	1.77	0.0433
0.28	0.0767	0.78	0.0612	1.28	0.0507	1.78	0.0431
0.29	0.0764	0.79	0.0610	1.29	0 0505	1.79	0.0430
0.30	0.0760	0.80	0.0607	1.30	0.0503	1.80	0.0429
0.31	0.0756	0.81	0.0605	1.31	0.0502	1.81	0.0428
0.32	0.0752	0.82	0.0602	1.32	0.0500	1.82	0.0427
0.33	0 0749	0.83	0.0600	1.33	0.0498	1.83	0.0425
0.34	0.0745	0.84	0.0597	1.34	0.0497	1.84	0.0424
0.35	0.0741	0.85	0.0595	1.35	0.0495	1.85	0.0423
0.36	0.0738	0.86	0.0593	1.36	0.0493	1.86	0.0422
0.37	0.0734	0.87	0.0590	1.37	0.0492	1.87	0.0420
0.38	0.0731	0.88	0.0588	1.38	0.0490	1.88	0.0419
0.39	0.0727	0.89	0.0586	1.39	0.0488	1.89	0.0418
0.40	0.0724	0.90	0.0587	1.40	0 0487	1.90	0.0417
0.41	0.0720	0.91	0.0581	1.41	0.0485	1.91	0.0415
0.42	0.0717	0.92	0.0579	1.42	0.0483	1.92	0.0414
0.43	0.0714	0.93	0.0576	1.43	0.0482	1.93	0.0413
0.44	0.0710	0.94	0.0574	1.44	0.0480	1.94	0.0412
0.45	0.0707	0.95	0.0572	1.45	0.0479	1.95	0.0411
0.46	0.0704	0.96	0.0570	1.46	0.0477	1.96	0.0410
0.47	0.0700	0.97	0.0568	1.47	0.0475	1.97	0.0408
0.48	0.0697	0.98	0.0565	1.48	0.0474	1.98	0.0407
0.49	0.0694	0.99	0.0563	1.49	0.0472	1.99	0.0406
0.50	0.0691	1.00	0.0561	1.50	0.0471	2.00	0.0405

Bibliography

1. Lykov, A.V. Teoriya teploprovodnosti (The Theory of Thermal Conductivity). — Gostekhizdat. 1952.
2. Rykalin, N.N. Teplovye osnovy svarki (The Thermal Principles of Welding). — Izd. AN SSSR. 1947.
3. Maslov, E.N. Osnovy teorii shlifovaniya (Principles of the Theory of Grinding). — Mashgiz. 1951.
4. Podzei, A.V. Opredelenie temperaturnogo polya v detalyakh pri obrabotke shlifovaniem (Determination of the Temperature Field in Workpieces during Grinding). — Oborongiz. 1960.
5. Red'ko, S.G. Protsessy teploobrazovaniya pri shlifovanii metallov (Generation of Heat during Grinding of Metals). — Izd. Saratovskogo Universiteta. 1962.
6. Isaev, A.I. and S.S. Silin. — Vestnik Mashinostroeniya, No. 5. 1957.
7. Shatunov, M.P. and V.F. Sovkin. — IFZh, No. 11. 1962.
8. Shatunov, M.P. and V.F. Sovkin. — Izvestiya Vysshikh uchebnykh zavedenii. Mashinostroenie, No. 2. 1962.
9. Pilinskii, V.I. and Yu.A. Novoselov. — Vestnik mashinostroeniya, No. 11. 1963.

A. G. Temkin

*RECONSTRUCTION OF THE HEAT AND MASS CONTENT FIELDS OF A COLLOIDAL BODY**

HEAT AND MASS TRANSFER EQUATIONS FOR A COLLOIDAL BODY. THE PROBLEM OF FIELD RECONSTRUCTION

The process of drying of a colloidal body, for which the Soret coefficient is extremely small, is described by a system of equations proposed by Lykov /1, 2, 3/

$$\frac{\partial u}{\partial \tau} = a' \nabla^2 u, \tag{1}$$

$$\frac{\partial t}{\partial \tau} = a \nabla^2 t + \frac{\varepsilon \rho}{c} \frac{\partial u}{\partial \tau}, \tag{2}$$

where u is the mass content g/g; a' is the potential conductivity coefficient of the colloidal substance, m^2/sec; a is the thermal diffusivity of the substance, m^2/sec; ε is a dimensionless number (the "phase transformation criterion"); ρ is the heat of phase transformation, j/g; c is the heat capacity of the body, calculated on the basis of one gram of absolutely dry body, j/g°C; t is the temperature, °C; and τ is the time, sec.

The Laplacian operator has been taken in the one-coordinate form /4, 5/. It is most convenient to use the radius of the body as the characteristic dimension /5, 6/. After conversion to a dimensionless form, the drying equations assume the form

$$\frac{\partial u}{\partial H} = \mathrm{Lu}\left[\frac{\partial^2 u}{\partial N^2} + \frac{k-1}{N}\frac{\partial u}{\partial N}\right], \tag{3}$$

$$\frac{\partial T}{\partial H} = \frac{\partial^2 T}{\partial N^2} + \frac{k-1}{N}\frac{\partial T}{\partial N} + \varepsilon \mathrm{Ko}\frac{\partial u}{\partial H}. \tag{4}$$

For the surface of the body the dimensionless single coordinate N is equal to unity. The Kossovich number has been defined /2/ as

$$\mathrm{Ko} = \frac{\rho \Delta u}{c \Delta t}, \tag{5}$$

the homochronicity complex is as in /5/, and the Lykov number (coupling number) is

$$\mathrm{Lu} = \frac{a'}{a}. \tag{6}$$

* [Printed here as a discussion.]

The problem of energy and mass transfer is usually solved for given boundary conditions /7 — 10/ existing on the surface of the body. The boundary conditions describing the interaction of the body with its surroundings are assumed to be known. In many cases /14/ the heat and mass transfer conditions are unknown, but the experimenter is able to record the changes of the mean moisture content of the body and one or several local temperatures.

The solution of the system of transfer equations (1) and (2) that satisfies the conditions within the bulk of the body (and not on its surface) is known as the reconstruction of the mass- and heat-content fields. The field reconstruction is carried out on the basis of parameters whose values are known either for some points in the interior of the body or as mean values for the bulk. In reconstruction problems, such experimentally determined values replace the boundary conditions used in boundary problems. An example of the reconstruction of symmetrical and asymmetrical temperature fields on the basis of one and two temperature measurements in the interior of a solid body has been described in the literature /11, 12/.

The problems related to the reconstruction of temperature fields on the basis of internal measurements may be represented in accordance with Laplace. However, such a representation has no original. For instance, when the temperature is measured at the center of a plate /11/

$$t(0, H) = t_1(H) \doteqdot \theta_1(s) \tag{7}$$

the representation of the temperature field

$$\theta(N, s) = \operatorname{ch} N\sqrt{s}\,\theta_1(s) \tag{8}$$

does not permit the determination of the original by means of an inversion formula since

$$\operatorname{ch} N\sqrt{s} \doteqdot \sum_{n=0}^{\infty} \frac{N^{2n}}{(2n)!}\delta^{(n)}(H). \tag{9}$$

However, the use of the natural method, which consists in expanding the solution into a series in terms of derivatives of the measured values, makes it possible to determine the main part of the temperature field — the action field

$$t_a(N, H) = \sum_{n=0}^{\infty} t_1^{(n)}(H)\frac{N^{2n}}{(2n)!}, \tag{10}$$

while the use of the Fourier integral leads to the calculation of the residual field, i.e., the after-effect field

$$t_r(N, H) = \frac{-2}{\pi}\int_0^{\infty}\exp(-\eta_i^2 H)\cos\eta N\, d\eta \times$$
$$\times\int_0^1\sum_{n=0}^{\infty} t_1^{(n)}(0)\frac{\xi^{2n}}{(2n)!}\cos\xi\eta\, d\xi, \tag{11}$$

and the sum of these fields describes the temperature field of the plate for a centrally located measuring element

$$t(N, H) = t_a(N, H) + t_r(N, H). \tag{12}$$

The sum of these two components satisfies the condition of internal measurement (7), the symmetry condition, and the condition of homogeneous initial temperature distribution.

RECONSTRUCTION OF THE MOISTURE FIELD

The determination of the moisture field by its mean value

$$u_v(\tau) = \frac{k}{R^k}\int_0^R u(r,\tau)\, r^{k-1} dr \qquad (13)$$

is exactly equivalent to the integration of the mass conductivity equation (1) for a boundary condition of the second kind. In this case the reconstruction problem is reduced to a boundary problem.

The specific flow of the substance on the surface of the body

$$q_m = -a'\gamma_0 \nabla u(R,\tau) \qquad (14)$$

is proportional to the variations in the mean moisture content

$$q_m = \frac{l_v^k}{l_s^{k-1}}\gamma_0 \frac{du_v}{d\tau}, \qquad (15)$$

where γ_0 is the density of the absolutely dry substance, g/cm^3. An obvious relationship exists between the drying rate and the moisture gradient on the surface of the body:

$$-\nabla u(R,\tau) = \frac{R}{k}\frac{du_v}{d\tau}, \qquad (16)$$

where the radius of the body R has been determined /5, 6/ while k is the number of finite dimensions of the body. Using dimensionless variables, the above relationship is written as follows:

$$Q_m(H) = \frac{\partial}{\partial N} u(1,H) = \frac{1}{k\,\mathrm{Lu}}\frac{du_v}{dH} \qquad (17)$$

or, if the product of the Fourier, Lobachevskii, and Lykov numbers is taken as the homochronicity complex

$$H' = \mathrm{Lu\,Lo\,Fo}, \qquad (18)$$

it will be written in a simplified form

$$Q_m(H') = \frac{\partial}{\partial N} u(1,H') = \frac{1}{k}\frac{du_v}{dH'}. \qquad (19)$$

The dimensionless mean (with respect to volume) moisture content is given by the integral

$$u_v(H') = k\int_0^1 u(N,H')\, N^{k-1}\, dN. \qquad (20)$$

The temperature field satisfying the boundary condition of the second kind is described /13/ by a series:

$$u(N,H') = \sum_{n=0}^{\infty} Q_m^{(n-1)}(H')\, L_{2n}(N,0,k) + \sum_{n=0}^{\infty} Q_m^{(n-1)}(0) L_{2n}(N,H',0,k), \qquad (21)$$

in which $L_{2n}(N,0,k)$ are radial polynomials of the second kind, and $L_{2n}(N,H',0,k)$ are the respective generalized radial functions. In cases in which the mean

mass content of the body is known, the moisture field may evidently be presented as a series expanded in terms of the mass-content derivatives

$$u(N,H') = \frac{1}{k}\left[\sum_{n=0}^{\infty} u_v^{(n)}(H') L_{2n}(N,0,k) + \right.$$

$$\left. + \sum_{n=1}^{\infty} u_v^{(n)}(0) L_{2n}(N,H',0,k) \right]. \qquad (22)$$

The radial polynomials that were derived in /13/ as sums of lambda-function series may be determined recurrently:

$$L_{2n}(N,0,k) = \int_0^N r_l^{1-k}\, d r_l \int_0^{r_l} \xi^{k-1} L_{2n-2}(\xi,0,k)\, d\xi - k \times$$

$$\times \int_0^1 N^{k-1}\, dN \int_0^N r_l^{1-k}\, d r_l \int_0^{r_l} \xi^{k-1} L_{2n-2}(\xi,0,k)\, d\xi \qquad (23)$$

or by using the integral operator (∇^{-2}) for this problem,

$$\nabla^{-2} F = \int_0^N r_l^{1-k}\, d r_l \int_0^{r_l} F(\xi)\, \xi^{k-1} d\xi\,; \qquad (24)$$

by using the notation for the mean value (with respect to volume) of the function

$$\overline{F} = k \int_0^1 N^{k-1} F(N)\, dN, \qquad (25)$$

the radial polynomials corresponding to the boundary conditions of the second kind may be written

$$L_{2n}(N,0,k) = \nabla^{-2} L_{2n-2}(N,0,k) - \overline{\nabla^{-2} L_{2n-2}(N,0,k)}. \qquad (26)$$

The generalized radial functions for boundary conditions of the second kind

$$L_{2n}(N,H',0,k) = (-1)^n \sum_{p=1}^{\infty} \frac{2r(\mu_p N,k)}{\mu_p^{2n}\, r(\mu_p,k)} \exp(-\mu_p^2 H') \qquad (27)$$

are characteristic numbers, while μ_p are the roots of the derivative

$$r'(\mu_p,k) = 0. \qquad (28)$$

The generalized radial functions rapidly approach zero as the time is increased; hence, the second series in the sum (22) represents the after-effect field. In the case of large values of the homochronicity complex H' the main part of the mass content field consists of the action field

$$u_a(N,H') = \frac{1}{k} \sum_{n=0}^{\infty} u_v^{(n)}(H')\, L_{2n}(N,0,k). \qquad (29)$$

The sum of the action and after-effect fields /22/ satisfies the symmetry condition

$$\frac{\partial}{\partial N} u(0,H') = 0, \qquad (30)$$

the condition for averaging with respect to the volume (20) and, at the starting moment

$$u(N,0) = u_v(0). \tag{31}$$

RECONSTRUCTION OF THE TEMPERATURE FIELD OF A MOIST BODY

The temperature field of a moist body is described by equation (4), which after substituting

$$\varepsilon \mathrm{Ko}\,\frac{\partial u(N,H')}{\partial H} = \varepsilon\,\mathrm{Ko}\,\mathrm{Lu}\,\frac{\partial u(N,H')}{\partial H'}$$

by the respective partial derivative of the action field of the mass content (29) assumes the form

$$\frac{\partial T}{\partial H} = \frac{\partial^2 T}{\partial N^2} + \frac{k-1}{N}\frac{\partial T}{\partial N} +$$

$$+ \frac{\varepsilon\,\mathrm{Ko}\,\mathrm{Lu}}{k}\sum_{n=0}^{\infty}\frac{u_v^{(n+1)}(H)}{\mathrm{Lu}^{n+1}}L_{2n}(N,0,k). \tag{32}$$

The problem of reconstructing the symmetrical temperature field of a moist body on the basis of temperature measurements at one point is exactly the same as the analogous problem for an exothermic body with known heat sources. In this case it is necessary to find a solution of the equation

$$\frac{\partial T}{\partial H} = \frac{\partial^2 T}{\partial N^2} + \frac{k-1}{N}\frac{\partial T}{\partial N} + W(N,H), \tag{33}$$

which is symmetrical at the center of the body

$$\frac{\partial}{\partial N}T(0,H) = 0 \tag{34}$$

and at the point of measurement N_0. The position of that point is known:

$$T(N_0,H) = T_0(H). \tag{35}$$

For the problem discussed here it is expedient to determine the integral operator

$$\nabla^{-2}F(N) = \int_{N_0}^{N}\eta^{1-k}d\eta\int_{0}^{\eta}F(\xi)\xi^{k-1}d\xi, \tag{36}$$

which together with its higher powers satisfies the symmetry condition at the center of the body

$$\frac{d}{dN}\left[\nabla^{-2}F(N)\right]_{N=0} = 0 \tag{37}$$

and the condition for internal temperature measurement at the point N_0

$$\nabla^{-}F(N_0) = 0. \tag{38}$$

Any linear combination of the powers of the operator

$$V(N) = \Sigma C_n \nabla^{-2n} F(N) \tag{39}$$

possesses the qualities (37) and (38) if the function $F(N)$ is satisfactory.

The action field of (33) — (35) consists of a sum of two series, the first of which is expanded in terms of derivatives of the measured temperature and powers of the integral operator (36), applied to unity, while the second series is expanded in terms of increasing powers of the same operator, applied to the time derivatives of the intensity of internal heat sources

$$T_a(N,H) = \sum_{n=0}^{\infty} T_0^{(n)}(H) \nabla^{-2n} \cdot 1 - \sum_{n=0}^{\infty} \nabla^{-2n-2} W^{(n)}(N,H) \tag{40}$$

or, in an expanded form,

$$\begin{aligned} T_a(N,H) = T_0(H) + T_0'(H) \nabla^{-2} \cdot 1 + T_0^{(2)}(H) \nabla^{-4} \cdot 1 + \ldots + \\ + T_0^{(n)}(H) \nabla^{-2n} \; 1 + \ldots - \nabla^{-2} W(N,H) - \\ - \nabla^{-4} W^{(1)}(N,H) - \nabla^{-6} W^{(2)}(N,H) - \ldots - \nabla^{-2n-2} W^{(n)}(N,H) - \ldots \end{aligned} \tag{41}$$

Direct substitution proves that the above sum satisfies the thermal conductivity equation for an exothermic body (33), the symmetry condition (34), and the condition for internal temperature measurement (35). The last is due to the fact that the higher powers of the integral operator (∇^{-2}) always satisfy conditions (37) and (38).

However, the dimensionless intensity of heat fluxes for a moist body is represented by the series

$$W(N,H) = \frac{\varepsilon \mathrm{Ko}}{k} \sum_{n=0}^{\infty} u_v^{(n+1)}(H) \, \mathrm{Lu}^{-n} L_{2n}(N,0,k). \tag{42}$$

and the application of the integral operation (36) to the above series yields the sum

$$\nabla^{-2m-2} W(N,H) = \frac{\varepsilon \mathrm{Ko}}{k} \sum_{n=0}^{\infty} \frac{u_v^{(n+1)}(H)}{\mathrm{Lu}^n} \nabla^{-2m-2} L_{2n}(N,0,k). \tag{43}$$

It must be taken into account that in a dimensional (with respect to time) form the action field for the mass content is

$$W(N,H) = \frac{\varepsilon \mathrm{Ko}}{k} \sum_{n=0}^{\infty} u_v^{(n+1)}(\tau) \left(\frac{R^2}{a'}\right)^n L_{2n}(N,0,k), \tag{44}$$

as the moisture content u_v is known as a function of time τ and not of some of the homochronicity complexes H or H'. Hence, the partial derivative of the sum (43) with respect to time will be expressed by the expansion

$$\begin{aligned} \nabla^{-2m-2} W^{(m)}(N,H) = \frac{\varepsilon \mathrm{Ko}}{k} \sum_{n=0}^{\infty} u_v^{(n+m+1)}(\tau) \times \\ \times \left(\frac{R^2}{a'}\right)^n \left(\frac{R^2}{a}\right)^m \nabla^{-2m-2} L_{2n}(N,0,k) = \\ = \frac{\varepsilon \mathrm{Ko}}{k} \sum_{n=0}^{\infty} u_v^{(n+m+1)}(H) \, \mathrm{Lu}^{-n} \nabla^{-2m-2} L_{2n}(N,0,k). \end{aligned} \tag{45}$$

In this way the action field for the temperature of a moist body that has been reconstructed on the basis of a single temperature measurement and the mean moisture content, will be described by the double series

$$T_a(N,H)=\sum_{n=0}^{\infty}T_0^{(n)}(H)\,\nabla^{-2n}\cdot 1-$$

$$-\frac{\varepsilon\,\mathrm{Ko}}{k}\sum_{m=0}^{\infty}\sum_{n=0}^{\infty}u_v^{(n+m+1)}(H)\,\mathrm{Lu}^{-n}\nabla^{-2m-2}L_{2n}(N,0,k) \qquad (46)$$

or, in detail,

$$T_a(N,H)=T_0(H)+T_0'(H)\,\nabla^{-2}\cdot 1+T_0''(H)\,\nabla^{-4}\cdot 1+\ldots+$$
$$+T_0^{(n)}(H)\nabla^{-2n}\cdot 1+\ldots-\frac{\varepsilon\,\mathrm{Ko}}{k}\{u_v'(H)\nabla^{-2}L_0(N,0,k)+$$
$$+u_v^{(2)}(H)\,\mathrm{Lu}^{-1}\nabla^{-2}L_2(N,0,k)+u_v^{(3)}(H)\mathrm{Lu}^{-2}\nabla^{-2}L_4(N,0,k)+\ldots\}+$$
$$+\{u_v^{(2)}(H)\,\nabla^{-4}L_0(N,0,k)+u_v^{(3)}(H)\,\mathrm{Lu}^{-1}\nabla^{-4}L_2(N,0,k)+$$
$$+u_v^{(4)}(H)\,\mathrm{Lu}^{-2}\nabla^{-4}L_4(N,0,k)+\ldots\}+\ldots$$
$$\ldots+\{u_v^{(m+1)}(H)\,\nabla^{-2m-2}L_0(N,0,k)+u_v^{(m+2)}(H)\,\mathrm{Lu}^{-1}\nabla^{-2m-2}L_2\times$$
$$\times(N,0,k)+u_v^{(m+3)}(H)\,\mathrm{Lu}^{-2}\nabla^{-2m-2}L_4(N,0,k)+\ldots]+\ldots\}. \qquad (47)$$

In the second sum, which is confined within the braces, it is possible to rearrange the terms and to isolate as factors the derivatives of the mean moisture content with respect to the homochronicity complex

$$T_a(N,H)=T_0(H)+T_0'(H)\,\nabla^{-2}\cdot 1+\ldots+T_0^{(n)}(H)\,\nabla^{-2n}\cdot 1+\ldots-$$
$$-\frac{\varepsilon\,\mathrm{Ko}}{k}\{u_v'(H)[\nabla^{-2}L_0(N,0,k)]+$$
$$+u_v^{(2)}(H)\,[\nabla^{-4}L_0(N,0,k)+\mathrm{Lu}^{-1}\nabla^{-2}L_2(N,0,k)]+$$
$$+u_v^{(3)}(H)\,[\nabla^{-6}L_0(N,0,k)+\mathrm{Lu}^{-1}\nabla^{-4}L_2(N,0,k)+\mathrm{Lu}^{-2}\nabla^{-2}L_4\times$$
$$\times(N,0,k)]+\ldots+u_v^{(m)}(H)\,[\nabla^{-2m}L_0(N,0,k)+\mathrm{Lu}^{-1}\nabla^{2-2m}\times$$
$$\times L_2(N,0,k)+\mathrm{Lu}^{-2}\nabla^{4-2m}L_4(N,0,k)+\ldots+$$
$$+\mathrm{Lu}^{1-m}\nabla^{-2}L_{2m-2}(N,0,k)]+\ldots\} \qquad (48)$$

or, in an abridged form, by arranging the expression depending on the moisture in terms of its derivatives

$$T_a(N,H)=\sum_{n=0}^{\infty}T_0^{(n)}(H)\,\nabla^{-2n}\cdot 1-$$
$$-\frac{\varepsilon\,\mathrm{Ko}}{k}\sum_{m=1}^{\infty}u_v^{(m)}(H)\sum_{p=0}^{m-1}\mathrm{Lu}^{-p}\nabla^{2p-2m}L_{2p}(N,0,k). \qquad (49)$$

When all other parameters are known the solution of the above expression makes it possible to calculate the temperature gradient on the surface of the body and to determine the Biot number for heat transfer complicated

by mass transfer. When the thermal diffusivity, the phase transformation number ε, and the Lykov number are unknown, additional temperature measurements at one or three points would make it possible to determine the thermal parameters of the substance and to solve from there the inverse heat and mass transfer problem /14, 15/.

The dimensional with respect to all variables (except the coordinate N) form of the expansion (49) for a classical body is

$$t_a(N,\tau) = \sum_{n=0}^{\infty} t_0^{(n)}(\tau)\left(\frac{R^2}{a}\right)^n \nabla^{-2n}\cdot 1 - \\ -\frac{\varepsilon\rho}{kc}\sum_{m=1}^{\infty} u_\varepsilon^{(m)}(\tau)\left(\frac{R^2}{a}\right)^m \sum_{p=0}^{m-1} \mathrm{Lu}^{-p}\nabla^{2p-2m} L_{2p}(N,0,k). \qquad (50)$$

By measuring the temperature at several more points, the parameters a, ε, Lu, and a' may be determined from (50).

Bibliography

1. Lykov, A.V. Teoriya sushki (Theory of Drying). — GEI. 1950.
2. Lykov, A.V. Yavleniya perenosa v kapillyarnoporistykh telakh (Transfer Phenomena in Capillary-porous Bodies). — GITTL. 1954.
3. Lykov, A.V. Teplo- i massoobmen v protsessakh sushki (Heat and Mass Transfer in Drying Processes). — GEI. 1956.
4. Temkin, A.G. Vsesoyuznoe nauchno-tekhnicheskoe soveshchanie po intensifikatsii protsessov sushki. Energeticheskaya sektsiya (All-Union Scientific-Technological Conference on the Intensification of Drying Processes. Power-Engineering Section). — Profizdat. 1958.
5. Temkin, A.G. — IFZh, No.4. 1962.
6. Temkin, A.G. — ZhTF, No.3. 1955.
7. Smirnov, M.S. — Trudy NIKFI, No.2. 1958.
8. Prudnikov, A.P. — Doklady AN SSSR, Vol.120, No.2. 1958.
9. Lykov, A.V. and Yu.A. Mikhailov. Teoriya perenosa energii i veshchestva (Theory of Heat and Mass Transfer). — Izd. AN BSSR. 1959.
10. Polonskaya, F.M. — IFZh, No.2. 1958.
11. Temkin, A.G. — IFZh, No.4. 1961.
12. Temkin, A.G. — IFZh, No.5. 1961.
13. Temkin, A.G. — IFZh, No.1. 1960.
14. Kavkazov, Yu.L. Vsesoyuznoe nauchno-tekhnicheskoe soveshchanie po intensifikatsii protsessov sushki. Energeticheskaya sektsiya (All-Union Scientific-Technological Conference on the Intensification of Drying Processes. Power-Engineering Section). — Profizdat. 1958.
15. Bab'ev, N.N. — Trudy MTIPP, No.6. 1956.

G.I. Bobrova and G.D. Rabinovich

DETERMINATION OF THE SORET COEFFICIENTS AND THE CONCENTRATION DIFFUSION COEFFICIENTS BY AN UNSTEADY-STATE METHOD

In the computation of thermal diffusion columns the important parameters that markedly affect the separation effectiveness are the Soret coefficient σ and the concentration diffusion coefficient D_{12}. Usually, the diffusion coefficient is determined under isothermal conditions by steady-state or unsteady-state methods /1, 2/. The use of the results thus obtained for the calculation of thermal diffusion columns must always introduce an error in the final result since a temperature gradient exists in the column and the values of D_{12} on the cold and hot walls of the apparatus may differ markedly. Since in liquids D_{12} is a complex function of the temperature /3/, the determination of a mean value of D_{12} for the calculations is very complicated. Hence, the development of a method for the determination of D_{12} under non-isothermic conditions (corresponding to the real conditions of operation of a thermal diffusion column) is of practical value.

The method we propose makes it possible to determine in a single experiment both the Soret coefficient σ and the concentration diffusion coefficient.

If the mixture to be investigated is placed between two parallel horizontal surfaces (Figure 1 b) the distance between which is much smaller than their diameter (in the case of a circular cell), and the temperatures T_1 and T_2 ($T_1 > T_2$) are maintained on the surfaces, a thermal diffusion process starts in the mixture; it is accompanied by conventional concentration diffusion that tends to equalize the concentrations over the height of the gap.

The molecular transfer process is described by the equation

$$\rho \frac{\partial c}{\partial \tau} = -\operatorname{div} j, \tag{1}$$

where

$$j = -\rho D_e \left[\frac{\partial c}{\partial x} - \sigma c (1-c) \frac{\partial T}{\partial x} \right]. \tag{2}$$

Since under the above conditions δ is much smaller than the diameter of the cell surface the problem may be considered as one-dimensional and edge effects may be neglected. Since the heat and mass streams are countercurrent, the gradients have opposite signs. The term D_e in (2) is the effective concentration diffusion coefficient, i.e., the mean value taking into account the non-isothermal nature of the process and remaining constant throughout the experiment. The dependence of the density of the

liquid mixture ρ on the temperature may be neglected under the conditions of the experiment. Since in the experimental cell (Figure 1 *a*) the transfer of heat from the hot to the cold surface is by thermal conductivity alone, the temperature distribution is a linear function of the coordinate x, i.e.,

$$\frac{\partial T}{\partial x} = \frac{T_1 - T_2}{\delta} = \frac{\Delta T}{\delta}. \tag{3}$$

This is valid only after the establishment of a steady temperature field, the steady state being approached after a time determined from

$$\mathrm{Fo} = \frac{a\tau}{\delta^2} > 3. \tag{4}$$

In aqueous solutions the thermal diffusivity coefficient has a value of ~ 5 cm^3/hr; hence, when the distance between the plates is one cm the time needed for the establishment of a linear temperature distribution would be 0.5 hrs (in accordance with /4/). In the problem discussed here the diffusion process reaches a steady state within the time

$$\tau = 0{,}5\,\delta^2/D \quad (\mathrm{Fo}_m = 0.5). \tag{5}$$

Since in liquids the value of D is of the order of 10^{-5} cm^2/sec, we have $\tau \approx 15$ hrs for $\delta = 1$ cm, i.e., the time of existence of a transient temperature field is about 3% of the above value. In view of this, it is possible to assume in the formulation of boundary conditions that equation (3) is practically valid from the start of the experiment.

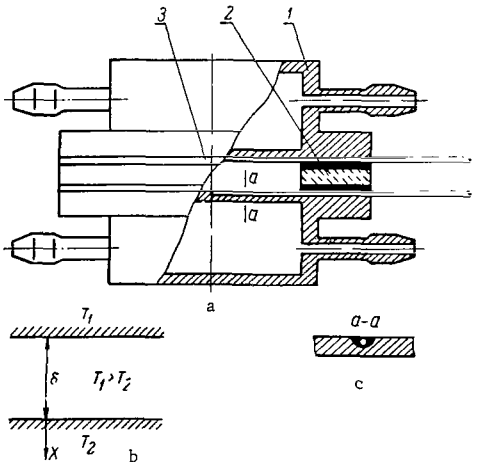

FIGURE 1. Schematic view of the apparatus.

a – schematic view of the cell surface; b – cell;
c – needle embedded on the cell surface.

Using the notation

$$\sigma \Delta T/\delta = \beta \tag{6}$$

and taking into account the above considerations we obtain (after mathematical transformations) an equation

$$\frac{\partial c}{\partial \tau} = D\left[\frac{\partial^2 c}{\partial x^2} - \beta \frac{\partial c(1-c)}{\partial x}\right]. \tag{7}$$

Equation (7) is non-linear and its solution is very difficult. It is of interest to note that an equation of the same type is used to describe the transient transfer in thermal diffusion columns; the solution obtained by Berdin and Debye /4/ is valid in cases in which $c \ll 1$.

Equation (7) may be solved also for cases in which

$$c(1-c) = a + bc \tag{8}$$

in the expected range of concentrations, or if the product $c(1-c)$ is assumed to be constant (which is fairly accurate in the range $0.3 < c < 0.7$). It has been assumed /5/ that $c(1-c)$ may be regarded as constant even if c does not fall in the above range. The author apparently bases the above assumption on the fact that in experiments for the determination of the Soret coefficient the absolute variations in the above product are very small. We shall prove below that this assumption is erroneous. The method recommended in /5/ has a disadvantage associated with the fact that in experiments the separation by thermal diffusion must be carried out to a state near to the steady state, since the Soret coefficient is determined by means of an equation satisfying the condition $\mathrm{Fo}_m \to \infty$.

In order to obtain a solution of a more general nature, we assumed the validity of a linear approximation as determined by equation (8). It is easily proved that the constant b lies in the range $-1 < b < 1$ and that $b > 0$ when the concentration of the studied component is below 0.5 while $b < 0$ when $c > 0.5$. At $c = 0.5$, $b = 0$. However, the last case is practically impossible, since even a small shift in concentration caused by thermal diffusion results in b other than zero.

Thus, instead of (7) we obtain another equation

$$\frac{\partial c}{\partial \tau} = D\left(\frac{\partial^2 c}{\partial x^2} - b\beta \frac{\partial c}{\partial x}\right), \tag{9}$$

which after substitution of variables yields

$$c - c_0 = \vartheta, \quad x/\delta = z, \quad D\tau/\delta^2 = \mathrm{Fo}_m \tag{10}$$

and introduction of the notation ε yields

$$\frac{\partial \vartheta}{\partial \mathrm{Fo}_m} = \frac{\partial^2 \vartheta}{\partial z^2} - 2\varepsilon \frac{\partial \vartheta}{\partial z}, \tag{11}$$

where $\varepsilon = \dfrac{b\beta\delta}{2}$.

Since the currents on the surfaces confining the cell are equal to zero, we obtain for $\mathrm{Fo}_m > 0$ the following boundary conditions:

$$\frac{\partial \vartheta}{\partial z} = 2\varepsilon\left(\frac{a}{b} + c_0 + \vartheta\right) \text{ at } \begin{cases} z = 0 \\ z = 1 \end{cases} \tag{12}$$

and the initial condition

$$\vartheta\,|_{\mathrm{Fo}_m = 0} = 0. \tag{13}$$

Solution of (11) by the integral transform method yields the following expression satisfying conditions (12) and (13):

$$b\frac{c-c_0}{c_0(1-c_0)} = \varepsilon\frac{\exp\{-\varepsilon(1-2z)\}}{\operatorname{sh}\varepsilon} - 1 + 4\pi\varepsilon(\exp-\varepsilon+1)\exp\varepsilon z \times$$

$$\times\sum_{k=0}^{\infty}\frac{2k+1}{[\varepsilon^2+\pi^2(2k+1)^2]^2}[\varepsilon\sin\pi(2k+1)z + \pi(2k+1)\cos\pi(2k+1)z]\exp\{-[\varepsilon^2+\pi^2(2k+1)^2]\,\mathrm{Fo}_m\}. \quad (14)$$

Since liquid samples for analysis are withdrawn at the two thermostated surfaces (i.e., at $z = 0$ and $z = 1$) equation (14) assumes for the above cases a simpler form:

for $z = 0$

$$b\frac{c-c_0}{c_0(1-c_0)} = \frac{\varepsilon\exp-\varepsilon}{\operatorname{sh}\varepsilon} - 1 + 4\pi^2\varepsilon[\exp(-\varepsilon)+1]\times$$

$$\times\sum_{k=0}^{\infty}\frac{(2k+1)^2}{[\varepsilon^2+\pi^2(2k+1)^2]^2}\exp\{-[\varepsilon^2+\pi^2(2k+1)^2]\,\mathrm{Fo}_m\}, \quad (14a)$$

and for $z = 1$

$$b\frac{c-c_0}{c_0(1-c_0)} = \frac{\varepsilon\exp\varepsilon}{\operatorname{sh}\varepsilon} - 1 - 4\pi^2\varepsilon(\exp\varepsilon+1)\times$$

$$\times\sum_{k=0}^{\infty}\frac{(2k+1)^2}{[\varepsilon^2+\pi^2(2k+1)^2]^2}\exp\{-[\varepsilon^2+\pi^2(2k+1)^2]\,\mathrm{Fo}_m\}. \quad (14b)$$

Equations (14a) and (14b) show that the changes in concentration on the two surfaces are not equal, i.e., the changes are asymmetrical with respect to the starting concentration. At the same time, the analytical solution /5/ indicates that the concentration changes at the hot and cold ends of the cell are equal in absolute values. This conclusion was reached by assuming that $c(1-c) = \text{const}$, which corresponds to a value $b = 0$ in equations (8), (14a), and (14b). In such a case the last two equations become identical. Thus, although in experiments for the determination of the Soret coefficient the value of $c(1-c)$ changes very slightly, the value of b will nevertheless differ noticeably from zero. For instance, when the concentration in the cell changes from 0.10 to 0.11 equation (8) assumes the form $c(1-c) = 0.8c - 0.1$, i.e., $b = 0.8$.

When $b > 0$, i.e., $c < 0.5$ we have for a steady state ($\mathrm{Fo}_m \to \infty$) $< c_0$ for $z = 0$ and $c > c_0$ for $z = 1$. It is evident that the above conclusion is also valid for an unsteady state.

It is of interest to elucidate the direction of the above-mentioned asymmetry in the concentration changes; this is most conveniently done for a steady state. Using the notation

$$\frac{c-c_0}{c_0(1-c_0)} = c_1^*, \quad \frac{c_0-c}{c_0(1-c_0)} = c_0^*, \quad (15)$$

we obtain that for $\mathrm{Fo}_m \to \infty$

$$c_1^* - c_0^* = \frac{2}{b}\left(\frac{\varepsilon}{\operatorname{th}\varepsilon} - 1\right). \quad (16)$$

Since the right-hand part of equation (16) is always positive, the concentration change would be greater in the range of accumulation of the component with concentration $c < 0.5$.

The value of ε is usually small, and as a result the effect described by equation (16) is also small. The observation that in some experiments /6/ the difference between the changes in concentration on the hot and cold sufaces is more pronounced than the difference calculated by means of equation (16) is attributed to the fact that equation (2) describing the material flow is approximate and does not take into account the dependence of the Soret coefficient on the concentration; experimental studies /7 — 10/ show that the effect of temperature may be substantial.

Taking into account the small value of ε and the resultant approximate relationships

$$\exp \varepsilon \approx 1 + \varepsilon,\ \operatorname{sh} \varepsilon \approx \varepsilon,\ \varepsilon^2 + \pi^2 (2k+1)^2 \approx \pi^2 (2k+1)^2,$$

we can replace (14a) and (14b) by

$$c_0^* = \frac{\varepsilon}{b}\left\{1 - \frac{8}{\pi^2}\left(1 - \frac{\varepsilon}{2}\right)\sum_{k=0}^{\infty} \frac{\exp\left[-\pi^2 (2k+1)^2 \operatorname{Fo}_m\right]}{(2k+1)^2}\right\}, \tag{17}$$

$$c_1^* = \frac{\varepsilon}{b}\left\{1 - \frac{8}{\pi^2}\left(1 + \frac{\varepsilon}{2}\right)\sum_{k=0}^{\infty} \frac{\exp\left[-\pi^2 (2k+1)^2 \operatorname{Fo}_m\right]}{(2k+1)^2}\right\}. \tag{17a}$$

For a steady state equations (17) and (17a) give

$$c_0^* = \varepsilon/b,\ c_1^* = \varepsilon/b,$$

and from here

$$\sigma_{z=1} = \frac{c_{z=1} - c_0}{\Delta T} \cdot \frac{2}{c_0 (1 - c_0)};\ \sigma_{z=0} = \frac{c_0 - c_{z=0}}{\Delta T} \cdot \frac{2}{c_0 (1 - c_0)}. \tag{18}$$

If $c_{z=1} \neq c_{z=0}$ the value of the Soret coefficient must be taken as the arithmetic mean of the two values as determined by (18):

$$\sigma = \frac{\sigma_{z=1} + \sigma_{z=0}}{2} = \frac{c_{z=1} - c_{z=0}}{\Delta T} \cdot \frac{1}{c_0 (1 - c_0)}, \tag{19}$$

i.e., an expression analogous to the de Groot equation /11/. For sufficiently long times corresponding to $\operatorname{Fo}_m > 0.05$ in equations (17) and (17a) we may confine ourselves to the first term in the series

$$\left.\begin{aligned} c_1^* &= \frac{\varepsilon}{b}\left[1 - \frac{8}{\pi^2}\left(1 + \frac{\varepsilon}{2}\right)\exp(-\pi^2 \operatorname{Fo}_m)\right] \\ c_0^* &= \frac{\varepsilon}{b}\left[1 - \frac{8}{\pi^2}\left(1 - \frac{\varepsilon}{2}\right)\exp(-\pi^2 \operatorname{Fo}_m)\right] \end{aligned}\right\}. \tag{20}$$

By using the above equations for two moments of time τ_1 and τ_2 it becomes possible to calculate the Soret coefficient and the concentration diffusion coefficient.

By taking the time in a way such that $\tau_2 = 2\tau_1$, and taking into account the fact that $\varepsilon \ll 1$ it is possible to transform the equations into a form more convenient for calculations:

$$D_{z=0} = -\frac{\delta^2}{\pi^2\tau_1}\ln\left[\frac{c^*_{0_2}}{c^*_{0_1}} - \sqrt{\left(\frac{c^*_{0_2}}{c^*_{0_1}}\right)^2 - \frac{\pi^2}{4}\left(\frac{c^*_{0_2}}{c^*_{0_1}} - 1\right)}\right], \tag{21}$$

$$\sigma_{z=0} = \frac{2}{\Delta T}\,\frac{c^*_{0_1}}{1 - \frac{8}{\pi^2}\exp\left(-\pi^2 \mathrm{Fo}_{m_1}\right)}, \tag{22}$$

where $c^*_{0_1}$ and $c^*_{0_2}$ are the values of $c^*_{0_i}$; at τ_1 and $\tau_2 = 2\tau_1$, respectively. Similar equations would be valid also for $D_{z=1}$ and $\sigma_{z=1}$ when $c^*_{1_i}$ is substituted for $c^*_{0_i}$. If $c^*_0 \neq c^*_1$ we must use the arithmetic mean of D and σ for $z = 0$ and $z = 1$.

For short times ($\mathrm{Fo}_m < 0.05$) it is expedient to use for the sum of series in equations (17) and (17a) the Debye approximation /4/:

$$\frac{8}{\pi^2}\sum_{k=0}^{\infty}\frac{\exp\left[-\pi^2(2k+1)\,\mathrm{Fo}_m\right]}{(2k+1)^2} = 1 - 4\sqrt{\frac{\mathrm{Fo}_m}{\pi}} + \frac{32}{\pi^2}(\mathrm{Fo}_m)^{3/2}\exp\left(-\frac{1}{\mathrm{Fo}_m}\right) + \ldots$$

By confining ourselves to the first two terms in the above expansion, we obtain from (17) and (17a)

$$c^*_0 = \frac{\varepsilon}{b}\left[1 - \left(1 - \frac{\varepsilon}{2}\right)\left(1 - 4\sqrt{\frac{\mathrm{Fo}_m}{\pi}}\right)\right],$$

$$c^*_1 = \frac{\varepsilon}{b}\left[1 - \left(1 + \frac{\varepsilon}{2}\right)\left(1 - 4\sqrt{\frac{\mathrm{Fo}_m}{\pi}}\right)\right]. \tag{23}$$

Like equation (20), the last two equations may be used to determine the required coefficients if the values of c^* are known for any two moments of time, i.e.,

$$\sigma_{z=0} = \frac{1}{\Delta T}\sqrt{\frac{2\left(c^*_{0_1} - \sqrt{\tau_1/\tau_2}\,c^*_{0_2}\right)}{b\left(1 - \sqrt{\tau_1/\tau_2}\right)}},$$

$$\sigma_{z=1} = \frac{1}{\Delta T}\sqrt{\frac{2\left(c^*_{1_2} - \sqrt{\tau_2/\tau_1}\,c^*_{1_1}\right)}{b\left(\sqrt{\tau_2/\tau_1} - 1\right)}}.$$

$$D_{z=0} = \frac{\pi\delta^2}{16\tau}\left(\frac{b}{\varepsilon}c^*_0 - \frac{1}{2}\varepsilon\right)^2,\quad D_{z=1} = \frac{\pi\delta^2}{16\tau}\left(\frac{b}{\varepsilon}c^*_1 + \frac{1}{2}\varepsilon\right)^2. \tag{24}$$

An experimental determination of the concentration changes in thermal diffusion separation was carried out in the cell schematically described in Figure 1 a. The cylindrical copper-made upper and lower sections (1) with an external diameter of 92 mm were joined to one another by a plexiglass ring (2). The height of the ring and the total thickness of the two rubber spacers (3) determined the height of the cell. In our experiments the cell height was constant, 7.75 ± 0.02 mm. Each section was ground and a check was made to determine whether the two planes were parallel. The cell was mounted, the uniformity of the gap was checked by micrometer, and the cell was placed on a surface whose level was aligned with a fair degree of accuracy. By means of the polished plexiglass ring, which made it possible to observe what was happening within the cell, we checked the absence of air in the cell after each introduction of the mixture (an aqueous

sucrose solution was used). The temperatures of the upper and lower surfaces were maintained constant at 65° and 23°C, respectively.

The samples were withdrawn exactly from the center of each surface. To do this long hypodermic needles were fitted into grooves on the inner surface of each section, and the space between the groove walls and the needle was then filled with epoxy resin, as shown in Figure 1 b. After the withdrawal of each sample a vacuum was created in the cell and the cell was again filled with a solution of the initial concentration. The samples were analyzed on a refractometer with an accuracy of ±0.04%.

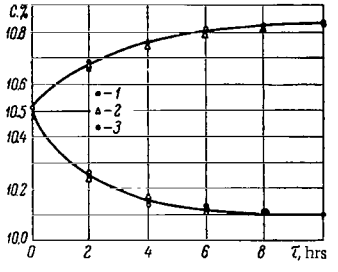

FIGURE 2. Dependence of the concentration of sucrose on the cold and hot surface of the cell on the duration of experiment.

1 – first series of experiments;
2 – second series of experiments;
3 – third series of experiments.

The changes in sucrose concentration at the hot and cold surfaces of the cell are shown in Figure 2. The observed asymmetry of the curves is in the opposite direction to that predicted by a theoretical analysis of the process. As we showed above, this can be attributed to the fact that the Soret coefficient and the diffusion are affected by the temperature. The diffusion and thermal diffusion coefficients were determined for the above change in concentration by means of equations (22) and (23), as the arithmetic means for the top and the bottom. The results of the calculations are shown in the table. The values of D and σ are in good agreement with data from the literature. The Soret coefficient for an aqueous solution of cane sugar of the same concentration as in our experiments is reported by Tanner /12/ as $\sim 2.30 \times 10^{-3}$ (1/degree). The discrepancy between our data and the data of Tanner is 13%, which lies within the range of experimental error. Unfortunately, no data corresponding exactly to the conditions of our experiments have been published in the literature, but nevertheless the available data are in good agreement with ours. Thus, for $\bar{t} = 12$°C and a sugar solution of a concentration of one mole/l Arrhenius /13/ obtained $D = 2.94 \times 10^{-6}$ cm^2/ sec. According to Morris et al. /3/ the diffusion coefficient depends on the temperature and to a lesser extent on the concentration. When the average experimental temperature is increased from 12 to 43°C (as was the case in the above experiment), and when the concentration is also increased, it could be assumed that the diffusion coefficient would be higher than 2.94×10^{-6} cm^2/sec.

TABLE

Experimental and calculated data from the determination of the coefficients D and σ for an aqueous sucrose solution of concentration $c_0 = 10.51\%$

τ_1	τ_2	c_1, %		c_2, %		$c^*_{0_1} \cdot 10^2$		$c^*_{0_2} \cdot 10^2$		$\bar{\sigma} \cdot 10^3$	$\bar{D} \cdot 10^6$
hours		cold	hot	cold	hot	cold	hot	cold	hot	$\frac{1}{\text{deg}}$	cm^2/sec
3	6	10.72	10.19	10.80	10.125	2.24	3.4	3.09	4.1	1.96	6.50
4	8	10.75	10.16	10.82	10.115	2.56	3.73	3.3	4 2	1.91	6.50
5	10	10.775	10.13	10.83	10.10	2.82	4.05	3.41	4.36	1.96	6.48

The values of D obtained by us are in good agreement with the data of Morris et al. /3/.

SYMBOLS

ρ — density; c — concentration by weight; j — flow; τ — time; D_e — effective diffusion coefficient; σ — Soret coefficient; T — temperature; δ — distance between the hot and cold surfaces; Fo — Fourier number; a — thermal diffusivity coefficient; Fo_m — Fourier coefficient for mass transfer.

Bibliography

1. Kafarov, V.V. Osnovy massoperedachi (Principles of Mass Transfer). — Moskva, Gosizdat. 1962.
2. Johonson, P.A. and A.H. Babb. — Chemical Reviews, Vol.56, No.3. 1956.
3. Jost, W. Diffusion in Solids — Liquids — Gases. New York. 1952.
4. Johns, K. and V. Furry. Separation of Isotopes by Thermal Diffusion. [Russian translation. 1947.]
5. Zhuravleva, V.P. — IFZh, No.9. 1963.
6. Growther, P. and C. Raw. —Proceedings of the Physical Society, 73, 4, No.472. 1959.
7. Prigogine, J., Z. De Brouckère, and R. Amand. — Physica, Vol.16(11-12). 1950.
8. Thomass, G. — Physica, Vol.17(10). 1951.
9. Rauch, B. and G. Meyerhoff. — The Journal of Physical Chemistry, Vol.67, No.4. 1963.
10. Hershey, D. and J.W. Prados. — The Journal of Physical Chemistry, Vol.67:6. 1963.
11. De Groot, S.R. Thermodynamics of Irreversible Processes. [Russian translation. 1956.]
12. Grew, K.E. and T.L. Ibbs. Thermal Diffusion in Gases. [Russian translation. 1956.]
13. Handbook of Chemistry and Physics, Vol.2. Cleveland, Ohio. 1955 — 1956.

22049

6 G.I. Bobrova and G.D. Rabinovich 6

3 INTENSIFICATION OF THE THERMAL DIFFUSION SEPARATION PROCESS IN A CLUSIUS-DICKEL COLUMN 6

The intensification of thermal diffusion separation processes is of great importance for improving the effectiveness of those processes. It is well known that among the separation methods based on diffusion, the thermal diffusion process has the lowest thermodynamic efficiency — of the order of 10^{-8}, i.e., about one order of magnitude lower than that in mass-diffusion and two orders of magnitude lower than in gas-diffusion processes.

However, as compared with the above two methods, the thermal diffusion method has the clear advantage of making it possible to carry out the separation in the liquid phase and of using very simple equipment.

The intensification of the separation of liquid mixtures by thermal diffusion in Clusius-Dickel columns has been recently the subject of several papers /1, 9, 12 — 14/ which show that their authors have been able to achieve substantial improvements by creating in the columns hydrodynamic conditions that had a favorable effect on the separation process (rotating columns, packed columns, etc.). Unfortunately, no experimental data are available that would make it possible to describe the mechanism of motion of the liquid in thermal diffusion separation columns, i.e., in slits 0.2 — 0.5 mm wide.

Hydrodynamic studies in narrow vertical slits under natural convection conditions, which have been described elsewhere /2, 4, 7/, were carried out with much greater gaps and may serve only as a partial basis for the creation of a physical model of the process discussed here. Those data indicated that the motion of currents in a thermal diffusion column differ substantially from the idealized model proposed by Jones and Furry used to formulate a theory for the calculation of such equipment. It should be assumed that the hydrodynamic interaction of both currents is accompanied by disturbances at the contact boundary, caused by the penetration of moles of liquid from one current to the other, i.e., the actual process is characterized not only by molecular but also by macroscopic mass transfer. The macroscopic transfer is an interfering factor and must have an unfavorable effect on the ultimate separation effect. The above assumption is supported by the results reported in several papers /5, 8, 10, 11/. Some of the experiments on separation were carried out with Clusius-Dickel columns /5, 10/. It was found that the actual separations obtained in the experiments were much lower than the values calculated on the basis of the Jones and Furry theory. It should be mentioned here that the authors of the above theory suggested the possible occurrence of parasitic currents

(caused by irregularities in the gap, imperfect vertical alignment, and asymmetry effects) that could reduce the separation effect.

An accurate evaluation of the effect of such parasitic currents /5/ showed that the great difference between the actual experimental results and those calculated on the basis of the ideal model cannot be attributed to parasitic currents since their proportion is very small.

Eddies which arise at the interaction boundary of the two currents may be suppressed substantially by introducing into the column space a barrier whose location should correspond roughly to the supposed natural boundary between the two currents. Naturally, the barrier must be perforated in order to permit transverse molecular transfer in the thermal diffusion process. Such a barrier is essentially different from the barriers used in gas diffusion, in which the pore size must be of the same order as the mean free path of the molecules. The barrier proposed by us has the single purpose of creating an ordered liquid flow (from the hydrodynamics standpoint) with simultaneous transverse transfer. Since in thermal diffusion columns an enrichment effect is observed only after circulation of the liquid repeated many times, the upper and lower ends of the barrier must be fitted with openings ("windows") that permit a free turning of the convective current at the ends of the column.

The above considerations were checked experimentally in an apparatus whose construction is shown schematically in Figure 1. Well polished and chromium-plated steel plates (1) with a size of 40×10×30 mm were fastened (with screws) on a frame (2) using a gasket (3). The uniformness of the tightening was checked by means of a micrometer. The distance between the plates (i.e., between the hot and cold walls) was equal to the combined thickness of the two gaskets between the plates (1), the frame (2), and the barrier (4), which in the compressed state served also as a gasket for the plates. The gap uniformness over the height of the apparatus was checked by micrometer and maintained at about 20μ.

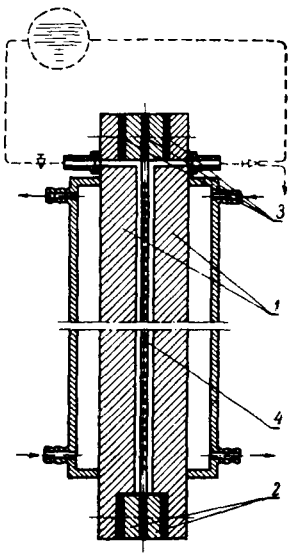

FIGURE 1. Schematic view of the apparatus.

Since the slit dimensions are small (of the order of 0.6 — 1.1 mm), the barrier must be completely uniform in thickness, must be completely free of undulations, must not be deformed by the temperature, must not swell, and must be chemically inert with respect to the liquid to be separated. We carried out experiments with several materials: steel, glass-Textolite, varnished fabric, polyethylene, and rubberized fabric. We were unable to eliminate the undulations over the height of steel and glass-Textolite with a thickness of 0.25 — 0.3 mm, and for this reason those barriers touched the column walls. Rubberized fabric was found to be the best material. A rubberized fabric barrier, carefully stretched during the assembly, satisfied the requirements listed above. One side of the column was cooled while the other was heated by running

water from thermostats. The temperature of the plate surfaces was measured with copper-constantan thermocouples placed in grooves in the internal surfaces of the plates.

TABLE

Separation as a function of the temperature gradient between the column walls

$\Delta\bar{t}$, °C	Sugar concentration at the top of the column, $\bar{c}_T$, %			Sugar concentration at the bottom of the column, $\bar{c}_B$, %			$\Delta\bar{C} = \bar{c}_B - \bar{c}_T$, %
9.45	2.93	2.93	2.93	4 00	3.42	4.10	0.91
14.0	2.93	2.93	—	4.69	4.63	—	1.73
19 6	2.83	2 83	2.83	6.29	5.89	6.16	3.28
24 20	2.93	2.93	—	6.94	6.38	—	3.98

Note. The data were obtained 2 hrs after the start of the experiment. The experiments were carried out in a column fitted with a barrier having an open area of 22%, a perforation diameter of 2 mm and in which the distance between the column walls was 0.86 mm.

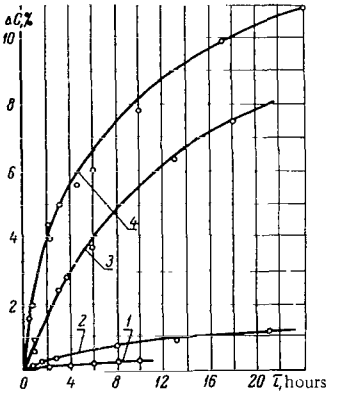

FIGURE 2. Degree of separation expressed by the difference between the concentration at the top and bottom of the column as a function of the diameters of the barrier perforation. Wall distance 0.86 mm, temperature gradient between the walls 19.6°C.

1 – column without barrier; 2 – column with barrier, perforation diameter = 5 mm, open area of the barrier = 22%; 3 – perforation diameter = 3.5 mm, open area of the barrier = 12%; 4 – perforation diameter = 2 mm, open area of the barrier = 22%.

Prior to its filling with the mixture to be separated, the working space of the column was evacuated thoroughly by means of a vacuum pump. The mixture was also exposed to a vacuum. A saccharose mixture served as the test object. Using a plumb line, the column was aligned before the experiments to an accurately vertical position in order to prevent the appearance of additional currents. In the upper part of the column the solution concentration was maintained at the same level as the initial concentration by continuous circulation of the liquid phase (the circulation circuit is shown in Figure 1 by a dashed line). The samples were withdrawn from the lower part of the column. Since the working space of the column was only 6 — 11 cm^3, it was essential to prevent any substantial changes in the concentration distribution (over the column height) as a result of the withdrawal of samples. For this reason, the height of the withdrawn liquid was only 1/80 of the column height, and the total volume of the samples withdrawn during the experiment did not exceed 10 — 15% of the total column volume.

We carried out four series of experiments in which the variables were: the open area of the barrier, diameter of the perforations, the wall temperatures, and the distance between the walls. The experimental results are shown in Figures 2 — 4 and in the table.

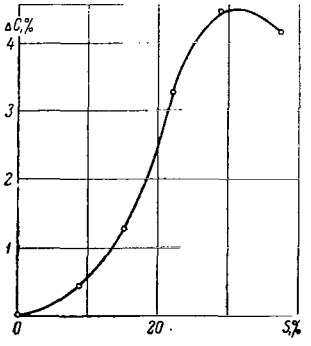

FIGURE 3. Separation in a column as a function of the open area of the barrier. Distance between the walls, 0.86 mm, temperature gradient between the walls 19.6°C, perforation diameter in the barrier, 2 mm.

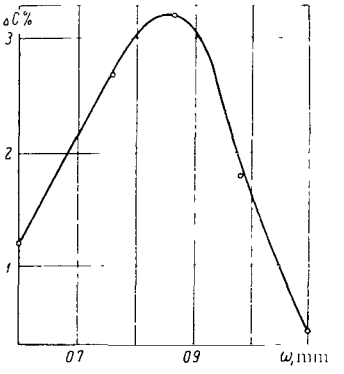

FIGURE 4. Separation in a column as a function of the distance between the walls. Temperature gradient between the walls, 19.6°C, open area of the barrier, 22%, perforation diameter in the wall 2 mm.

The data in Figure 2 show that a sharp improvement in the separation was obtained as a result of the use of a barrier. After twenty hours of operation, the separation coefficients obtained in a column with a barrier were 5 times the values obtained without a barrier. While in a column without a barrier the separation was virtually terminated after 8 — 10 hours of operation, separation in a column with a barrier was even more rapid. A steady state was established for much longer than in a column without a barrier. It may be assumed that close to the steady state the separation

coefficient in a column with a barrier had many times the value obtained in columns without barriers. In columns with barriers the maximum separation rate was observed within the first two or three hours of operation. For a given constant time, the concentration gradient between the top and bottom of the column decreased as the perforation diameter was increased. This is attributed to the increased contact area between the currents at each perforation that resulted in macroscopic transfer at the contact boundary. The validity of our assumptions concerning the occurrence of mixing at the contact area between the currents in the column is illustrated by the curves.

In Figure 3, the point corresponding to a zero concentration gradient between the top and the bottom was obtained in a column with a compact barrier fitted at its upper and lower ends with windows that provided for circulation of the liquid. Such a barrier has a zero open area; hence there is no transverse transfer and the separation is virtually zero.

According to the theory of Jones and Furry, the separation effect must be enhanced as the distance between the column walls is reduced. This is indeed observed until the gap becomes so small (Figure 4) that any further decrease causes a decrease in the separation effect (and even so, the gap is always much larger than the theoretically calculated gap that would effect maximum separation). This may be attributed to the fact that when the distance between the walls is reduced, the distance between a column wall and the barrier decreases much more rapidly since the barrier thickness remains constant. The parasitic currents associated with the uneveness of the gap have an unfavorable influence on the separation effect. This conclusion is supported by experimental results /14/. It is supported also by the results obtained in a column without barrier where the distance between the walls is 0.3 mm. The results obtained in that column were characterized by a wide dispersion and poor reproducibility.

However, it should be mentioned that the degree of separation achieved in a column with a barrier and with a gap of 0.6 mm was indeed lower than the separation achieved in a column with a gap of 0.86 mm, but at the same time it was much higher than the separation achieved in the same column without a barrier. The separation of columns of improved accuracy is very difficult and results in an increase in the cost of the apparatus. The method we propose (separation in a column fitted with a barrier) makes it possible to achieve the same degree of separation with much wider gaps, i.e., in much larger spaces, which is equivalent to a reduction of the energy consumption per unit of enriched product.

Bibliography

1. Alkhazov, D.G., A.N. Murin, and A.R. Ratner. — Izv. AN SSSR, Otdelenie Khimicheskikh Nauk, No. 1. 1943.
2. Boyarintsev, D.M. — ZhTF, No. 9. 1950.
3. Johns, K. and V. Furry. Separation of Isotopes by Thermal Diffusion. [Russian translation. 1947.]
4. Ostroumov, G.A. Svobodnaya konvektsiya v usloviyakh vnutrennei zadachi (Free Convection under the Conditions of the Internal Problem). — GITTL. 1954.

5. Panchenkov, G.M., V.D. Moiseev, and Yu.A. Lebedev.— ZhFKh, Vol.30: 10. 1956.
6. Rozen, A.M. Teoriya razdeleniya izotopov v kolonakh (The Theory of Isotope Separation in Columns).— Atomizdat. Moskva. 1960.
7. Sorokin, M.P.— IFZh, VI, No.2. 1961.
8. Brewer, A.K. and A. Bramley.— Physical Review, Vol.55: 550. 1939.
9. Debye, P. United States Patent, 2567765. 1946.
10. Cooke, B.A., J. Hewes, and H.A. Mackenzie.— Journal of Science; American Chemical Institute, Vol.7: 11. 1954.
11. Groth, W.— Naturwissenschaften, Vol.27, p.260. 1939.
12. Powers, J. and C.A.I. Wilke.— Ch. E. Journal, 3(2): 213. 1957.
13. Sullivan, I.J., T.C. Ruppel, and C.B. Willingham.— Industrial and Engineering Chemistry, 47(2): 208. 1957; 49(1): 110. 1957.
14. Washall, F.A. and F.M. Melpolder.— Industrial and Engineering Chemistry. Process Design and Development, 1(1): 1. 1962.

P. A. Novikov

EFFECT OF THE VIBRATION RATE OF A BODY ON HEAT AND MASS TRANSFER UNDER THE CONDITIONS OF VACUUM SUBLIMATION

Recent investigations /1, 3/ have established that artificially-induced vibrations cause an increase in heat transfer rates. This attracted our interest to the study of the effect of some physical variables (in this case — vibrations) on heat and mass transfer during vacuum sublimation. The main vibration parameters are the amplitude and frequency.

Vibrations are induced by hydraulic shock, pulsations, during the operation of a piston pump, during the throttling of a liquid, and also during the very rapid motion of bodies. In addition, an oscillating motion may be induced with the purpose of intensifying various technological processes.

The recent advances in some branches of industry have necessitated the intensification of heat and mass transfer processes without an excessive increase in temperature. Such is the case primarily with condenser-evaporators, marine installations, drying of biological preparations and foods, etc.

In the present paper we report the results of an experimental study of heat and mass transfer during the vibrations of a substance undergoing vacuum sublimation.

The experiments were carried out within a wide range of frequencies (from 20 to 150 cps), with an oscillation amplitude of 1 — 18 mm and a total pressure of the surroundings ranging from atmospheric pressure down to 0.1 mm Hg. The temperature of the surroundings was maintained constant (18°C). A schematic view of the experimental setup is shown in Figure 1.

The vacuum chamber consisted of a cylindrical vessel 420 mm in diameter, fitted with lids and a peep hole. The required vacuum was created by means of an oil vacuum pump. A receiver was placed between the vacuum chamber and the pump which attenuated all disturbances created by the operation of the pump in the medium. The required pressure in the working chamber was provided by a diaphragm-type air inlet. The overall pressure in the chamber was measured by means of a U-tube pressure gage and also by a thermocouple vacuum gage. The partial pressure of dry air was measured by means of a compression McLeod gage.

Two traps were installed between the vacuum chamber and the McLeod gage, one of them being filled with liquid oxygen the other with calcium chloride. The temperature of the vapor-water mixture and the surface of the subliming material were measured with a copper-constantan thermocouple.

Moreover the changes of temperature in the medium and on the surface of the subliming material were checked with a special alcohol thermometer.

The material studied was a spherical body (diameter 14 mm) made of naphthalene.

The rate of heat exchange between the subliming body and the medium was determined by the rate of sublimation of the body investigated. The sublimation rate was determined from the decrease in the weight of the vibrating body, which was measured by simultaneous weighing (on analytical balance) of two samples undergoing sublimation; the measurements were made at predetermined time intervals. The samples were spherical, had identical volumes and weights, and were subjected to the same working conditions in the vacuum chamber. One of the samples served as a standard and was at rest, while vibrations with a given frequency and amplitude were imparted to the second sample.

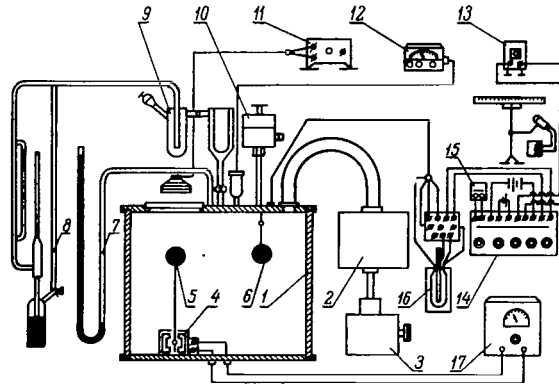

FIGURE 1. Main scheme of the test apparatus.

1 – vacuum chamber; 2 – receiver; 3 – vacuum pump; 4 – electromagnetic vibrator; 5 – sample; 6 – standard; 7 – U tube mercury vacuum gage; 8 – mercury compression McLeod gage; 9 – trap; 10 – air inlet; 11 – stroboscope; 12 – thermocouple vacuum meter; 13 – mirror galvanometer; 14 – low-resistance potentiometer; 15 – center-zero galvanometer; 16 – Dewar flask with melting ice; 17 – tone generator.

The sample to be investigated was placed in the vacuum chamber on the thin rod of an electromagnetic vibrator. The electromagnetic vibrator consisted of two electromagnets with a core and a rod fitted between them on an axis with bearings. The distance between the magnets and the core was regulated within the required range by means of special screws. The electromagnetic vibrator operated at the output frequencies of a tone generator. The vibration amplitude was controlled by means of a stroboscope. The vibration amplitude was measured with the aid of a special scale. The variations in the temperature of the substance undergoing sublimation were recorded during the vibrations by means of a special alcohol thermometer, with a thin layer of the material undergoing sublimation fused on its head. The thermometer was fastened to the rod of the electromagnetic vibrator and was thus subjected to oscillations with a given frequency. The thermometer scale readings were taken with the aid of a stroboscope. Moreover, the temperature of the sublimated material was

measured with the aid of copper-constantan thermocouples, with a thin layer of the sublimated material fused on their tips.

The amount of sublimated material was determined by measuring the difference in the weight of the investigated body before and after the experiment, taking into account the amount sublimed during the introduction of the body into the vacuum chamber and its evacuation to the required working pressure:

$$\Delta G = G_1 - G_2 - \Delta G',$$

where G_1 is the weight of the body before the experiment, G_2 is its weight after the experiment, and $\Delta G'$ is the decrease in weight during the introduction of the body in the vacuum chamber and its evacuation to the required working pressure.

For a given period of time the sublimation rate was determined from the equation

$$q_m = \frac{\Delta G}{F\tau},$$

where F is the sublimation surface, $м^2$ and τ is the time, hours.

The mean square value of the velocity was calculated from the equation

$$\overline{V} = \frac{2\pi fA}{\sqrt{2}},$$

where A is the vibration amplitude, m, and f is the vibration frequency in cps. In our experiments the velocity ranged from 0 to 1.6 m/sec.

In our experiments the temperature of the medium in the vacuum chamber was equal to the wall temperature, and hence the rate of convective heat transfer during sublimation under steady-state conditions was expressed by the equation

$$\alpha_k = \frac{1}{\Delta T}\left\{q_m r - C_c \times \left[\left(\frac{T_w}{100}\right)^4 - \left(\frac{T_{vb}}{100}\right)^4\right]\right\},$$

where $\Delta T = T_w - T_{vb}$, r is the latent heat of sublimation, j/kg, and C_c is the corrected radiation coefficient.

Figure 2 is a graphical presentation of the dependence of the sublimation rate on the mean square values of the velocity of the body at various pressures of the surroundings.

The figure shows that the sublimation rate increases with increasing velocity. In the pressure range studied (from atmospheric down to 4 mm Hg) the dependence of the sublimation rate on the velocity had an almost analogous form at any pressure. When the total pressure was reduced below 4 mm Hg, the effect of the velocity on the sublimation rate became negligible. In the case of a body with the given characteristic dimensions, the velocity had no observable effect on the sublimation rate when the pressure was 0.1 mm Hg. At the same time, in the pressure range studied there was a critical velocity above which there was a marked increase in the sublimation rate. The increase in the sublimation rate in the presence of vibrations (as compared with the rate in the absence of vibrations) was manifest to a different extent at different pressures of the surroundings.

For instance, at atmospheric pressure and a velocity of 1.56 m/sec (vibration frequency = 22 cps, vibration amplitude = 16 mm) the sublimation

rate of the vibrating body was 5 times the rate in the absence of vibrations. At a total pressure of 400 mm Hg the above ratio was 4, while at a pressure of 100 mm Hg it was below 2. As the total pressure was reduced, the difference between the sublimation rates in the presence and the absence of vibrations became gradually smaller; at a total pressure (of the surroundings) below 4 mm Hg a small difference was observed only at large amplitudes. At pressures below 0.1 mm the sublimation rates in the absence and the presence of vibrations were the same. In the presence of vibrations, the main factor affecting the sublimation rate is the amplitude. As compared with an increase in the vibration frequency, an increase in the vibration amplitude had a much greater effect on the heat and mass transfer rates. For instance, in our experiments vibrations with a small amplitude (A = 1 mm) at a frequency f = 150 cps had a negligible effect on the sublimation rate.

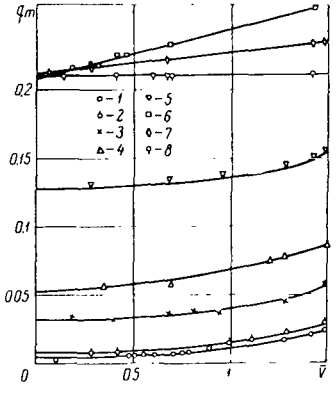

FIGURE 2. Dependence of the sublimation rate q_m on the velocity of the body $\bar{V}$ at various pressures of the surroundings.

1 – 745; 2 – 400; 3 – 100; 4 – 50; 5 – 20; 6 – 4; 7 – 1; 8 – 0.1 mm Hg.

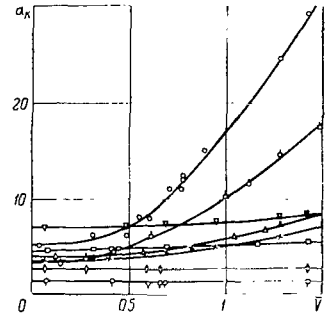

FIGURE 3. Dependence of the coefficient of convective heat transfer on the velocity of a body undergoing sublimation, at various total pressures (the notation used is the same as in Figure 2).

Figure 3 is a graphical presentation of the changes in the convective heat transfer coefficient as a function of the mean square value of the velocity of a spherical body undergoing sublimation, at various pressures of the surroundings. The figure shows that the heat transfer coefficient increases with increasing velocity. At atmospheric pressure and a velocity of 1.6 m/sec (frequency f = 22 cps, amplitude A = 16 mm) the value of the heat transfer coefficient was 6 times the value of the same coefficient for a body undergoing sublimation in the absence of vibrations. At the same time, the effect of the velocity on the rate of convective heat transfer decreased sharply as the total pressure was reduced. In our experiments, at pressures below 20 mm Hg the velocity had a very slight effect on the rate of convective heat transfer, while at a pressure of 0.1 mm Hg the velocity had no effect on the rate of convective heat transfer. It should be mentioned that the velocity of the body had an effect on the

temperature of the substance undergoing sublimation only if the vibrations had a large amplitude. In our experiments the temperature changed when the amplitude of the body undergoing sublimation was higher than 8 mm. At low amplitudes the temperature of the material undergoing sublimation remained constant at any frequency in the range studied. At a total pressure of 0.1 mm Hg the temperature of the material undergoing sublimation remained constant within the whole investigated range of vibration parameters. This again shows that the rate of convective heat transfer is independent of the velocity of the body at a total pressure of 0.1 mm Hg.

The results of our experiments showed that the effect of vibrations of the body on the sublimation rate and the rate of convective heat transfer becomes noticeable only if the vibrations have a large amplitude. An especially marked effect is obtained when the amplitude is greater than the characteristic size of the body undergoing sublimation.

Bibliography

1. Kovalenko, V. F. Vliyanie vibratsii na teploperedachu (Effect of Vibrations on Heat Transfer). — Teploenergetika, Vol. 5, p. 112. 1958.
2. Kubanskii, P.N. — ZhTF, Vol. 22, No. 4. 1952.
3. Lemlich. Effect of Vibrations on Natural Convective Heat Transfer. — Industrial and Engineering Chemistry, Vol. 47. 1955.

P.A. Novikov and B.M. Smol'skii

THE MECHANISMS OF HEAT AND MASS TRANSFER DURING THE VIBRATIONS OF A BODY UNDERGOING SUBLIMATION IN A RARIFIED GASEOUS MEDIUM UNDER THE CONDITIONS OF FREE CONVECTION

The existing data on the effect of body vibrations on the rates of heat and mass transfer are insufficient and in some cases they are even contradictory. This may be attributed on the one had to the wide variety of physical phenomena encountered by the worker during the experiments, and on the other hand to the variety of experimental procedures. In each case the simultaneous action of the variable physical factors may have a different effect on the heat and mass transfer processes occurring. In the presence of vibrations the heat and mass transfer mechanisms are very complex. Many of the factors affecting the heat and mass transfer under regular conditions (in the absence of vibrations) are still of an unknown nature. Hence, in view of the present level of our knowledge, it is very difficult to carry out an accurate analysis of the process taking place or to find an analytical solution of the problems characterizing the heat and mass transfer in bodies in an oscillating motion.

The main vibration parameters affecting the heat and mass transfer are the amplitude and frequency. Experimental studies show that those parameters may be combined in derivative parameters which give the vibration velocity. This velocity is proportional to the product of the frequency and amplitude.

Heat and mass transfer in the presence of an oscillatory motion may be studied by two methods. The oscillatory motion may be caused in the surrounding medium by a sonic field, pulsations, vibrations or some other perturbation source while the investigated body is kept stationary, or the oscillatory motion may be imparted directly to the body, which then vibrates at a certain amplitude and frequency.

The two methods are similar but not identical, and the selection in each case depends on the more advantageous use of the experimental apparatus.

The extent to which the vibrations affect the heat and mass transfer depends on the physical properties of the surrounding medium, the directions and velocities of the fluid stream, etc. At the same time, no increase in the heat transfer coefficient was observed in some systems in the presence of vibrations, because of the predominant effect of several physical variables. In the case of a vigorously boiling liquid, vibration of the heating surface can even have a negative effect on the heat transfer. This indicates that in the case of heat and mass transfer with vibrations there exists a combination of a large number of physical effects.

It has been established by experiments that for most systems there exists a certain critical frequency, above which the heat transfer rate increases sharply with increasing amplitude.

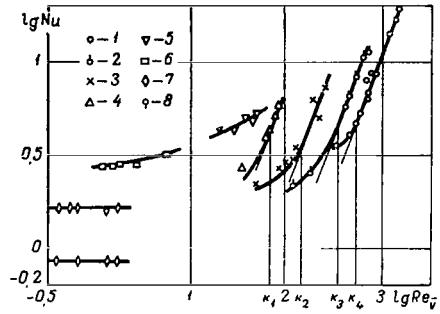

FIGURE 1. Dependence of the heat transfer rate Nu on the vibration velocity $Re_{\bar{v}}$ of a body undergoing sublimation, at different pressures of the surroundings.

1 - 745 mm; 2 - 400 mm; 3 - 100 mm; 4 - 50 mm; 5 - 20 mm; 6 - 4 mm; 7 - 1 mm; 8 - 0.1 mm Hg.

We carried out an experimental study in order to establish the effect of the velocity of a body on the heat and mass transfer during vacuum sublimation. The experiments were carried out under steady-state and free-convection conditions. The total pressure of the surroundings was varied within a wide range: from 745 mm Hg to 0.1 mm Hg.

The dependence of the heat transfer rate on the vibration velocity of a body undergoing sublimation at various pressures of the surroundings is shown in a dimensionless form in Figure 1, in which Nu is plotted as a function of $Re_{\bar{v}}$ in logarithmic coordinates.

The Reynolds number of vibration $Re_{\bar{v}}$ was calculated on the basis of the mean velocity of the body and the physical properties of the surrounding vapor—gas mixture, taking the sphere diameter as the characteristic body dimension.

The curves representing the above relationships show that at total pressures of the surroundings from atmospheric down to 50 mm Hg, i.e., the sections of the curves ($Nu = f(Re_{\bar{v}})$ corresponding to $Re_{\bar{v}}$ above the critical value, were parallel to one another. This indicates that in the above range of pressures and at low sublimation rates the mass transfer did not have a substantial effect on the nature of the heat transfer in the boundary layer, where the low velocity of detachment of the vapor from the surface and its molecular transfer had no substantial effect on the nature of the temperature distribution round the surface of the body. As the total pressure was reduced below 50 mm Hg there was a decrease in the slope of the curves and at pressures equal to 0.1 mm Hg the slope approached zero. At a total pressure of 0.1 mm Hg the heat transfer rate became independent of the velocity of the body. It should be mentioned that the critical value of $Re_{\bar{v}}$ (above which there was a marked increase in

heat transfer rate) decreased as the total pressure was reduced from 745 to 50 mm Hg. When the Reynolds number of vibration $Re_{\bar{v}}$ was lower than its critical value, the Nusselt number Nu was virtually independent of the Reynolds number. The graph shows that no inflection in the curves was observed at pressures below 50 mm Hg. This means that in a low-density medium the critical $Re_{\bar{v}}$ loses its physical meaning, i.e., the $Re_{\bar{v}}$ is degenerated.

A sharp increase in the heat transfer rate is observed when $Re_{\bar{v}}$ exceeds the critical value. As the mean velocity of the body drops below the critical value, the heat transfer rate approaches the rate obtained under the conditions of free convection. In Figure 1 the transition to critical $Re_{\bar{v}}$ values is shown by an inflection in the curves (points κ_1, κ_2, κ_3, κ_4) beyond the boundaries of the transition zone; in logarithmic coordinates Nu as a function of $Re_{\bar{v}}$ is represented by straight lines.

An analysis of the above relationships leads to the conclusion that in the pressure range between 745 and 50 mm Hg and for $Re_{\bar{v}}$ values below the critical, the heat transfer is affected mainly by the free convection in which gravitational forces are more important (for the convective heat transmission) than the force field created by the velocity of the body at low $Re_{\bar{v}}$ values. As the $Re_{\bar{v}}$ is increased above the critical value (at low sublimation rates) the inertia forces created as a result of the body vibrations become the main factor affecting the heat transfer.

The experimental data obtained at pressures between 745 and 50 mm Hg for $Re_{\bar{v}}$ values above the critical satisfy the equation

$$Nu = 0.95\, Re_{\bar{v}}\, Gu^{0.9}$$

At pressures between 50 and 0.1 mm Hg the heat transfer process cannot be described by a general equation, since the nature of the heat transfer on the surface undergoing sublimation is affected to a very marked degree by the mass transfer. In the above case, when the total pressure is reduced the heat transfer due to vaporization predominates over the heat transfer occurring under the effect of inertia forces.

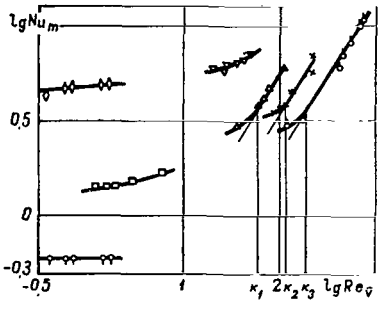

FIGURE 2. Dependence of the mass transfer rate Nu_m on the velocity $Re_{\bar{v}}$ of the body undergoing sublimation, at various pressures of the surroundings (the notation used is the same as in Figure 1).

A similar relationship is observed when we plot the mass transfer parameters.

The relationship $Nu_m = \varphi(Re_{\bar{v}})$ is shown in Figure 2 in logarithmic coordinates. At pressures between 745 and 50 mm Hg and $Re_{\bar{v}}$ values above the critical the mass transfer rate is described by the equation

$$Nu_m = 0.425\, Re_{\bar{v}} Gu^{0.74}$$

The correlation of the experimental data obtained at pressures between 745 and 50 mm Hg is shown in Figure 3. In the above pressure range a good correlation between the heat and mass transfer data is obtained by introducing the parametric Gukhman number Gu into the equation $Nu = f(Re_{\bar{v}})$; in the above case Gu is identical with the transfer potential governing free convection.

On the basis of the experimental data it is possible to describe the mechanism of the heat and mass transfer around the surface undergoing sublimation, in the presence of vibrations. In the case of vibrations with a small amplitude and at relatively low sublimation rates the increase in the rates of heat and mass transfer is insignificant. At the same time the perturbations caused by the vibrations within the boundary layer surrounding the body undergoing sublimation have a negligible effect. It may be assumed here that the body undergoing sublimation vibrates within a thin, closed layer of the vapor-air mixture, and that the boundary layer adjacent to the surface (which, as is well known, constitutes the main resistance to the heat and mass transfer) is not destroyed.

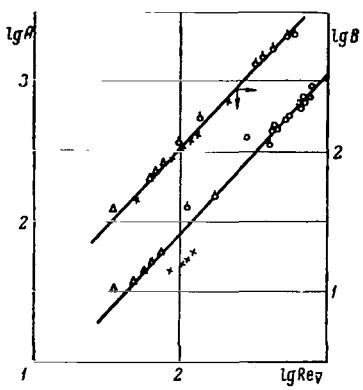

FIGURE 3. Correlation of experimental data on the heat transfer $A = \frac{Nu}{0.95Gu^{0.9}}$ and mass transfer $B = \frac{Nu}{0.425Gu^{0.74}}$ in the case of a body undergoing vacuum sublimation in the presence of vibrations.

In the case of vibrations with a small amplitude (when $A/d \ll 1$) the heat and mass transfer process is governed by a conventional transfer mechanism, as in the case of free convection in the absence of vibrations.

In the case of vibrations with a large amplitude the vibrating body creates a strong perturbation in its immediate surroundings, and each cycle of motion contributes to the perturbations. As the number of such perturbations (per second) increases, there is an increase in the magnitude of their effect on the boundary layer round the surface undergoing sublimation. In the above case the vibrations may be regarded as means for the destruction and creation of turbulence in the boundary layer adjacent to the surface undergoing sublimation. In the case of slow sublimation at pressures between 745 and 50 mm Hg the velocity (with an amplitude $A/d \gg 1$) is the main factor governing the whole hydrodynamic behavior of the medium in the vicinity of the surface undergoing sublimation. The degree of turbulence of the boundary layer

of the vapor-air mixture in the presence of vibrations depends on the number of motion cycles of the body undergoing sublimation, on the displacement of the body, the density of the medium in the boundary layer, etc.; but the main parameter governing the degree of turbulence of the boundary layer is the density of the vapor-air mixture. For vibrations of given identical parameters, the density of the boundary layer (adjacent to the surface undergoing sublimation) decreases with decreasing total pressure which decreases the turbulence of the boundary layer. This in turn reduces the influence of the velocity on the heat and mass transfer rates.

An analysis of the experimental data shows that none of the motion processes (including accelerated motion of the body, vibration, etc.) has such a strong destructive effect on the boundary layer and causes such a sharp improvement in heat transfer as rapid vacuum vaporization. During rapid sublimation the rate of vapor detachment from the surface (vaporization rate) can cause such a marked change in the physical properties of the medium surrounding the surface undergoing sublimation that the flow pattern of the vapor-air mixture cannot be affected substantially by the velocity of the body.

The mass transfer occurring during the vacuum sublimation of a substance is the dominant factor affecting the development of the hydrodynamic conditions during the process, and it governs the heat transfer rate. At first approximation, the ratio of the sublimation rate (it characterizes the rate of penetration of the bulk of the vapor into the surrounding medium) to the mean velocity of the body may serve as a quantitative measure of the intensity of hydrodynamic phenomena during the heat and mass transfer process. The above ratio may be accepted as a dimensionless criterion

$$\varepsilon = \frac{w^*}{v}.$$

If $\varepsilon \ll 1$ the heat transfer caused by the vibration forces exceeds the heat transfer determined by the vaporization rate.

If $\varepsilon \gg 1$ the influence of vaporization is higher in the transfer process than that of vibration forces. The experimental results show that the application of vibration as means of increasing the sublimation rate does not always cause an increase in the heat and mass transfer rates. The extent to which the effect of vibration is felt will depend on the ratio of the turbulent perturbations (caused by the vibrating body) to the natural vapor-formation processes. At low vaporization rates the use of artificially-induced vibration may have a substantial effect and, inversely, in the case of rapid vaporization the artificially-induced vibration does not increase the heat and mass transfer rates.

At high vaporization rates a decrease in the total pressure gradually eliminates the influence of induced vibration. For each separate case there are certain critical values of the amplitude and frequency, above which induced vibration causes no increase in the heat and mass transfer rates and may even cause a drop in them.

The rate of heat and mass transfer in the presence of vibration also depends on the direction of movement of the oscillating surface with respect to the direction of gas flow. If the oscillating surface is normal to the gas flow the vapor-air layer adjacent to the surface undergoing sublimation is repulsed and destroyed, thus causing an increase in the heat and mass transfer rates.

When the oscillatory motion is in the same direction as the gas flow the destruction of the boundary layer does not take place; only a decrease in the thickness of the boundary layer occurs and, naturally, the increase in the rates of heat and mass transfer is not as pronounced as in the previous case.

SYMBOLS

$\mathrm{Nu} = \frac{\alpha_k d}{\lambda}$ — the thermal Nusselt number; $\mathrm{Nu}_m = \frac{\alpha_m d}{D}$ — the diffusion Nusselt number; $\mathrm{Re}_{\bar{v}} = \frac{\bar{v} d}{\nu}$ — the Reynolds number of vibration; $\mathrm{Gu} = \frac{T_{vg} - T_{ss}}{T_{vg}}$ — the Gukhman number; α_k — the convective heat transfer coefficient; α_m — the mass transfer coefficient; d — the sphere diameter; λ — thermal conductivity coefficient of the mixture; D — the diffusion coefficient; ν — the kinematic viscosity of the mixture; T_{vg} — the absolute temperature of the vapor-gas mixture; T_{ss} — the absolute temperature of the surface of the material undergoing sublimation; $\bar{v} = \frac{2\pi f A}{\sqrt{2}}$ — the mean vibration velocity of the body; f — the vibrations frequency; A — the vibration amplitude; $w^* = \frac{m}{\rho}$ — the vaporization rate; $m = q/r$ — the mass of vapor formed; q — the amount of heat transferred to the material undergoing sublimation, per unit time and unit surface; r — the latent heat of sublimation; ρ — the vapor density at the vaporization surface.

Bibliography

1. Lemlich. — Chemical Engineering, Vol. 68, No. 10. 1961.

L. M. Nikitina

THE MASS TRANSFER COEFFICIENT OF AIR

A condition of the third kind is often used as the boundary condition in studies of the mass transfer between a capillary-porous body and its surroundings. In the case of boundary conditions of the third kind, the system of differential equations for heat and mass transfer may describe a very extensive group of phenomena, such as non-isothermic dissolution, heterogeneous reactions governed by diffusion kinetics, convective drying, electrodiffusion, etc. /1/. In this case the boundary conditions relate the transfer potentials on the body surface to the corresponding potentials of the medium by means of the given values of the heat and mass transfer coefficients or, in other words, by means of the laws of convective heat transfer and of mass transfer on the surface.

Thus, for the case of convective drying the boundary condition of the third kind is written as /2/

$$j = \beta\rho(u_p - u_r). \tag{1}$$

As is well known, the mass transfer coefficient is numerically equal to the mass transfer rate when the moisture concentration gradient between the material surface and the surrounding medium equals unity /2/. Since the mass transfer coefficient generally depends on the conditions and the state of the material surface (the mass transfer decreases with increasing (mass) density /2/), the fixing of its value is difficult and hence the boundary condition (1) becomes unsatisfactory in the case of unsteady mass transfer (as is the case in drying processes).

In studies of the moisture transfer between a capillary-porous body and the surrounding medium it is advantageous to use boundary conditions of the fourth kind, for which the density of the moisture flow on the boundary surface between the capillary-porous body and its surroundings is assumed to be equal to their respective potentials, namely,

$$\left.\begin{aligned} \mu_\tau &= \mu_c \\ -\lambda_\tau \nabla\mu_\tau &= -\lambda_c \nabla\mu_c \end{aligned}\right\}. \tag{2}$$

For the effective use of (2) let us derive an expression for the mass transfer coefficient in terms of experimentally determinable values.

It is known that the density of the diffusion flow /3/

$$j = -D_{12}\frac{M_1}{M}\rho_c \nabla P_{10}, \tag{3}$$

where $P_{10} = p_1/P$ is the ratio of the partial vapor pressure to the total (barometric) pressure of the vapor-gas mixture.

TABLE

The mass transfer coefficient of air

T,°K \ φ	0.10	0.15	0.20	0.25	0.30	0.35	0.40	0.45	0.50	0.55
273	4.79	7.19	9.59	11.98	14.38	16.78	19.17	21.57	23.97	26.36
283	9.64	14.46	19.28	24.1	28.92	33.74	38.57	43.39	48.21	53.03
293	18.36	27.54	36.72	45.9	55.08	64.27	73.45	82.63	91.81	100.99
303	33.31	49.96	66.62	83.27	99.93	116.58	133.24	149.89	166.55	183.2
313	57.91	86.87	115.82	144.78	173.73	202.69	231.64	260.6	289.55	318.51
323	96.84	145.26	193 68	242.1	290.5	338.94	387.36	435.78	484.2	532.62
333	156.39	234.6	312.79	391	469.18	547.38	625.58	703.77	781.97	860.17
343	244.64	366.96	489.28	611.6	733.9	856.24	978.56	1100.88	1223.2	1345.52
353	371.72	557.59	743.45	929.3	1115.17	1301.04	1486.9	1672.76	1858.62	2044.48
363	550.42	825.62	1100.83	1376.04	1651.25	1926.45	2201.66	2476.87	2752.08	3027.28
373	795.56	1193.35	1591.13	1988.91	2386.7	2784.48	3182.26	3580.04	3977.82	4376.6

T,°K \ φ	0.60	0.65	0.70	0.75	0.80	0.85	0.90	0.95	1
273	28.76	31.16	33.55	35.95	38.35	40.74	43.14	45.54	47.93
283	57.85	62.67	67.49	72.31	17.13	81.95	86.77	91.59	96.41
293	110.17	119.35	128.53	137.71	146.89	156.07	165.25	174.43	183.61
303	199.86	216.51	233.17	249.82	266.48	283.13	299.79	316.44	333.1
313	347.46	376.42	405.37	434.33	463.28	492.24	521.19	550.15	579.1
323	581.04	629.46	677.88	726.3	774.73	823.15	871.57	920	968.41
333	938.36	1016.56	1094.76	1172.95	1251.15	1329.35	1407.55	1485.74	1563.94
343	1467.84	1590.16	1712.48	1834.8	1957.12	2079.45	2201.77	2324.1	2446.41
353	2230.35	2416.21	2602.07	2787.93	2973.8	3159.66	3345.5	3531.38	3717.24
363	3302.49	3577.7	3852.9	4128.11	4403.3	4678.5	4953.7	5228.95	5504.15
373	4773.38	5171.16	3568.95	5966.73	6364.5	6762.3	7160.08	7557.86	7955.01

By applying the Clapeyron equation to the case of moist air we obtain

$$j = - D_{12} \frac{M_1 P}{RT} \nabla P_{10}. \tag{4}$$

Since by definition $p_1 = PP_{10}$, we have

$$j = -D_{12} \frac{M_1}{RT} \nabla p_1. \tag{5}$$

Using the identity

$$\nabla p_1 \equiv \left(\frac{\partial p_1}{\partial \mu} \right)_\tau \nabla \mu, \tag{6}$$

we ultimately obtain

$$j = -D_{12} \frac{M_1}{RT} \left(\frac{\partial p_1}{\partial \mu} \right)_\tau \nabla \mu. \tag{7}$$

From (7) we obtain the following expression for the mass transfer coefficients:

$$\lambda = \frac{D_{12} M_1}{RT} \left(\frac{\partial p_1}{\partial \mu} \right)_\tau. \tag{8}$$

Equation (8) may be transformed by using the known expression for the chemical potential of mass transfer in the hygroscopic range $\mu = RT \ln \varphi$ /4/.

Indeed, we may write that

$$\left(\frac{\partial p_1}{\partial \mu} \right)_\tau = \left(\frac{\partial p_1}{\partial \varphi} \right)_\tau \left(\frac{\partial \varphi}{\partial a} \right)_\tau. \tag{9}$$

But since $\left(\frac{\partial p_1}{\partial \varphi} \right)_\tau = p_s$ and $\left(\frac{\partial \varphi}{\partial \mu} \right)_\tau = \frac{\varphi}{RT}$ we obtain

$$\left(\frac{\partial p_1}{\partial \mu} \right)_\tau = p_s \frac{\varphi}{RT}. \tag{10}$$

In that case (8) may be written

$$\lambda = \frac{D_{12} M_1 p_s \varphi}{(RT)^2}. \tag{11}$$

The molecular diffusion coefficient of vapor from the surface of the capillary-porous body may be determined from the following equation /2/

$$D_{12} = D_0 \left(\frac{T}{273} \right)^n \frac{760}{P}, \tag{12}$$

where D_0 is the molecular diffusion coefficient of the vapor at 273°K and $1.01 \cdot 10^5$ N/m^2. For water vapor $D_0 = 0.22 \cdot 10^{-4}$ m^2/sec; n is a coefficient whose value lies between 1.75 and 2.0 /2/. In our calculations we used $n = 2.0$ and $p = 745$ mm Hg.

By substituting (12) in (11) and using the values reported above, we obtain the following expression for the mass transfer coefficient of air:

$$\lambda = 0.77 \cdot 10^{-15} p_s \varphi \left[\frac{\text{kg·mole}}{\text{m·j·sec}} \right]. \tag{13}$$

Using equation (13) we calculated the values of the mass transfer coefficient of air (see the table). The results may be used for the calculation of the mass transfer between a capillary-porous body and the surrounding medium.

SYMBOLS

j — density of the moisture flow, kg/m^2·sec; β — mass transfer coefficient, m/sec; ρ —density of the material, kg/m^3; u —specific mass content kg/kg; λ — mass transfer coefficient, kg-mole/m·j·sec; D_{12} — molecular diffusion coefficient of the vapor from the surface of the capillary-porous body 1 into the surrounding medium 2, m^2/sec; M_1 — molecular weight of the vapor; M — molecular weight of the binary (vapor-gas) mixture; ρ_c — density of the binary mixture, kg/m^3; R — the gas constant; T — absolute temperature; p_s — pressure of the saturated vapor; φ — relative humidity of the air.

Bibliography

1. Lykov, A.V. and Yu.A. Mikhailov. Teoriya teplo- i massoperenosa (The Theory of Heat and Mass Transfer). — Gosenergoizdat. 1963.
2. Lykov, A.V. Teoriya sushki (The Theory of Drying). — Gosenergoizdat. 1950.
3. Lykov, A.V. Teoreticheskie osnovy stroitel'noi teplofiziki (Theoretical Foundations of Structural Thermophysics). — AN BSSR. 1961.
4. Nikitina, L.M. — IFZh, No.4, 1963.

L. M. Nikitina

THE SPECIFIC ISOTHERMAL MASS CAPACITY OF HUMID AIR

The true specific isothermal mass capacity of humid air may be determined either by means of *Id*- diagrams or by calculations with the aid of known equations.

It is well known /1/ that the moisture content of humid air is determined by means of the equation

$$x = 0.622 \frac{p_p}{P_b - p_p}. \tag{1}$$

We may write

$$x = 0.622 \frac{p_p/p_s}{(P_b - p_p)/p_s} = 0.622 \frac{\varphi}{\frac{P_b}{p_s} - \varphi}. \tag{2}$$

Then

$$\left(\frac{\partial x}{\partial \varphi}\right)_T = \frac{0.622 P_b/p_s}{\left(\frac{P_b}{p_s} - \varphi\right)^2}. \tag{3}$$

It is known, also, that the chemical potential of mass transfer in the hygroscopic range $\mu = RT \ln \varphi$ /2/, hence, $(\partial\varphi/\partial\mu)_T = \varphi/RT$; ultimately, we obtain the following expression for the true specific isothermal mass-absorption capacity of humid air

$$c'_m = \left(\frac{\partial x}{\partial \mu}\right)_T = \left(\frac{\partial x}{\partial \varphi}\right)_T \left(\frac{\partial \varphi}{\partial \mu}\right)_T = \frac{0.622 P_b/p_s}{\left(\frac{P_b}{p_s} - \varphi\right)^2} \frac{\varphi}{RT}. \tag{4}$$

We calculated the values c'_m of humid air at temperatures between 273 and 373°K and relative humidities $\varphi = 0.1 - 1.0$.

On the basis of the data on the true specific isothermal mass capacity we calculated the mean specific isothermal mass capacity of humid air $\bar{c}_m$. The calculated values are tabulated.

The table shows that the specific isothermal mass capacity (true and mean) of humid air depends on the temperature (contrary to the case of colloidal capillary-porous bodies). Thus, when the temperature of the humid air is increased from 273 to 368°K the mean specific isothermal mass capacity increases from $0.0092 \cdot 10^{-7}$ to $8.9 \cdot 10^{-7}$ moles/j,

i.e., by about three orders of magnitude. According to equation (4), at $\varphi = 1.0$ and $T = 373°K$ we have $c'_m = \infty$.

TABLE

The true ($c'_m \cdot 10^7$, moles/j) and mean ($\bar{c}_m \cdot 10^7$, moles/j) specific isothermal mass capacities of humid air

Temperature, °K	Relative humidity of air										$\bar{c}_m$
	0.1	0.2	0.3	0.4	0.5	0.6	0.7	0.8	0.9	1.0	
273	0.00160	0.00325	0.00486	0.00654	0.0082	0.01	0.0114	0.013	0.0148	0.0164	0.0092
278	0.00227	0.00455	0.00682	0.00913	0.0115	0.0138	0.0161	0.0184	0.0207	0.023	0.0125
283	0.00315	0.0063	0.0095	0.013	0.0159	0.0192	0.0223	0.0257	0.0289	0.032	0.0178
288	0.0043	0.0086	0.013	0.0174	0.0218	0.0263	0.0307	0.0354	0.0398	0.0443	0.0212
293	0.0058	0.0117	0.0175	0.0235	0.0297	0.0357	0.0417	0.048	0.054	0.0604	0.0328
298	0.00776	0.0154	0.0236	0.0314	0.040	0.048	0.0564	0.065	0.073	0.082	0.0437
303	0.0102	0.0206	0.031	0.042	0.053	0.064	0.075	0.087	0.098	0.11	0.0604
308	0.0134	0.0271	0.0412	0.0554	0.0703	0.0851	0.1	0.116	0.132	0.149	0.078
313	0.0174	0.0353	0.0537	0.0728	0.0926	0.113	0.133	0.155	0.177	0.2	0.1064
318	0.0221	0.0452	0.069	0.0938	0.119	0.146	0.174	0.204	0.234	0.265	0.16
323	0.0285	0.0582	0.0894	0.123	0.158	0.194	0.233	0.274	0.316	0.361	0.163
328	0.036	0.0752	0.116	0.16	0.207	0.257	0.311	0.369	0.434	0.497	0.246
333	0.0429	0.089	0.139	0.195	0.252	0.317	0.387	0.463	0.547	0.639	0.311
338	0.0556	0.118	0.186	0.26	0.345	0.437	0.539	0.655	0.78	0.931	0.43
343	0.0702	0.149	0.239	0.342	0.457	0.59	0.747	0.927	1.31	1.366	0.556
348	0.086	0.187	0.306	0.443	0.609	0.804	1.038	1.316	1.65	2.068	0.81
353	0.107	0.236	0.392	0.589	0.827	1.128	1.502	1.98	2.61	3.41	1.22
358	0.132	0.30	0.515	0.79	1.155	1.633	2.29	3.19	4.48	6.4	1.94
363	0.161	0.376	0.667	1.066	1.62	2.418	3.625	5.564	8.73	14.625	3.33
368	0.198	0.477	0.898	1.485	2.432	3.99	6.72	11.96	23.99	58.9	8.9
373	0.243	0.615	1.21	2.20	3.94	7.37	15.318	39.215	178.514	∞	—

A knowledge of the specific isothermal mass capacity of humid air is necessary for the calculation of the mass transfer of a substance from a colloidal capillary-porous body to air (and vice versa) when a difference in the chemical potential of mass transfer exists between them.

SYMBOLS

P_b — barometric pressure; p_p — partial pressure of the vapor; p_s — pressure of the saturated vapor; φ — relative humidity of the air; R — gas constant; T — temperature.

Bibliography

1. Lykov, A.V. Teoriya sushki (The Theory of Drying). — Gosenergoizdat. 1950.
2. Nikitina, L.M. — IFZh, No.4. 1963.

I. F. Pikus

SOME PROBLEMS OF THE FLUIDIZED-BED DRYING OF HEAT-SENSITIVE MATERIALS IN A CYCLIC REGIME

The different time dependence of the moisture and temperature fields, which is characteristic of all heat-sensitive materials (Lu $\ll 1$), is the cause of the different rates of heat and mass transfers during the fluidized-bed drying of such materials; heating of the particles is much more rapid than their dehydration /3, 7, 8, 10/. This imposes a limitation on the possibilities of intensifying the process, and hence reduces the effectiveness of utilization of fluidized-bed techniques for the drying of disperse heat-sensitive materials under conditions of continuous heating. Indeed, an increase in the initial temperature of the heating medium (all other conditions being equal) causes an even greater difference between the heat and mass transfer rates; at the same time the comparatively rapid increase in the temperature of the material in a fluidized bed makes it impossible to remove the required amount of moisture without exceeding the maximum permissible temperature for the heat-sensitive material and hence without impairing the quality of the material.

The need to maintain the quality of heat-sensitive materials during their rapid fluidized-bed drying makes it necessary to use a cyclic regime — successive heating-cooling cycles at predetermined time intervals. The cyclic drying ensures the required decrease in the moisture content of the material to be dried, without impairing its quality, and also results in a high-efficiency process /7, 8, 10/.

It is clear that the achievement of the optimum efficiency in the fluidized-bed drying of disperse heat-sensitive materials under cyclic conditions depends to a great extent on the adequate selection of the parameters of the drying agent (primarily, the temperature and velocity of the hot gases and of the air used as coolant), the specific load on the grid, and adequate conditions of cycling. The velocity of the drying agent is usually limited by the value at which the whole fluidized bed is mixed fairly vigorously, while the specific load of material on the grid is determined by the requirements for minimum specific consumption of heat and energy.

The conditions of cycling are determined by the ratio of the heating time of the material in each cycle to the cooling time $\Delta\tau_h/\Delta\tau_c$ as well as by the duration of each cycle $T=\Delta\tau_h+\Delta\tau_c$ (or the frequency of the cycle $\nu=1/T$). By increasing the frequency it is possible to use heating media at higher temperatures in the above process without the hazards of overheating and without impairing the quality of the heat-sensitive material. This is explained by two main facts: in the first place, the higher the cycle

frequency the smaller is the range of fluctuations in the temperature of the material to be dried, so that the mean temperature of the material during drying may be maintained much nearer to the maximum permissible temperature; in the second place, maintaining of quality of most heat-sensitive materials depends to a great extent on the holding time at the maximum temperature /3/ and hence the thermostability limit of heat-sensitive materials becomes higher as the half-time for heating during drying in cycles is reduced.

However, if the cycle frequency is too high the process may be affected by the heat resistance of the material particles, since the penetration of a heat wave into a body heated in accordance with a certain periodic rule (cyclic conditions) is, in particular, a reciprocal function of the frequency of fluctuation of the temperature of the heating medium (drying agent) /6/. As a result the difference between the surface temperature of the particles and their mean temperature may become quite substantial during the half-time of heating, and this may ultimately affect the value of the maximum permissible temperature of the heat-sensitive material.

The selection of the optimum conditions of cycling must be based not only on the specific properties of the material to be dried (heat sensitivity, ratio of heating to dehydration rates, particle size, etc.) but also on the possibility of using the simplest and most convenient drying equipment. As a result, it appears that the most advantageous and economical drying of disperse heat-sensitive materials is by a fluidized-bed technique using high-frequency cyclic regimes, with symmetrical cycles, i.e., with heating and cooling half-times of equal duration: $\Delta\tau_h = \Delta\tau_c$ (or $\Delta\tau_h/\Delta\tau_c = 1:1$). Like the selection of too high a cycle frequency, the use of a cyclic process with non-symmetrical cycles may require more complex equipment.

The selection of the temperature of the drying agent (which is the main control parameter of the process) must be carried out with special care. It is significant that the efficiency of drying under cyclic conditions in the case of heat-sensitive materials is determined not only by the use of hot gases but also by the selection of an adequate temperature of the cooling air. In the half-time (phase) of cooling, the material to be dried is cooled both by evaporation and by direct transfer of heat to the "cold" air. Evidently, under cyclic conditions the cooling of the material must be arranged in such a way that the heat losses with the cooling air are reduced to a minimum. An increase in the thermal efficiency of the drying equipment may be achieved by reducing the temperature gradient between the cooling air and the material to be cooled. In this way cooling of the material would occur mainly at the expense of the heat utilized by spontaneous evaporation of the material /1/. Thus, in each subsequent cycle the temperature of the cooling air should increase in accordance with the increase in the material temperature during the drying process. However, in practice, it is very difficult to achieve variable cycling conditions with a constantly increasing temperature, and for the drying of most materials it is not economically justified. Hence, it is advantageous to keep the temperature of the cooling air at a value intermediate between the starting and the final (maximum permissible) temperature of the material during the drying process (t_c^{opt}) /8/.

It is evident that the temperature of the cooling air must be selected to conform with the other process parameters. The selection must be such

that it provides for optimum heating and dehydration rates and for satisfactory technological and economical parameters of the process without impairing the quality of the product. It should be noted that the cooling air may be heated to the optimum temperature t_c^{opt} by recirculation of a fraction of the spent gases and their mixing with external air.

The thermal calculation of drying equipment for heat-sensitive materials, operating by the above method, consists in essence of the determination of the drying time, taking into account the heating of the material to the maximum permissible temperature /7, 8/. It should be noted that analytical studies of the fluidized-bed drying of heat-sensitive materials under cyclic conditions, with the aim of describing mathematically the related phenomena of heat and mass transfer, are very complicated. This is due in the first place to the fact that the heat transfer in the alternating heating-cooling cycles is an unsteady process that occurs generally in the presence of a negative internal heat source which changes with time and, in addition, at a variable temperature of the drying agent. It is clear that a strictly analytical solution of the above complex problem (which is described by a system of complex differential equations characterizing the heat and moisture transfer both inside the material to be dried and within the drying chamber) is very difficult. Hence, in practice, acceptable calculation formulas are obtained by making some simplifying assumptions and by the processing of experimental data.

In this paper we shall present equations for the approximate calculation of the kinetics of heating of a moist disperse material, which may be applied to fluidized-bed cyclic drying (with high-frequency cycles) during the stages of constant and decreasing drying rates. It is known that the rapid drying of heat-sensitive materials (e.g., the fluidized-bed drying of grain) takes place with a continuous increase in the temperature of the material, even if the drying rate is constant /2, 7/.

In solving the above problem we made the following simplifying assumptions.

At any given moment of time the material within the whole bulk of the fluidized-bed is at a given constant temperature, and at a certain specific load the temperature of the spent drying agent is equal to the temperature of the material ($t_2^{ex} = \vartheta$). This condition is determined by the optimum hydrodynamic conditions for fluidization /4, 5, 7/.

The temperature gradient between the particles in the bed is negligible.

It should be noted that the above assumptions make it possible to calculate the heat transfer during drying by means of the relatively simple equation for the thermal balance of the fluidized bed, without requiring a knowledge of the values of the heat transfer coefficient and the mean temperature gradient, the accurate determination of which is rather difficult /4, 7, 11/.

Under symmetrical cyclic conditions the temperature of the drying agent at the entrance to the bed changes in accordance with the cosine law:

$$t = t_m + A\cos\frac{2\pi}{T}\tau, \qquad (1)$$

where

$$t_m = \frac{t_h + t_c}{2}; \quad A = t_m - t_c = t_h - t_m.$$

The validity of the above assumption has been confirmed experimentally. Evidently, the fact that the change in the temperature of the drying agent at the inlet to the bed is governed by a law resembling the law of simple harmonic oscillations is associated with the time-lag of the cyclic equipment, and with the thermal lag in the air-conducting pipes and the gas-dispersing grid.

It was assumed that the same law governs the drying rate during both the heating and the intermediate cooling half-times (phases). During the stage of constant drying rate

$$\frac{dW}{d\tau} = N = \text{const.} \tag{2}$$

The value of N is determined by the parameters of the process (the temperatures of the hot gases and the cooling air, the mass velocity of the drying agent, the specific load of the material) and depends also on the size and shape of the particles of the material /7, 9/.

It may be assumed (with an accuracy sufficient for technological calculations) that in the second stage of drying the drying rate changes in accordance with the equation /2/

$$\frac{dW}{d\tau} = kN(W_{ce} - W_e)\exp(-kN\tau), \tag{3}$$

where k is an empirical drying coefficient, i.e., a constant whose value is determined experimentally.

In view of the specific features of the process, it may be assumed that the errors introduced into the calculations by the above assumptions are small. Indeed, during high-frequency cyclic drying the temperature of the material changes only slightly in each of the short (of the order of seconds) half-times of heating and cooling. Hence, the decrease in the drying rate during the intermediate cooling phases (which is caused by a certain decrease in the temperature of the material) can be neglected. Moreover, it should be noted that in the intermediate cooling phases the drying is assisted by the so-called heat-and-moisture conductance.

Let us neglect the heat losses into the surrounding medium.

Taking into account the above assumptions, we shall derive a differential equation for the thermal balance, to be applied to cyclic drying of a moist material in a fluidized bed,

$$F_g v\gamma c\left(t_m + A\cos\frac{2\pi}{T}\tau - \vartheta\right)d\tau = Gc_м d\vartheta + G\frac{dW}{100+W}r. \tag{4}$$

It is characteristic that the optimum mass velocity of the drying agent v_γ is usually taken as constant during the cycles. The heat capacity c of the drying agent is determined from the mean air temperature t_m, while the heat of vaporization r is generally determined by means of the following approximate equation /11/:

$$r = 597 - 0.56\vartheta_m + r_{E_n}. \tag{5}$$

For the stage of constant drying rate we have

$$W = W_1 - N\tau; \tag{6}$$

$$G = G_1 \frac{100 + W_1 - N\tau}{100 + W_1}; \tag{7}$$

$$c_м = c_{dm} + (1 - c_{dm}) \frac{W}{100 + W} = \frac{100 c_{dm} + W_1 - N\tau}{100 + W_1 - N\tau}. \tag{8}$$

By substituting (7) and (8) into equation (4) and making some modifications taking into account equation (2), we obtain

$$\frac{d\vartheta}{d\tau} = \vartheta \frac{Fgv\gamma c\,(100 + W_1)}{G_1\,(100 c_{dm} + W_1 - N\tau)} =$$

$$= \frac{Fgv\gamma c\,(100 + W_1)\left(t_m + A\cos\frac{2\pi}{T}\tau\right)}{G_1\,(100 c_{dm} + W_1 - N\tau)} - \frac{Nr}{100 c_{dm} + W_1 - N\tau}. \tag{9}$$

Let us use the notation

$$\frac{Fgv\gamma c\,(100 + W_1)}{G_1} = B; \tag{10}$$

$$100 c_{dm} + W_1 = M_1; \tag{11}$$

$$Nr = D_1. \tag{12}$$

Then

$$\frac{d\vartheta}{d\tau} + \vartheta \frac{B}{M_1 - N\tau} = \frac{B\left(t_m + A\cos\frac{2\pi}{T}\tau\right) - D_1}{M_1 - N\tau}. \tag{13}$$

By solving the non-homogeneous linear equation of the first order (13) for a boundary condition $\vartheta|_{\tau=0} = \vartheta_0$ we obtain

$$\vartheta = t_m - \frac{D_1}{B} + \left(\vartheta_0 - t_m + \frac{D_1}{B}\right)\left(\frac{M_1 - N\tau}{M_1}\right)^{\frac{B}{N}} +$$

$$+ AB(M_1 - N\tau)^{\frac{B}{N}} \int_0^{\tau} (M_1 - N\tau)^{-\frac{B}{N}} \cos\frac{2\pi}{T}\tau\, d\tau. \tag{14}$$

A general solution of the definite integral of equation (14) has the form

$$S(\tau) = \int_0^{\tau} p(\tau)\cos b\tau\, d\tau = \sin b\tau \left[\frac{p(\tau)}{b} - \frac{p''(\tau)}{b^3} + \ldots\right] +$$

$$+ \cos b\tau \left[\frac{p'(\tau)}{b^2} - \frac{p'''(\tau)}{b^4} + \ldots\right] - \left[\frac{p'(0)}{b^2} - \frac{p'''(0)}{b^4} + \ldots\right], \tag{15}$$

where

$$p(\tau) = (M_1 - N\tau)^{-\left(\frac{B}{N}+1\right)}; \quad b = \frac{2\pi}{T}.$$

By substituting the value of $p(\tau)$ and its derivaties in (15) it can be seen that the square brackets comprise decreasing alternating series; an analysis

shows that in general for practical calculations it is sufficient to take the first terms of each of those series. Omitting the intermediate rearrangements, we obtain

$$S(\tau) = \frac{(M_1 - N\tau)^{-\left(\frac{B}{N}+1\right)} \sin\frac{2\pi}{T}\tau}{\frac{2\pi}{T}} + \frac{(M_1 - N\tau)^{-\left(\frac{B}{N}+2\right)}(B+N)\cos\frac{2\pi}{T}\tau}{\left(\frac{2\pi}{T}\right)^2} - \frac{(B+N)(M_1)^{-\left(\frac{B}{N}+2\right)}}{\left(\frac{2\pi}{T}\right)^2}. \quad (16)$$

Substitution of (16) in (14) finally yields

$$\vartheta = t_m - \frac{D_1}{B} + \left[\vartheta_0 - t_m + \frac{D_1}{B} - \frac{AB(B+N)}{\left(\frac{2\pi}{T}\right)^2 M_1^2}\right]\left(\frac{M_1 - N\tau}{M_1}\right)^{\frac{B}{N}} + \frac{AB\sin\frac{2\pi}{T}\tau}{\frac{2\pi}{T}(M_1 - N\tau)} + \frac{AB(B+N)\cos\frac{2\pi}{T}\tau}{\left(\frac{2\pi}{T}\right)^2 (M_1 - N\tau)^2}. \quad (17)$$

Thus, equation (17) may be used for the approximate calculation of the kinetics of high-frequency symmetric heating in cycles of a moist material in a fluidized bed, applicable to cyclic drying (during the constant drying rate stage).

For the stage of the decreasing drying rate, the equation for the calculation of the kinetics of heating of a moist material in the above process has the following form /11/, taking into account equations (1) and (3):

$$\frac{d\vartheta}{d\tau} + \vartheta \frac{B\exp(kN\tau)}{M\exp(kN\tau) + W_{ce} - W_e} = \frac{B\exp(kN\tau)\left(t_m + A\cos\frac{2\pi}{T}\tau\right) - D}{M\exp(kN\tau) + W_{ce} - W_e}, \quad (18)$$

where

$$M = 100c_{dm} + W_p; \quad D = kN(W_{ce} - W_e)r.$$

For a boundary condition $\vartheta|_{\tau=0} = \vartheta_1$ the solution of the non-homogeneous linear equation of the first order (18) has the form

$$\vartheta = t_m + (\vartheta_1 - t_m)\left[\frac{M + W_{ce} - W_e}{M\exp(kN\tau) + W_{ce} - W_e}\right]^{\frac{B}{MkN}} + S_1(\tau) - S_2(\tau), \quad (19)$$

where ϑ_1, is the initial temperature of the material in the decreasing drying rate stage;

$$S_1(\tau) = AB[M\exp(kN\tau) + W_{ce} - W_e]^{-\frac{B}{MkN}} \times$$

$$\times \int_0^\tau \cos\frac{2\pi}{T}\tau \exp(kN\tau)[M\exp(kN\tau) + W_{ce} - W_e]^{\frac{B}{MkN}-1} d\tau; \qquad (20)$$

$$S_2(\tau) = D[M\exp(kN\tau) + W_{ce} - W_e]^{-\frac{B}{MkN}} \times$$

$$\times \int_0^\tau [M\exp(kN\tau) + W_{ce} - W_e]^{\frac{B}{MkN}-1} d\tau. \qquad (21)$$

According to (11) it may be assumed with a high degree of accuracy that

$$S_2(\tau) = \frac{D}{\exp(kN\tau)(B - MkN)} -$$

$$- \frac{D}{B - MkN}\left[\frac{M + W_{ce} - W_e}{M\exp(kN\tau) + W_{ce} - W_e}\right]^{\frac{B}{MkN}}. \qquad (22)$$

By using the above method of approximate integration ((15) and (16)) we obtain

$$S_1(\tau) = \frac{AB\exp(kN\tau)\sin\frac{2\pi}{T}\tau}{\frac{2\pi}{T}[M\exp(kN\tau) + W_{ce} - W_e]} +$$

$$+ \frac{AB(B - MkN)\exp(2kN\tau)\cos\frac{2\pi}{T}\tau}{\left(\frac{2\pi}{T}\right)^2[M\exp(kN\tau) + W_{ce} - W_e]^2}$$

$$- \frac{AB(B - MkN)}{\left(\frac{2\pi}{T}\right)^2(M + W_{ce} - W_e)^2}\left[\frac{M + W_{ce} - W_e}{M\exp(kN\tau) + W_{ce} - W_e}\right]^{\frac{B}{MkN}}. \qquad (23)$$

By substituting (22) and (23) in (19) we obtain finally

$$\vartheta = t_m + \left[\vartheta_1 - t_m + \frac{D}{B - MkN} - \frac{AB(B - MkN)}{\left(\frac{2\pi}{T}\right)^2(M + W_{ce} - W_e)^2}\right] \times$$

$$\times \left[\frac{M + W_{ce} - W_e}{M\exp(kN\tau) + W_{ce} - W_e}\right]^{\frac{B}{MkN}} + \frac{AB\exp(kN\tau)\sin\frac{2\pi}{T}\tau}{\frac{2\pi}{T}[M\exp(kN\tau) + W_{ce} - W_e]} +$$

$$+ \frac{AB(B - MkN)\exp(2kN\tau)\cos\frac{2\pi}{T}\tau}{\left(\frac{2\pi}{T}\right)^2[M\exp(kN\tau) + W_{ce} - W_e]^2} - \frac{D\exp(-kN\tau)}{B - MkN}. \qquad (24)$$

The applicability of the above approximate method for the kinetics of heating of a moist material in periodic drying in a fluidized bed under

conditions of high-frequency cycling was confirmed by experiments. The reliability of the above equations was checked by comparing with their results our experiments on drying of potatoes and fruits (cut into cubes) as well as with experimental data /8/ on drying of grain. The discrepancy between the calculated and the experimental data did not exceed 10 — 12%.

SYMBOLS

t; t_h t_c — respectively, the current temperature of the drying agent, the temperature of the hot gases, and the temperature of the cooling air; A — the range of fluctuations of the drying agent temperature; T — the fluctuation time; v; γ; and c are, respectively, the velocity, specific gravity, and specific heat of the drying agent; F_g — surface area of the gas-dispersing grid; G — the weight of the material at a moisture content W; ϑ — temperature of the material; c_{dm} — heat capacity of the dry matter W_1, W_{ce} and W_e are, respectively, the initial, the critical equivalent and the equilibrium moisture contents of the material; τ — time; N — drying rate in the constant drying rate stage; c_M — heat capacity of the material; r — heat of vaporization; ϑ_{tm} — mean temperature of the material over the time τ; $r_{E.m}$ — the mean integral value of the moisture-material bond energy in the range of moisture to be removed.

Bibliography

1. Lyuboshits, I.L. Teplo i massoperenos (Heat and Mass Transfer), Vol. 4. — Gosenergoizdat. 1963.
2. Lykov, A.V. Teplo i massoobmen v protsessakh sushki (Heat and Mass Transfer in Drying Processes). — Gosenergoizdat. 1956.
3. Ginzburg, A.S. Sushka pishchevykh produktov (The Drying of Foodstuffs). — Pishchepromizdat. 1960.
4. Zabrodskii, S.S. Gidrodinamika i teploobmen v psevdoozhizhennom sloe (Hydrodynamics and Heat Transfer in Fluidized Beds). — Gosenergoizdat. 1963.
5. Fedorov, I.M. Teoriya i raschet protsessa sushki (The Theory and the Calculation of Drying Processes). — Gosenergoizdat. 1955.
6. Lykov, A.V. and Yu.A. Mikhailov. Teoriya teplo i massoperenosa (The Theory of Heat and Mass Transfer). — Gosenergoizdat. 1963.
7. Ginzburg, A.S. and V.A. Rezchikov. — IFZh, No.8. 1962.
8. Slobodkin, L.S. — IFZh, No.3. 1964.
9. Grishin, M.A. — IFZh, No.5. 1960.
10. Zhidko, V.I. Teplo i massoperenos (Heat and Mass Transfer), Vol. 4. — Gosenergoizdat. 1963.
11. Pikus, I.F. — In Sbornik: "Teplo i massoobmen v dispersnykh sistemakh." Minsk, Izd. Nauka i Tekhnika. 1965.

A. I. Lyuboshits

EXPERIMENTAL DETERMINATION OF THE MASS TRANSFER COEFFICIENT IN THE COOLING OF MOIST GRAIN AFTER DRYING IN MULTISECTIONAL PACKED HEAT EXCHANGERS

In order to secure the preservation of grain after drying, it must be cooled from 50 — 60°C to a temperature near the temperature of the external air.

At present, after drying the grain is cooled in shafts divided into compartments — multisectional packed heat exchangers. The recent literature contains no data on evaporation from the grain during the cooling — a process that is called below spontaneous evaporation.

The actual values of the mass transfer coefficient during spontaneous evaporation were determined experimentally, in separate measurements for each material studied.

In order to obtain conditions similar to those existing in industrial processes, we carried out the experiments in an apparatus of the same construction as a multisectional packed heat exchanger.

In cooling a moist disperse material by pumping air through the bed, the temperature is reduced by two simultaneous processes: convective heat transfer from the particles of the moving material to the cooling air, and evaporation of moisture from the hot material.

Depending on the values of the various parameters, the relative contributions of each of those processes may be different. In this paper we shall discuss only the process of spontaneous evaporation. In this process evaporation occurs not at the expense of heat supplied from the outside but at the expense of the enthalpy of the material itself. Throughout the whole process the temperature of the material is higher than that of the cooling air.

An important feature of spontaneous evaporation during cooling of moist grain is the negligible decrease in moisture content (about 1%, i.e., from 15 to 14%), which cannot have a substantial influence on the redistribution of the moisture within the material. At the same time there occurs a noticeable additional decrease in the temperature of the material.

It should be born in mind that the mass transfer coefficient referred to the nominal (total) surface (i.e., the true coefficients) are much higher than the effective values. The rate of spontaneous evaporation referred to one m^2 of the total geometric surface of all particles in the layers is determined by the equation

$$S = \psi(H - h). \qquad (1)$$

The mass transfer coefficient in spontaneous evaporation ψ depends on the gas velocity and the nature of the flow round the particles. The partial pressure of water vapor over the surface of the material H is a function of the nature of the material, its temperature and moisture content. The partial pressure of water vapor h depends on the moisture content of the surrounding air. The influence of the factors affecting the value of H was studied without blowing air through the bed, i.e., under conditions of natural cooling. The experiments were carried out at different initial temperatures of the material (35, 50, 65°C) and at a moisture content of 15% (i.e., the moisture content characteristic for cooling of grain after drying).

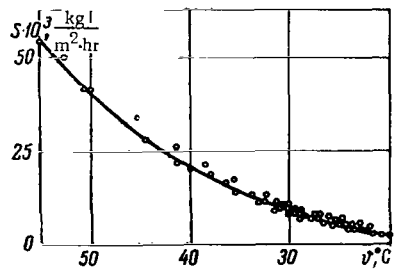

FIGURE 1. Dependence of the rate of spontaneous evaporation $S \cdot 10^3$ kg/m^2·hr on the temperature of the grain ϑ°C for a moisture content $\omega = 15\%$.

The experimental results are shown in Figure 1. An analysis of the data shown in that figure indicates that the value of H may be calculated (with an accuracy satisfactory for practical purposes) from the equation

$$H = 5.3\vartheta^2. \qquad (2)$$

The experiments for the determination of ψ during blowing of air through the layers were carried out with grain of the same moisture content as above. Processing of the experimental results yielded the Kossovich number Ko, while the value of ψ was determined from equation

$$\mathrm{Ko} = \frac{r\psi(5.3\vartheta_m^2 - h)}{\alpha(\vartheta - t)_m} \qquad (3)$$

The experiments were carried out at various mass velocities of the air (v_γ), between 0.1 and 0.4 kg/sec·m^2. The effect of the mass velocity of the air on the mass transfer coefficient ψ is shown in Figure 2. The line in this figure satisfies the equation

$$\psi = 0.18 \cdot 10^{-8} (v_\gamma)^{0.21} \text{ kg/sec·m}^2\text{·m} \qquad (4)$$

Equation (4) shows that the air velocity has relatively little influence on the value of ψ, and that this effect is much less pronounced than its effect on the heat transfer coefficient α. This may be seen by comparing equation

(4) with the dimensionless equation for the heat exchange between a gas and a moving grain layer. According to our experiments the equation is

$$Nu = 0.043\,Re^{0.78}.$$

Thus, when the mass velocity of air is increased the heat consumed for the process of spontaneous evaporation increases much more slowly than the heat consumed for heating of the cooling air. This is characterized by a decrease in the Kossovich number. A curve representing the effect of the mass velocity of air in the cooling column of a grain drier on the Kossovich number is shown in Figure 3; the curve was plotted on the basis of equation (3).

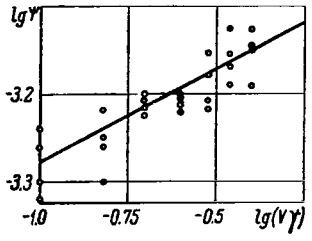

FIGURE 2. Effect of the mass velocity of air on the mass transfer coefficient

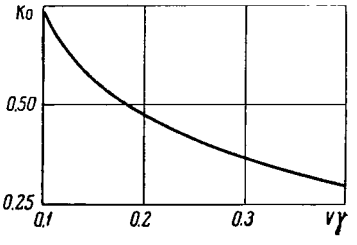

FIGURE 3. Effect of the mass velocity of air on the Kossovich number.

SYMBOLS

ϑ — temperature of the material; t — air temperature; r — heat of evaporation; $(\vartheta - t)_m$ — the mean temperature gradient between the grain and the air

A. I. Lyuboshits

DETERMINATION OF THE OPTIMUM THICKNESS OF LAYERS IN MULTISECTIONAL PACKED HEAT EXCHANGERS

Multisectional packed heat exchangers consist of a shaft filled with open-bottom compartments /1/. Under the effect of gravity the packing moves from the top to the bottom. Rows of inlet compartments (through which the gases enter the heat exchanger) alternate with rows of exit compartments. Hence, such a heat exchanger is a multisectional one, and in it the concurrent and countercurrent flows alternate.

The vertical distance between rows of compartments determines the thickness of the packing layer in each section, i.e., the parameter that determines the two main indices of performance of the heat exchanger: the effectiveness of the heat exchanger and its resistance to the gas flow.

It is evident that both the effectiveness of the heat exchange and the energy consumption increase as the layer thickness is increased. For this reason it is very important to determine the optimum thickness of the layer for which the technological-economic indices of performance of a multisectional packed heat exchanger have the optimum values.

In order to solve this problem, we shall use an equation (derived in /1/) for "pure" heat transfer (dry packing) in a multisectional packed heat exchanger

$$\frac{\vartheta_2 - t_1}{\vartheta_1 - t_1} = \exp[-R\varepsilon]. \qquad (1)$$

Calculations of multisectional packed heat exchangers are usually based on given values of ϑ_1, ϑ_2, and t_1; it is necessary to determine the dimensions of the heat exchanger.

By substituting in (1) the value of R

$$R = \frac{c_p L}{c_M G},$$

we obtain

$$L = G\,\frac{c_M}{c_p}\,\frac{\ln\dfrac{\vartheta_1 - t_1}{\vartheta_2 - t_1}}{\varepsilon}. \qquad (2)$$

Equation (2) shows that L, and hence at a given gas velocity the dimensions of the heat exchanger, are inversely proportional to the coefficient of effectiveness of the heat exchanger ε which in turn is a function of the complex A:

$$\varepsilon = 1 - \exp[-A]. \tag{3}$$

where

$$A = \frac{\alpha\delta f \eta_3}{c_p(v\gamma)}. \tag{4}$$

The value of f is determined from the equation

$$f = \frac{6(1-m)}{d}. \tag{5}$$

The complex A comprises the Stanton number

$$\mathrm{St} = \frac{\mathrm{Nu}}{\mathrm{Re\,Pr}} = \frac{\alpha}{c_p(v\gamma)}. \tag{6}$$

By substituting (5) and (6) in equation (4) we obtain

$$A = 6(1-m)\eta_3 \mathrm{St}\frac{\delta}{d}. \tag{7}$$

In the case of packed heat exchangers the power of Re in the dimensionless equation showing Nu as a function of Re is almost unity (according to some authors it is equal to unity). Hence, the Nu/Re ratio may be regarded with a fair degree of accuracy as constant (independent of v and d). The Prandtl number is also constant. Therefore, the Stanton number in (7) may also be regarded as constant.

Since the porosity ratio m has a definite value for the packing used, while the filling ratio η_3 is also constant for the given design of the heat exchanger, (7) shows that ultimately the value of A, and hence of the coefficient of effectiveness ε (see (3)), are determined solely by the δ/d ratio, i.e., by the ratio of layer thickness to the diameter of the particles in the packing.

Increasing the δ/d ratio above a certain limit is not to be recommended since the proportional increase in the resistance of the layer will result in a very small increase in ε. This is shown in the following example.

According to (3), a value of $A = 2.3$ corresponds to $\varepsilon = 0.9$. Let us assign the following values to the terms in A: $m = 0.5$, and $\eta_3 = 0.7$.

According to our experiments on the heat exchange between the gas and the packing in a multisectional packed heat exchanger, St = 0.029. Substituting in equation (7) the values of m, η_3, and St we obtain

$$\frac{\delta}{d} = 37.5.$$

When the δ/d ratio, and hence the complex A, are increased by a factor of 5 (i.e., to $A = 11.5$) the value of ε will become equal to unity (in accordance with (3)). Thus, a five-fold increase in the δ/d ratio (which is accompanied by a five-fold increase in the layer resistance) increases the value of ε only from 0.9 to 1.0, i.e., in accordance with (2) the size of the heat exchanger is reduced by only 11%.

Hence, an increase in the δ/d ratio above 35 — 40 is not expedient, and at the above ratio the value of ε is sufficiently high (0.9). A further increase in δ/d results in a negligible increase in ε but at the same time causes a sharp increase in the layer resistance.

SYMBOLS

ϑ_1 — initial temperature of the material; ϑ_2 — final temperature of the material; t_1 — initial temperature of the gas; R — ratio of the water equivalents of the gas and the packing; ε — coefficient of effectiveness of the packed multisectional heat exchanger; c_p — heat capacity of the gas; L — gas throughput; c_M — heat capacity of the material; G — amount of material passing through the heat exchanger; α — heat exchange coefficient between the gas and the material; δ — layer thickness of the material in each section; f — specific surface area, referred to one cubic meter of the volume; η_3 — filling ratio of shaft; v — gas velocity; γ — specific gravity of the gas; m — porosity; d — particle diameter.

Bibliography

1. Lyuboshits, A.I. — IFZh, No. 11. 1963.

Yu. A. Finaev

DEPENDENCE OF THE COMBUSTION RATE OF COKE PARTICLES ON THE FLOW RATE ROUND THE PARTICLES, IN A GENERALIZED DIMENSIONLESS FORM

When coke particles burn in a gas-air stream, the flow velocity of the stream affects the rate of combustion of the particles. The essence of this effect is that the rear (with respect to the flow direction) sections of the particle surfaces are practically excluded from direct reaction with oxygen, since they are covered by the carbon monoxide formed during combustion and entrained with the gas stream. The analytical problem of the effect of the combustion of the carbon monoxide has not been solved as yet, but this effect may be accounted for by means of certain coefficients such as A or δ.

In the case of forced flow the diffusion limit of the specific rate of combustion satisfies the equation /1/

$$K_s^c = \frac{12}{32} A(1 + \xi') c_0 \sqrt{\frac{wD}{d}}, \qquad (1)$$

where $A = \delta/\sqrt{\pi}$; K_s^c is the rate of combustion of the specific surface of the coke particles; d is the particle diameter; c_0 is the oxygen concentration at a distance from the burning particle; D is the diffusion coefficient; w is the flow velocity round the particle; and ξ' is a term in the equation used to calculate the effect of the limiting conditions of combustion when the process is accompanied by the formation of CO only ($\xi' = 1$) or CO_2 only ($\xi' = 0$).

With the aid of certain transformations (1) may be presented in a dimensionless form

$$\frac{K_s^c d}{c_0 D} = \frac{12}{32} (1 + \xi') A \sqrt{\frac{wd}{D}}. \qquad (2)$$

If combustion occurs under molecular diffusion conditions, the limiting equation for the specific rate of combustion is

$$K_s^c = \frac{24}{32} \frac{c_0 D}{d} \qquad (3)$$

or, in a dimensionless form,

$$\frac{K_s^c d}{c_0 D} = \text{const} = \frac{24}{32} = 0.75. \qquad (4)$$

Equations (4) and (2) show that the value of the dimensionless complex $K_s^c d/c_0 D$ may vary from a constant (0.75) in the case of molecular diffusion to a value determined by the dimensionless complex $\sqrt{\omega d/D}$ at higher stream velocities.

L. N. Khitrin showed the data of his experiments /1/ and the experiments of other authors /2 — 5/ on the burning of electrode graphite, anthracite, and brush graphite on a generalized graph (using logarithmic coordinates) in the form of an empirical equation

$$\frac{K_s^c d}{c_0 D} = f\left(\frac{\omega d}{D}\right). \tag{5}$$

The graph is shown in Figure 1. The graph contains also the results of our experimental studies of the rate of combustion of peat coke particles of a diameter of 4.5, 8, and 12 mm as well as of electrode graphite particles 5 mm in diameter, at a furnace temperature of 1270°K and a flow velocity (of the gas round the particles) of 0.2 — 1.35 m/sec /6/.

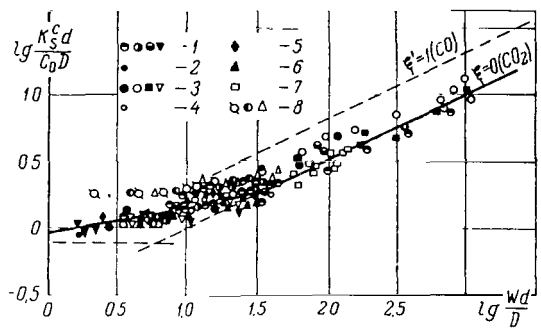

FIGURE 1. Generalized graphical presentation of $K_{sd}^c c_0 D$ as a function of $\omega d/D$.

Electrode graphite (1 — Khitrin /1/; 2 — Blinov and Khaikina /5/; 3 — Tsukhanova and Kolodkina /4/; 4 — Smith and Gudmundsen /2/; 5 — author's data /6/); anthracite (6 — Khitrin /1/); brush graphite (7 — Tu, Davis and Hottel /3/); peat coke (8 — author's data /6/).

We determined the diffusion coefficient D by means of the equation /1/

$$D = 0.18\left(\frac{T}{273}\right)^2. \tag{6}$$

The calculation of the diffusion coefficient as a function of the square of the temperature yields results that are in good agreement with experimental data.

Let us analyze our experimental data. Figure 1 shows that the points characterizing the combustion of electrode graphite particles lie on the curve that averages the data reported in /1 — 5/. The points relating to

combustion of peat coke also form a definite curve with little scattering, but they lie somewhat above the averaged curve. This may be attributed to the fact that the specific rates of combustion calculated for peat coke K_s^c were a little too high since the calculations were based on the external geometrical surface area of the particles rather than on the real surface which was rough, fairly extensive and much larger than the geometrical surface. Our data support the conclusion that the reactivity of peat coke is greater than that of anthracite, electrode graphite, and brush graphite (on the average by 30%).

Figure 1 shows clearly the existence of two boundary states: at small wd/D values the curve approaches a constant value, while at high $/D$ values the curve becomes a straight line with a slope of 0.5. However, most of the experimental points (including those plotted from our data) lie within the range of transitional conditions, where the slope of the curve changes continuously. The best agreement between the theoretical and experimental data is obtained at $\xi' = 0$, i.e., when the reaction proceeds to the formation of CO_2.

Bibliography

1. Predvoditelev, A.S., L.N. Khitrin, O.A. Tsukhanova, Kh.I. Kolodtsev, and M.K. Grozdovskii. Gorenie ugleroda (Combustion of Carbon).— Izd. AN SSSR. 1949.
2. Smith, D. and A. Gudmundsen.— Ind. Eng. Ch., Vol.23: 277. 1931.
3. Tu, C.M., H. Davis, and H.C. Hottel.— Ind. Eng. Ch., Vol.26: 749. 1934.
4. Kolodkina, L.A., O.A. Tsukhanova, and O.N. Oleshchuk. Opredelenie skorosti goreniya ugol'nykh chastits pri obtekanii s bol'shimi skorostyami (Determination of the Rates of Combustion of Carbon Particles in Very Rapid Gas Streams).— VTI. 1937.
5. Blinov, V.I. and S.E. Khaikina.— Izvestiya VTI, No.6. 1935.
6. Finaev, Yu.A. Thesis.— Minsk. 1963.

A. I. Avakov, K. E. Garyainov, and L. T. Yakovlev

THERMAL STRESSES IN CELLULAR CONCRETES DURING HYDROTHERMAL PROCESSING

The hydrothermal processing of concrete causes a number of very complex chemical and physical processes that are associated with the hardening of the concrete, i.e., the formation of crystalline structures in a medium of variable temperature and moisture content.

The existence of such a medium leads to the formation of a temperature-moisture gradient in the concrete which leads to the creation of stresses in the processed material. Those stresses, whose magnitude depends on the physical-mechanical properties of the material, make it necessary to use very prolonged heating and cooling times.

In cellular concretes, i.e., materials of low thermal conductivity, the hydrothermal processing leads to large temperature gradients that may result in stresses leading to failure.

In this paper we have made an attempt to derive, by means of analytical methods, equations for the calculation of the temperature and the thermal stresses associated with it since the magnitude of these stresses determined the selection of the rate of temperature changes.

In a general form, the thermal stresses at the moment τ may be described by the equation

$$\sigma(t, \tau) = f(t_\tau - t_0).$$

In order to obtain an analytical expression for thermal stresses as a function of the temperature, the time and the current variable it is necessary to find

$$\sigma = f_1(t),\ t = \varphi(\tau, x),\ \text{i.e.,}\ \sigma = \psi(\tau, x).$$

A number of authors have reported that the temperature of the concrete does not agree exactly with the analytically calculated temperature, since heat is transferred with the moving moisture. This causes a change in all thermal constants of the processed material. However, for certain mean values of the thermal coefficients it is possible to obtain an analytical equation for the temperature which is in agreement with the experimental data.

Let us assume for the calculations the existence of an infinite plate with a thickness of $2R$, and an initial temperature of the medium and the material equal to t_0; the temperature of the medium t_{me} changes in accordance with the equation $t_{me} = t_0 + b\tau$, and the heat transfer is by convection.

The initial and boundary conditions are

$$t(x,\ 0) = t_0,\ \frac{\partial t(0,\ \tau)}{\partial x} = 0,$$

$$-\frac{\partial t(R,\ \tau)}{\partial x} + H[(t_0 + b\tau) - t(R,\ \tau)] = 0.$$

It is necessary to find $t(x, \tau)$, i.e., to solve the equation

$$\frac{\partial t}{\partial \tau} = a\frac{\partial^2 t}{\partial x^2}.$$

An analytical solution of the above equation at the given initial and boundary conditions has been found by Lykov /2/. In finding the solution Lykov assumes that λ, c, γ, a are constant. In the case discussed here the thermal parameters change as a function of the temperature or the time, or

$$\lambda = f_2(t,\ \tau),\ c = f_3(t,\ \tau),\ \gamma = f_4(t,\ \tau),\ a = \psi_1(t,\ \tau).$$

The determination of the above functions by an analytical method or by experiment is difficult.

An analytical equation for the determination of λ has been proposed /1/:

$$\lambda_{equ} = \frac{(t_{ok} - t_{sp})\gamma c}{2(t_{ps} - t_{cs})M_s^2\tau}. \qquad (1)$$

Equations (2) and (3) may be used to calculate the temperature fields in concrete during heating, by taking the experimental values of λ_{equ} for the time intervals of the determination and by assuming that c and γ are constant.

It is assumed that during the cooling the change in the temperature of the medium is an exponential function of time

$$t_{me} = t_m - (t_m - t_a)e^{-k\tau}.$$

The initial and boundary conditions for the above case have the form

$$t(x,\ 0) = t_a,\quad \frac{\partial t(0,\ \tau)}{\partial x} = 0,$$

$$-\frac{\partial t(R,\ \tau)}{\partial x} + H[t_m - (t_m - t_a)e^{-k\tau} - t(R,\ \tau)] = 0.$$

A solution of the thermal conductivity equation for the above boundary conditions has been reported in /2/.

In the case of autoclave processes the Fourier number is fairly high; hence, only the first terms of the series may be used in (2) and (3) without introducing a large error.

In order to compare the analytical solutions with experimental data we carried out calculations of a plate made of cellular concrete. The following values were used in the calculations:

λ_{equ} = 0.95 w/m·deg and α = 116 w/m^2·deg at $t \leqslant 100$°C

λ_{equ} = 2.33 w/m·deg and α = 580 w/m^2·deg at $t > 100$°C

$c = 2.1 \cdot 10^3$ j/kg·deg, $\gamma = 9810$ N/m^3, $R = 0.2$ m,

$$b = 3 \cdot 10^{-3} \text{ deg/sec}, \quad k = 5.6 \cdot 10^{-5} \text{ 1/sec}, \quad t_m = 20°\text{C},$$

$$t_0 = 20°\text{C}, \quad t_a = 100°\text{C}.$$

The experimental and calculated data are shown in Figure 1.

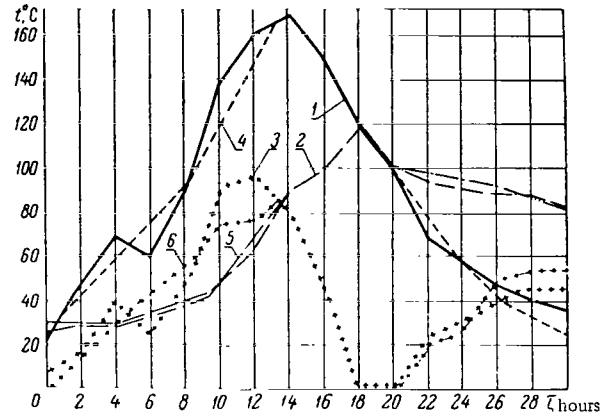

FIGURE 1. Graphical presentation of the calculated and actual temperatures.

1 – actual surface temperature; 2 – actual center temperature; 3 – actual temperature gradient between the center and the surface; 4 – calculated surface temperature; 5 – calculated center temperature; 6 – calculated temperature gradient between the center and the surface.

In the calculations, the values of λ_{equ} and α were taken as the average over the whole time.

Finally we have the change in the temperature:

a) for heating

$$t(x, \tau) - t_0 = 1.3\left\{b\tau - \frac{b}{2a}\left[R^2\left(1 + \frac{2}{\text{Bi}}\right) - x^2\right] + \right.$$

$$\left. + \frac{bR^2}{a}\frac{A_1}{\mu_1^2}\cos\mu_1\frac{x}{R}e^{-\mu_1^2\text{Fo}}\right\}, \qquad (2)$$

where 1.3 is the coefficient of gradient increase;

b) for cooling

$$t(x, \tau) - t_a = (t_m - t_a) \times$$

$$\times\left[1 - \frac{\cos\sqrt{\frac{k}{a}}x e^{-k\tau}}{\cos\sqrt{\frac{k}{a}}R - \frac{1}{H}\sqrt{\frac{k}{a}}\sin\sqrt{\frac{k}{a}}R} - \frac{A_1 e^{-\mu_1^2\text{Fo}}\cos\mu_1\frac{x}{R}}{1 - \frac{a\mu_1^2}{kR^2}}\right] \qquad (3)$$

As is evident from (2) and (3), thermal stresses are created in the concrete plate; the magnitude of those stresses may be calculated (for the case of

fairly distant points in an isotropic elastic body) by the reduced Gatewood equation /3/

$$\sigma_y = \sigma_z = -\frac{\alpha_y ET(x)}{1-\nu} + \frac{1}{2R(1-\nu)}\int_{-R}^{+R} \alpha_y ET(x)\,dx + \\ + \frac{3x}{2R^3(1-\nu)}\int_{-R}^{+R} \alpha_y ET(x)\,x\,dx. \qquad (4)$$

The third term of (4) $\frac{3x}{2R^3(1-\nu)}\int_{-R}^{+R} \alpha_y \times ET(x)\,x\,dx$ is eliminated in the case of a symmetrical temperature distribution in the plate. By substituting in the above equations (2) and (3) we obtain the following expression valid for the heating period of the plate:

$$\sigma_y = \sigma_z = \frac{1.3\alpha_y E b}{a(1-\nu)}\left[\frac{R^2 A_1 e^{-\mu_1^2 Fo}}{\mu_1^2} \times \left(\frac{\sin\mu_1}{\mu_1} - \cos\mu_1 \frac{x}{R}\right) + \frac{R^2}{6} - \frac{x^2}{2}\right], \qquad (5)$$

and for the cooling period

$$\sigma_y = \sigma_z = \frac{(t_m - t_a)\alpha_y E}{1-\nu}\left[\frac{A_1 e^{-\mu_1^2 Fo}}{1 - \frac{a\mu_1^2}{kR^2}}\left(\cos\mu_1 \frac{x}{R} - \frac{\sin\mu_1}{\mu_1}\right) + \right.$$

$$\left. + \frac{e^{-k\tau}\left(\cos\sqrt{\frac{k}{a}}\,x - \frac{\sin\sqrt{\frac{k}{a}}\,R}{\sqrt{\frac{k}{a}}\,R}\right)}{\cos\sqrt{\frac{k}{a}}\,R - \frac{1}{H}\sqrt{\frac{k}{a}}\sin\sqrt{\frac{k}{a}}\,R}\right]. \qquad (6)$$

Let us determine the maximum and minimum σ as a function of τ and x. To this end let us solve the system of equations $\frac{\partial\sigma}{\partial\tau} = 0$ and $\frac{\partial\sigma}{\partial x} = 0$ with respect to τ and x. By checking the obtained solutions against $\frac{\partial^2\sigma}{\partial\tau^2}$, $\frac{\partial^2\sigma}{\partial x^2}$ and $\frac{\partial^2\sigma}{\partial x\cdot\partial\tau}$ we obtain that for the heating period $\sigma = \sigma_{max}$ at $x = 0$ and $\tau = \infty$ while for the cooling period $\sigma = \sigma_{min}$ at $x = 0$,

$$\tau = \left\{\left[\ln\mu_1^2 a A_1\left(\cos\sqrt{\frac{k}{a}}\,R - \frac{1}{H}\sin\sqrt{\frac{k}{a}}\,R\sqrt{\frac{k}{a}}\right)\left(\frac{\sin\mu_1}{\mu_1} - 1\right)\right]\times\right.$$

$$\left.\times\left[(R^2k - a\mu_1^2)\left(1 - \frac{\sin\sqrt{\frac{k}{a}}\,R}{\sqrt{\frac{k}{a}}\,R}\right)\right]^{-1}\right\}\left(\frac{\mu_1^2 a}{R^2} - k\right)^{-1}. \qquad (7)$$

The above data show that the σ_{max} and σ_{min} obtained at $x = 0$ correspond to the mathematical maximum and minimum. Let us check the values of σ both at $x = 0$ and $x = \pm R$ (i.e., at the ends of the interval).

In their absolute value, the magnitudes of σ at $x = +R$ may be larger than at $x = 0$. The calculations show that the stress at the ends of the interval is about double the stress at $x = 0$.

An analysis of (5) and (6) leads to the conclusion that the stresses depend on the thermal and mechanical properties of the material (α_y, a, E, γ), on the rate of change of the temperature (b, k), on the geometric dimensions (R), on the nature of the heat exchange with the surface (μ_1, A_1, $H = \alpha/\lambda$) and on the time τ which is measured from the instant at which the change in temperature occurs.

During the cooling of the concrete the stress σ clearly depends on the difference between the initial and final temperatures.

Equations (5) and (6) were used to calculate the stresses developed in a cellular concrete plate under the above temperature conditions. The calculated moment of time was determined on the basis of the maximum stresses in the concrete. The calculated results are shown in Figure 2, expressed as relative values $\frac{\alpha_y E}{1-\nu}$.

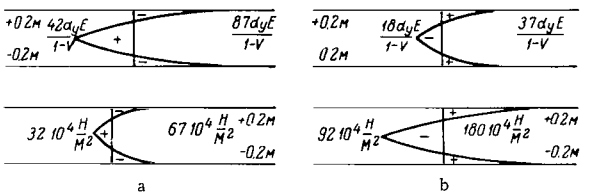

FIGURE 2. Curves showing the thermal stresses in a cellular concrete plate.

a – heating for τ = 14 hrs; b – cooling for τ = 9.5 hrs; + stretching; – compression.

The values of α_y and E, which change during the various stages of hydrothermal processing of various concretes, must be determined experimentally. For cellular concrete with a column weight of the order of 9810 n/m^3 we found that at the end of the heating period α_y was equal to $6 \cdot 10^{-6}$ deg^{-1} and E was equal to $9.81 \cdot 10^8$ n/m^2, while during the cooling period (at $P = 9.81 \cdot 10^4$ n/m^2) α_y was equal to $8 \cdot 10^{-6}$ deg^{-1} and E was equal to $49 \cdot 10^8$ n/m^2. The Poisson ratio (determined by Lindenberg) was assumed to be equal to 0.23. By substituting those values in equations (5) and (6) we obtained the absolute values of the stresses (Figure 2).

Thus, during the heating of cellular concretes their elasticity modulus and thermal stresses are smaller than during cooling. In the cooling period, after the completion of the chemical reactions in the concrete, the elasticity modulus increases markedly and the thermal stresses are higher than in the heating stage.

SYMBOLS

$\sigma(t, \tau)$ — thermal stresses at the moment of time τ; t_0 and t_τ — cross-section temperature — initial and in the period studied, deg; τ — duration of the time for which the calculations are carried out, min; M_s — surface modulus; t_{ok}, t_{sp}, t_{ps} and t_{cs} — the temperatures of fixed points, deg; t_m — temperature of the surrounding air or final temperature of the cellular concrete, deg; t_a — temperature at $P = 9.81 \cdot 10^4$ n/m^2, deg; k — coefficient characterizing the rate of cooling, sec^{-1}; a — thermal diffusivity coefficient, m^2/sec; λ — thermal conductivity coefficient, w/m·deg; c — heat capacity, j/kg·deg; γ — volume weight, n/m^3, α — convective heat transfer coefficient, w/m^2·deg; b — heating rate, deg/sec; R — half thickness of the plate, m; Bi — Biot number (Bi = $\alpha/\lambda R = HR$); Fo — Fourier number (Fo = $a\tau/R^2$); μ_1 — roots of the characteristic equation cot $\mu = \mu/\text{Bi}$; A_1 — initial thermal amplitude ($A_1 = \frac{2\sin\mu_1}{\mu_1 + \sin\mu_1 \cos\mu_1}$); α_y — coefficient for the expansion induced by heat and moisture, deg^{-1}; E — elasticity modulus, n/m^2; ν — Poisson ratio.

Bibliography

1. Goryainov, K.E., et.al. Krupnye gazobetonnye stenovye bloki (Large Cellular-concrete Wall Blocks).— Gosstroiizdat. 1959.
2. Lykov, A.V. Teoriya sushki (The Theory of Drying).— GITTL. 1952.
3. Gatewood, B.E. Thermal Stresses. [Russian translation. 1959.]

E. F. Vinokurov

THE ITERATION METHOD OF SOLVING THE PLANE ELASTIC-PLASTIC PROBLEM OF SOIL MECHANICS

The elastic-plastic deformation created in foundation soils under the effect of external loads may be calculated by means of the iteration method of solving the elastic-plastic problems of soil mechanics /1/.

Lamé-type equations that characterize the elastic-plastic deformation of soils without taking into account the body forces at the point i, j (the figure, *a*), are written in the following form in terms of finite differences /2/:

$$\frac{\kappa+1}{4}(v_{i+1,\,j-1}+v_{i-1,\,j+1}-v_{i-1,\,j-1}-v_{i+1,\,j+1})+(\kappa+2)\times$$
$$\times(u_{i+1,\,j}+u_{i-1,\,j}-2u_{i,\,j})+u_{i,\,j+1}+u_{i,\,j-1}-2u_{i,\,j}=\Delta h^2 R_x;$$
$$\frac{\kappa+1}{4}(u_{i+1,\,j-1}+u_{i-1,\,j+1}-u_{i-1,\,j-1}-u_{i+1,\,j+1})+(\kappa+2)\times$$
$$\times(v_{i,\,j+1}+v_{i,\,j-1}-2v_{i,\,j})+v_{i+1,\,j}+v_{i-1,\,j}-2v_{i,\,j}=\Delta h^2 R_y, \qquad (1)$$

where

$$\frac{\partial^2 u}{\partial x^2}=\frac{1}{\Delta x^2}(u_{i+1,\,j}+u_{i-1,\,j}-2u_{i,\,j});$$

$$\frac{\partial^2 u}{\partial y^2}=\frac{1}{\Delta y^2}(u_{i,\,j+1}+u_{i,\,j-1}-2u_{i,\,j});$$

$$\frac{\partial^2 v}{\partial x^2}=\frac{1}{\Delta x^2}(v_{i+1,\,j}+v_{i-1,\,j}-2v_{i,\,j});$$

$$\frac{\partial^2 v}{\partial y^2}=\frac{1}{\Delta y^2}(v_{i,\,j+1}+v_{i,\,j-1}-2v_{i,\,j});$$

$$\frac{\partial^2 v}{\partial x\partial y}=\frac{1}{4\Delta x\,\Delta y}(v_{i-1,\,j-1}+v_{i-1,\,j+1}-v_{i-1,\,j-1}-v_{i+1,\,j+1});$$

$$\frac{\partial^2 u}{\partial x\partial y}=\frac{1}{4\Delta x\,\Delta y}(u_{i+1,\,j-1}+u_{i-1,\,j+1}-u_{i-1,\,j-1}-u_{i+1,\,j+1});$$

$$R_x=2\frac{\partial\omega}{\partial x}(\varepsilon_x-\varepsilon_m)+\frac{\partial\omega}{\partial y}\gamma_{xy}+\omega\left(2\frac{\partial(\varepsilon_x-\varepsilon_m)}{\partial x}+\frac{\partial\gamma_{xy}}{\partial y}\right);$$

$$R_y=2\frac{\partial\omega}{\partial y}(\varepsilon_y-\varepsilon_m)+\frac{\partial\omega}{\partial x}\gamma_{xy}+\omega\left(2\frac{\partial(\varepsilon_y-\varepsilon_m)}{\partial y}+\frac{\partial\gamma_{xy}}{\partial x}\right);$$

$$\Delta x=\Delta y=\Delta h.$$

In terms of finite differences the expressions for R_x and R_y are:

$$R_x = \omega\left[\frac{1}{\Delta x^2}(u_{i+1,\,j} + u_{i-1,\,j} - 2u_{i,\,j}) + \frac{1}{\Delta y^2}(u_{i,\,j+1} + \right.$$

$$\left. + u_{i,\,j-1} - 2u_{i,\,j}) + \frac{1}{3}\left(\frac{\vartheta_{i+1,\,j} - \vartheta_{i,\,j}}{\Delta x}\right)\right] + 2\left(\frac{\omega_{i+1,\,j} - \omega_{i,\,j}}{\Delta x}\right) \times$$

$$\times\left[\left(\frac{u_{i+1,\,j} - u_{i,j}}{\Delta x}\right) - \frac{\vartheta_{i,j}}{3}\right] + \left(\frac{\omega_{i,j+1} - \omega_{i,j}}{\Delta y}\right) \times$$

$$\times\left[\left(\frac{u_{i,j+1} - u_{i,j}}{\Delta y}\right) + \left(\frac{v_{i+1,j} - v_{i,j}}{\Delta x}\right)\right];$$

$$R_y = \omega\left[\frac{1}{\Delta x^2}(v_{i+1,j} + v_{i-1,j} - 2v_{i,j}) + \frac{1}{\Delta y^2}(v_{i,j+1} + \right.$$

$$\left. + v_{i,j-1} - 2v_{i,j}) + \frac{1}{3}\left(\frac{\vartheta_{i,j+1} - \vartheta_{i,j}}{\Delta y}\right)\right] + 2\left(\frac{\omega_{i,j+1} - \omega_{i,j}}{\Delta y}\right) \times$$

$$\times\left[\left(\frac{v_{i,j+1} - v_{i,j}}{\Delta y}\right) - \frac{\vartheta_{i,j}}{3}\right] + \left(\frac{\omega_{i+1,j} - \omega_{i,j}}{\Delta x}\right) \times$$

$$\times\left[\left(\frac{v_{i+1,j} - v_{i,j}}{\Delta x}\right) + \left(\frac{u_{i,j+1} - u_{i,j}}{\Delta y}\right)\right];$$

$$\omega = 1 - \frac{\sigma_u}{3G\,\varepsilon_u}; \qquad \vartheta = 3\varepsilon_m.$$

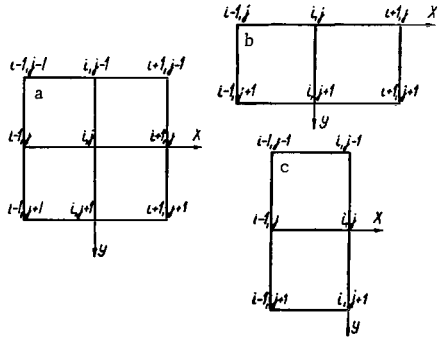

FIGURE. Calculation schemes.

a – lattice for the phase problems; b – boundary conditions for points on x-axis; c – boundary conditions on -axis.

In solving the problem by the method for the case of ideal elasticity /3/, the relationship between the stress components and the deformation components is expressed as follows:

$$\sigma_x = \overline{\sigma}_x - 2G\,\omega\,(\varepsilon_x - \varepsilon_m);$$
$$\sigma_y = \overline{\sigma}_y - 2G\,\omega\,(\varepsilon_y - \varepsilon_m);$$
$$\tau_{xy} = \overline{\tau}_{xy} - G\,\omega\,\gamma_{xy} \qquad (2)$$

Equations (2) are valid not only for internal points in the investigated region but also for points on the edge. At the same time the stress components on the edge must satisfy certain boundary conditions. Equation (2) may be written in terms of finite differences for the edge points i, j (the figure, *б, в*) in the form

$$\sigma_y^0 = \bar{\sigma}_y^0 - \frac{2G\omega}{3}\left(\frac{2v_{i,j+1} - 2v_{i,j}}{\Delta y} - \frac{u_{i+1,j} - u_{i,j}}{\Delta x}\right);$$

$$\tau_{xy}^0 = \bar{\tau}_{xy}^0 - G\omega\left(\frac{u_{i,j+1} - u_{i,j}}{\Delta y} + \frac{v_{i+1,j} - v_{i,j}}{\Delta x}\right);$$

$$\sigma_x^0 = \bar{\sigma}_x^0 - \frac{2G\omega}{3}\left(\frac{2u_{i,j} - 2u_{i-1,j}}{\Delta x} - \frac{v_{i,j+1} - v_{i,j}}{\Delta y}\right). \qquad (3)$$

In addition to (3), the following surface conditions must also be satisfied at the edge of the investigated region:

$$P_{xv} = \bar{P}_{xv} + GR_{xv};$$
$$P_{yv} = \bar{P}_{yv} + GR_{yv}, \qquad (4)$$

where

$$R_{xv} = -\omega\left[\left(\frac{u_{i+1,j} - u_{i,j}}{\Delta x}\right)2l + \left(\frac{u_{i,j+1} - u_{i,j}}{\Delta y}\right)m + \left(\frac{v_{i+1,j} - v_{i,j}}{\Delta x}\right)m\right];$$

$$R_{yv} = -\omega\left[\left(\frac{v_{i,j+1} - v_{i,j}}{\Delta y}\right)2m + \left(\frac{v_{i+1,j} - v_{i,j}}{\Delta x}\right)l + \left(\frac{u_{i,j+1} - u_{i,j}}{\Delta y}\right)l\right].$$

In solving plane elastic-plastic problems by the method for ideal elasticity it is assumed (at first approximation) that $\omega = 0$, i.e., we deal with a conventional problem of the theory of elasticity, whose solution (for the given boundary conditions) may be obtained in a closed form.

The main problems of soil mechanics have been solved by using the mathematical tools of the theory of elasticity. Hence, in solving the elastic-plastic problems at first approximation it is advantageous to make use of the existing solutions. In order to determine the displacement in first approximation, it is necessary in the first place to present the calculation scheme as a lattice-like region, and to represent the displacement of points on the edge by means of the displacement of internal points adjacent to the edge and by the boundary conditions.

The investigated infinite region (e.g., a half-plane) is replaced by regions of finite dimensions with applied loads corresponding to the internal stresses at the points, at the expense of the discarded section of the half-plane.

The equations relating the edge stresses to the displacement of edge points (except points on the corner) and the displacement of the internal points adjacent to the edge are derived by using equation (3) and the surface conditions (4). In this way the number of equations corresponds to the number of unknown components of the displacement of edge points. However, for the corner points of the lattice the relationship between the edge stresses and the displacement of edge points and of internal points adjacent to the edge is determined by three equations for each corner point in the lattice. Hence, the number of equations is greater than the number of required unknowns which introduces an uncertainty in the solution of the system of

equations. For this reason it is suggested that the displacement of the corner points of the lattice be calculated by methods that are developed on the basis of the general theory of bodies subjected to linear deformation, and that the obtained displacements be used to solve the elastic-plastic problem. In particular, when the half-plane surface is subject to the action of a local uniformly-distributed load the displacement of corner points of the lattice may be determined from /4/:

$$u = \frac{q}{\pi}\frac{1+\mu}{E}\left\{(1-2\mu)\left[(x-a)\operatorname{arctg}\frac{y}{x-a} - (x+a)\operatorname{arctg}\frac{y}{x+a}\right] + y(1-\mu)\ln\frac{(x-a)^2+y^2}{(x+a)^2+y^2} + (1-2\mu)a\pi\right\};$$

$$v = \frac{q}{\pi}\frac{1+\mu}{E}\left\{(1-\mu)\ln\frac{[(x+a)^2+y^2]^{(x+a)}}{[(x-a)^2+y^2]^{(x-a)}} - y(1-2\mu)\left(\operatorname{arctg}\frac{y}{x+a} - \operatorname{arctg}\frac{y}{x-a}\right)\right\} + C.$$

The displacement of the corner points of the lattice may be expressed also through the displacement of the points adjacent to the lattice, applying the Taylor series:

$$f(x, y) = f(a, b) + \frac{f'_x(a, b)}{1!}(x-a) + \frac{f'_y(a, b)}{1!}(y-b) + \frac{f''_x(a, b)}{2!}(x-a)^2 + \frac{f''_y(a, b)}{2!}(y-b)^2 + \ldots$$

In the determination of the displacement of internal lattice points, a system of equations (1) is established for each internal node. The displacements of the external points comprised in those equations must be presented as functions of the displacement of the internal points adjacent to the lattice and the edge stresses, and the surface displacements are thus included in the overall iteration process.

In this way the problem of determining the displacement of nodes in the lattice is reduced to the solution of a system of x equations with x unknowns; it is recommended that electronic computers be used to obtain this solution.

The method of solving elastic-plastic problems in second approximation is analogous to the method for their solution in first approximation, but $\omega \neq 0$. The function ω is determined on the basis of an experimental determination of the dependence of the deformation magnitude on the magnitude of the normal octahedral stress.

When solving the problems of soil mechanics by the methods for ideal elasticity, it is possible in a number of cases to be satisfied with the solution obtained in second approximation. However, if necessary, the above method in conjunction with the lattice method may also be used to solve elastic-plastic problems in third and subsequent approximations.

SYMBOLS

u, v — displacement components; κ — quotient of the Lamé coefficients λ to G; Δx, Δy — distances between nodes of the lattice; σ_u — magnitude of the

stress; ε_u — magnitude of the deformation; ε_m — mean elongation, %; ε_x, ε_y — elongations, %; γ_{xy} — relative slip; σ_x, σ_y, τ_{xy} — stress components; $\bar{\sigma}_x$, $\bar{\sigma}_y$, $\bar{\tau}_{xy}$ — elastic stress components; $\bar{P}_{xv}$; $\bar{P}_{yv}$ — surface loads for an ideally elastic body; l, m — cosines of the angles between the respective axes and the normal to the plane; μ — Poisson ratio; E — modulus of overall deformation; q — intensity of the uniformly distributed load; a — half of the lenght on which the uniformly distributed load has been applied.

Bibliography

1. Vinokurov, E. F. — IFZh, No. 1. 1965.
2. Varvak, P. M. Razvitie i prilozhenie metoda setok k raschetu plastinok (Development and Application of the Method of Lattice to the Calculation of Plates). — Izd. AN UkrSSR. 1952.
3. Il'yushin, A. A. Plastichnost' (Plasticity). — OGIZ. 1948.
4. Khakimov, Kh. R. Raschet osadki sooruzhenii na estestvennom osnovanii i opredelenie aktivnoi zony grunta (Calculation of the Sinking of Equipment on Natural Foundations and Determination of the Active Zone of Soils). — NKTP SSSR. 1936.

B. Berkovskii and Z. Shul'man

EXACT SOLUTION OF THE EQUATIONS FOR THE BOUNDARY LAYER OF PSEUDOPLASTIC FLUIDS ON A PERMEABLE FLAT PLATE AND IN THE VICINITY OF THE CRITICAL POINT

The boundary layer hypothesis, which is satisfactorily applied to Newtonian fluids, was found to be applicable and useful also for certain classes of non-Newtonian fluids. For instance, in the case of fluids obeying the exponential rheological law (pseudoplastic, dilatant) we have

$$\tau_{ij} = k\left|\frac{1}{2}e_{im}e_{ml}\right|^{\frac{n-1}{2}}e_{ij}. \tag{1}$$

Their properties have been discussed by Wilkinson /1/, Serrin /2/, Metzner /3/, etc.

Equations have been derived for two-dimensional /4/ and unsteady three-dimensional /5/ boundary layers. The integration of the boundary layer equation for a flat impermeable plate has been carried out in /6/, and of the equations of flat and axis-symmetrical streams in /7/. The transformations converting the two-dimensional boundary layer problem for elongated bodies of rotation into a plane problem have been reported in /5/.

We present below the exact numerical solutions of the boundary layer equations for non-compressible pseudoplastic fluids on a permeable flat plate and in the vicinity of the critical point.

THE BOUNDARY LAYER ON A FLAT PLATE

Let us examine the boundary layer on a plate in a steady-state uniform external current. Let the velocity of the current be U_∞. The x-axis is along the plate and the y-axis is normal to it. The origin of the coordinates is at the front edge of the plate. In such a case the equation describing motion will be:

$$u\frac{\partial u}{\partial x} + v\frac{\partial u}{dy} = n\frac{k}{\rho}\left|\frac{\partial u}{\partial y}\right|^{n-1}\frac{\partial^2 u}{\partial y^2},$$

$$\frac{\partial u}{\partial x} + \frac{\partial v}{\partial y} = 0. \tag{2}$$

Let us define the boundary conditions

$$u(x,\ 0) = 0,\quad v(x,\ 0) = v_0 = ax^{-\frac{n}{1+n}},$$

$$u(0,\ y) = U_\infty,\quad \lim_{y\to\infty} u = U_\infty = \text{const}. \tag{3}$$

The solution is sought in the form

$$u = U_\infty \frac{dF}{d\eta} = U_\infty F'(\eta),$$

$$v = x^{-\frac{n}{1+n}}(\eta F' - F)\frac{1}{1+n}\left[n(1+n)\frac{k}{\rho}U_\infty^{2n-1}\right]^{\frac{1}{1+n}}, \tag{4}$$

$$\eta = yx^{-\frac{1}{1+n}}\left[\frac{U_\infty^{2-n}\rho}{nk(1+n)}\right]^{\frac{1}{1+n}}. \tag{5}$$

Using the new variables, equations (2) and the boundary conditions (3) are reduced to

$$|F''|^{n-1}F''' + FF'' = 0, \tag{6}$$

$$F(0) = A, \quad F'(0) = 0, \quad \lim_{\eta \to \infty} F' = 1. \tag{7}$$

The numerical integration of equation (6) with boundary conditions (7) was carried out on the "Minsk-2" electronic computer by the "adjustment" method, for $0.5 \leqslant n \leqslant 1$ at increments of 0.1; $n = 0.72$, 0.66, and 0.58 corresponded to 0.09, 0.22, and 0.35% solutions of carboxymethylcellulose (CMC) in water /8/ and for nine values of A.

The values of the function $F(\eta)$ and its three derivatives at $A = 0$ are shown in Table 1. Table 2 lists the $F''(0)$ for all calculated values of A needed to determine the local friction stresses on the plate surface τ_0 and the total friction resistance W_f.

Let us introduce equations for the determination of τ_0 and W_f:

$$\tau_0 = k\left|\frac{\partial u}{\partial y}\right|_{y=0}^{n} = [F''(0)]^n\left[\frac{U_\infty^3\rho}{n(1+n)x}k^{\frac{1}{n}}\right]^{\frac{n}{1+n}},$$

$$W_f = 2b\int_0^L \tau_0\,dx = [F''(0)]^n \cdot 2b(1+n)\left[\frac{U_\infty^3\rho}{n(1+n)}(Lk)^{\frac{1}{n}}\right]^{\frac{n}{1+n}}. \tag{8}$$

Let us introduce two dimensionless complexes — the local friction coefficient and the total friction resistance coefficient:

$$c_f = \frac{\tau_0}{1/2\,\rho U_\infty^2} = 2\left[\frac{1}{n(1+n)}\right]^{\frac{n}{1+n}}[F''(0)]^n R_x^{-\frac{1}{1+n}},$$

$$C_f = \frac{W_f}{1/2\,\rho U_\infty^2 \cdot 2bL} = \tag{9}$$

$$= 2(1+n)[(1+n)n]^{-\frac{n}{1+n}}[F''(0)]^n R^{-\frac{1}{1+n}},$$

$$R_x = \rho\frac{U_\infty^{2-n}x^n}{k}, \quad R = \rho\frac{U_\infty^{2-n}L^n}{k}.$$

As is evident from (5), the thickness of the boundary layer is determined from the equation

$$\delta \sim \left[x\frac{n(1+n)k}{\rho}U_\infty^{n-2}\right]^{\frac{1}{1+n}} = \left[n(1+n)\right]^{\frac{1}{1+n}} xR_x^{-\frac{1}{1+n}}. \tag{10}$$

TABLE 1

Exact solutions of the equation $|F''|^{n-1} F''' + FF'' = 0$

τ_i	F	F'	F''	F'''
		$n = 1$		
0.00	0.0000	0.0000	0.4696	+0.0000
0.50	0.0586	0.2342	0.4650	—0.0273
1.00	0.2329	0.4606	0.4344	—0.1012
1.50	0.5150	0.6614	0.6318	—0.1863
2.00	0.8867	0.8166	0.2556	—0.2267
2.50	1.322	0.9168	0.1474	—0.1950
3.00	1.795	0.9690	0.0677	—0.1215
3.50	2.286	0.9907	0.0244	—0.0558
4.00	2.783	0.9977	0.0069	—0.0191
4.50	3.283	0.9995	0.0015	—0.0050
5.00	3.783	0.9999	0.0003	—0.0010
5.50	4.283	1.0000	0.0000	—0.0001
		$n = 0.9$		
0.00	0.0000	0.0000	0.4339	+0.0000
0.50	0.0542	0.2164	0.4302	—0.0214
1.00	0.2155	0.4268	0.4061	—0.0800
1.50	0.4776	0.6168	0.3483	—0.1497
2.00	0.8262	0.7701	0.2615	—0.1890
2.50	1.240	0.8774	0.1684	—0.1748
3.00	1.696	0.9416	0.0929	—0.1242
3.50	2.176	0.9749	0.0445	—0.0710
4.00	2.668	0.9900	0.0190	—0.0342
4.50	3.165	0.9962	0.0075	—0.0145
5.00	3.664	0.9986	0.0028	—0.0056
5.50	4.163	0.9995	0.0010	—0.0021
6.00	4.663	0.9998	0.0003	—0.0007
6.50	5.163	0.9999	0.0001	—0.0003
7.00	5.663	1.0000	0.0000	—0.0001
		$n = 0.8$		
0.00	0.0000	0.0000	0.3962	+0.0000
0.50	0.0495	0.1977	0.3934	—0.0162
1.00	0.1970	0.3908	0.3751	—0.0608
1.50	0.4377	0.5685	0.3308	—0.1160
2.00	0.7607	0.7175	0.2622	—0.1526
2.50	1.149	0.8292	0.1846	—0.1513
3.00	1.583	0.9038	0.1161	—0.1195
3.50	2.047	0.9486	0.0665	—0.0792
4.00	2.529	0.9734	0.0356	—0.0462
4.50	3.019	0.9864	0.0183	—0.0248
5.00	3.514	0.9931	0.0092	—0.0127
5.50	4.012	0.9964	0.0046	—0.0064
6.00	4.510	0.9983	0.0024	—0.0032
6.50	5.010	0.9989	0.0012	—0.0016
7.00	5.509	0.9994	0.0006	—0.0008
7.50	6.009	0.9996	0.0003	—0.0004
8.00	6.509	0.9998	0.0002	—0.0002
8.50	7.009	0.9998	0.0001	—0.0001

TABLE 1 (continued)

η	F	F'	F''	F'''
9.00	7.509	0 9999	0.0001	−0.0001
9.50	8.009	0.9999	0.0000	−0.0000
10.00	8.509	1.0000	0.0000	0.0000
		$n = 0.7$		
0.00	0.0000	0 0000	0.3567	+0.0000
0.50	0.0445	0 1781	0.3547	−0.0116
1.00	0.1775	0 3528	0.3415	−0.0439
1.50	0.3955	0.5164	0.3091	−0.0860
2.00	0.6904	0.6587	0.2572	−0.1181
2.50	1.049	0.7719	0.1951	−0.1254
3.00	1.457	0.8543	0.1358	−0.1087
3.50	1.899	0.9098	0.0883	−0.0809
4.00	2.363	0.9450	0.0547	−0.0541
4.50	2.842	0.9665	0.0331	−0.0338
5.00	3.328	0.9794	0.0198	−0.0203
5.50	3.820	0.9872	0.0119	−0.0120
6.00	4.315	0.9918	0.0072	−0.0071
6.50	4.812	0.9947	0.0045	−0.0042
7.00	5.310	0.9965	0.0028	−0.0025
7.50	5.808	0.9976	0.0018	−0.0016
8.00	6.307	0.9983	0 0012	−0.0010
8.50	6.806	0.9988	0.0008	−0.0006
9.00	7.306	0 9991	0.0005	−0.0004
9.50	7.806	0.9993	0.0004	−0.0003
10.00	8.305	0.9995	0.0003	−0.0002
10.50	8.805	0.9996	0.0002	−0.0001
11 00	9.305	0.9997	0.0001	−0.0001
11.50	9.805	0.9997	0.0001	−0 0001
12.00	10.30	0.9998	0.0001	0.0000
12.50	10.80	0.9998	0.0001	0.0000
13.00	11.30	0.9998	0 0000	0.0000
13.50	11.80	0.9999	0.0000	0.0000
14.00	12.30	0.9999	0.0000	0.0000
14.50	12.80	0.9999	0.0000	0.0000
15.00	13.30	0.9999	0.0000	0.0000
15.50	13.80	0.9999	0.0000	0.0000
16.00	14.30	0.9999	0.0000	0.0000
16.50	14.80	0.9999	0.0000	0.0000
17 00	15.30	1.0000	0.0000	0.0000
		$n = 0.6$		
0.00	0.0000	0.0000	0.3157	+0.0000
0.50	0.0394	0.1577	0.3143	−0.0078
1.00	0.1573	0.3131	0.3054	−0.0299
1.50	0.3512	0.4608	0.2831	−0.0600
2.00	0.6156	0.5936	0 2460	−0.0864
2.50	0.9413	0.7052	0.1991	−0.0983
3.00	1.3168	0.7925	0.1507	−0.0930
3.50	1.7300	0.8568	0.1079	−0.0767
4.00	2.1704	0.9020	0.0745	−0.0572
4.50	2.6297	0 9329	0.0503	−0.0400
5.00	3.1016	0.9536	0.0338	−0.0270
5.50	3.5821	0.9675	0.0227	−0.0179

TABLE 1 (continued)

η	F	F'	F''	F'''
6.00	4.0684	0.9769	0.0154	—0.0118
6.50	4.5586	0.9833	0.0106	—0.0078
7.00	5.0514	0.9877	0.0074	—0.0052
7.50	5.5461	0.9909	0.0052	—0.0035
8.00	6.0421	0.9931	0.0037	—0.0024
8.50	6.5391	0.9947	0.0027	—0.0017
9.00	7.0368	0.9959	0.0020	—0.0012
9.50	7.5349	0.9967	0.0015	—0 0008
10.00	8.0334	0.9974	0.0012	—0.0006
10.50	8.5323	0.9979	0.0009	—0.0005
11.00	9.0313	0.9983	0.0007	—0.0003
11.50	9.5305	0.9986	0 0005	—0.0003
12.00	10.0299	0.9988	0.0004	—0.0002
12.50	10.5294	0.9990	0.0003	—0.0001
13.00	11.0289	0.9992	0.0003	—0.0001
13.50	11.5285	0.9993	0.0002	—0.0001
14.00	12.0282	0.9995	0.0002	—0.0001
14.50	12.5279	0.9995	0.0002	—0.0001
15.00	13.0277	0.9996	0.0001	—0.0000
15.50	13.5275	0.9996	0.0001	—0.0000
16.00	14.0273	0.9997	0.0000	—0.0000
16.50	14.5272	0.9997	0.0000	—0.0000
17.00	15.0270	0.9997	0.0000	—0.0000
17.50	15.5269	0.9998	0.0000	—0.0000
18.00	16.0268	0.9998	0.0000	—0.0000
18.50	16.5267	0.9998	0.0000	—0.0000
19.00	17.0266	0.9998	0.0000	—0.0000
19.50	17.5266	0.9999	0.0000	—0.0000
20.00	18.0265	0.9999	0.0000	—0.0000
20.50	18.5264	0 9999	0.0000	—0.0000
21.00	19.0264	0.9999	0.0000	—0.0000
21.50	19.5263	0.9999	0.0000	—0.0000
22.00	20.0263	0.9999	0.0000	—0.0000
22.50	20.5263	0.9999	0.0000	—0.0000
23.00	21.0262	0.9999	0.0000	—0.0000
23.50	21.5262	0.9999	0.0000	—0.0000
24.00	22.0262	0.9999	0.0000	—0.0000
24.50	22.5261	1.0000	0.0000	—0.0000
		$n = 0.5$		
0.00	0.0000	0.0000	0.2735	+0.0000
0.50	0.0342	0.1366	0.2727	—0.0049
1.00	0.1364	0.2719	0.2671	—0.0188
1.50	0.3052	0.4022	0.2528	—0.0388
2.00	0.5370	0.5229	0.2283	—0.0586
2.50	0.8257	0.6291	0.1954	—0.0713
3.00	1.1632	0.7177	0.1587	—0.0736
3.50	1.5404	0.7881	0.1234	—0.0667
4.00	1.9485	0.8419	0.0928	—0.0551
4.50	2.3799	0.8819	0.0684	—0.0426
5.00	2.8287	0.9113	0.0500	—0.0316
5.50	3 2899	0.9327	0.0364	—0.0229

TABLE 1 (continued)

τ_1	F	F'	F''	F'''
6.00	3 7604	0.9484	0.0267	—0 0164
6.50	4.2376	0.9599	0.0197	—0.0117
7.00	4.7198	0.9684	0.0147	—0.0084
7.50	5.2057	0.9748	0.0111	—0.0061
8.00	5.6944	0.9797	0.0085	—0.0045
8.50	6.1852	0.9835	0.0066	—0.0033
9.00	6.6777	0.9864	0.0051	—0.0025
9.50	7.1715	0.9887	0.0041	—0.0019
10.00	7.6663	0.9905	0 0033	—0.0014
10.50	8.1619	0.9920	0.0026	—0.0011
11.00	8.6582	0.9931	0.0021	—0.0009
11.50	9.1555	0 9941	0.0018	—0.0007
12.00	9 6523	0.9949	0.0015	—0.0005
12.50	10.1499	0.9956	0.0012	—0.0004
13.00	10.6479	0.9961	0.0010	—0.0003
13 50	11.1461	0.9966	0.0009	—0.0003
14.00	11.6445	0.9970	0.0007	—0.0002
14.50	12.1431	0.9974	0.0006	—0.0002
15.00	12.6418	0.9977	0 0005	—0.0002
15.50	13.1407	0.9979	0.0005	—0.0001
16.00	13.6398	0.9981	0.0004	—0.0001
16.50	14.1389	0.9983	0.0004	—0.0001
17.00	14.6381	0 9985	0.0003	—0.0001
17.50	15.1373	0.9986	0.0003	—0.0001
18.00	15.6367	0.9988	0.0002	—0.0001
18.50	16.1361	0.9989	0.0002	—0.0001
19.00	16.6356	0.9990	0 0002	—0.0000
19.50	17.1351	0.9991	0.0002	—0.0000
20.00	17.6346	0.9991	0.0001	—0.0000
20.50	18.1342	0.9992	0.0001	—0.0000
21 00	18.6339	0.9993	0.0001	—0 0000
21.50	19.1335	0.9993	0.0001	—0.0000
22.00	19.6332	0 9994	0 0001	—0.0000
22.50	20.1329	0.9994	0.0000	—0 0000
23.00	20.6326	0.9995	0.0000	—0.0000
23.50	21.1324	0.9995	0.0000	—0.0000
24.00	21.6322	0.9996	0.0000	—0.0000
24.50	22.1319	0.9996	0.0000	—0.0000
25.00	22.6318	0.9996	0.0000	—0.0000
25.50	23.1316	0.9997	0 0000	—0.0000
26.00	23.6314	0.9997	0.0000	—0.0000
26.50	24.1213	0.9997	0.0000	—0.0000
27.00	24.6311	0.9997	0.0000	—0.0000
27.50	25.1310	0.9997	0.0000	—0.0000
28.00	25.6309	0.9998	0.0000	—0.0000
28.50	26.1308	0.9998	0.0000	—0.0000
29.00	26.6307	0.9998	0.0000	—0.0000
29.50	27.1306	0.9998	0.0000	—0.0000
30.00	27.6305	0.9998	0 0000	—0.0000
30.50	28.1304	0.9998	0.0000	—0.0000
31.00	28.6304	0.9999	0.0000	—0.0000
31.50	29.1303	0.9999	0.0000	—0.0000
32.00	29.6302	0.9999	0.0000	—0.0000
32.50	30.1301	0.9999	0.0000	—0.0000
33.00	30.6301	0.9999	0.0000	—0.0000
33.50	31.1300	0.9999	0.0000	—0.0000
34.00	31.6300	0.9999	0.0000	—0.0000
34.50	32.1299	0.9999	0.0000	—0.0000
35.00	32.6299	0.9999	0.0000	—0.0000
35.50	33.1299	0.9999	0.0000	—0.0000
36.00	33.6299	0.9999	0.0000	—0.0000
36.50	34.1298	0.9999	0.0000	—0.0000
37.00	34.6298	1.0000	0.0000	—0.0000

TABLE 2

Values of $F''(0)$ from the results of the numerical calculations

$F(0)$ \ n	1	0.9	0.8	0.7	0.6	0.5	0.72	0.66	0.58
+3.0	3.1451	3.1977	3.2272	3.2168	3.1428	2.9727	—	—	3.1180
+1.0	1.2836	1.2138	1.1289	1.0278	0.9097	0.7764	1.0490	0.9820	0.8841
+0.5	0.8579	0.7960	0.7269	0.6510	0.5687	0.4819	0.6666	0.6193	0.5524
0.0	0.4696	0.4339	0.3962	0.3567	0.3157	0.2735	0.3651	0.3404	0.3070
−0.5	0.1485	0.1530	0.1541	0.1522	0.1461	0.1376	0.1522	0.1498	0.1453
−0.8	0.0175	0.0414	0.0594	0.0723	0.0806	0.0846	—	—	0.0817
−1.0	—	—	—	—	—	—	0.0341	0.0427	0.0521
−1.5	—	—	—	—	—	—	—	—	0.01
−2.0	—	—	—	—	—	—	—	—	0.001

The meaning of $F(0)$ is made clear in the equation

$$F(0) = -\frac{v_0}{U_\infty} R_x^{\frac{1}{1+n}} (1+n)[n(1+n)]^{-\frac{1}{1+n}}. \tag{11}$$

As in the case of Newtonian fluids (which is a particular case of the above problem) the above solution is probably not applicable for the vicinities of the front and rear edges of the plates, for which the boundary layer hypothesis is not valid.

THE BOUNDARY LAYER IN THE VICINITY OF THE CRITICAL POINT

Let us discuss the plane-parallel flow in the vicinity of the critical point. The x-axis is along the wall, the y-axis is normal to the wall, and the origin of coordinates is at the critical point. The equation describing motion and the boundary conditions will now be:

$$u\frac{\partial u}{\partial x} + v\frac{\partial u}{\partial y} = c^2 x + n\frac{k}{\rho}\left|\frac{\partial u}{\partial y}\right|^{n-1}\frac{\partial^2 u}{\partial y^2}, \tag{12}$$

$$\frac{\partial u}{\partial x} + \frac{\partial v}{\partial y} = 0,$$

$$u(x, 0) = 0, \quad v(x, 0) \quad v_0 = ax^{\frac{n-1}{1+n}}, \tag{13}$$

$$u(0, y) = 0, \quad \lim_{y\to\infty} u = U = cx.$$

As shown in /5/ the solution must be sought in the form

$$u = U\frac{dF}{d\eta} = cxF', \tag{14}$$

$$v = -x^{\frac{n-1}{1+n}}\left[F + \frac{1-n}{2n}\eta F'\right]\frac{2nc^3}{1+n}\left(\frac{kn}{\rho}\right)^{\frac{1}{1+n}},$$

TABLE 3

Exact solutions of the boundary layer equations for the vicinity of the critical point

η	F	F'	F''	F'''
		$n = 1$		
0.00	0.0000	0.0000	1.2326	—1.0000
0.20	0.0233	0.2266	1.0344	—0.9728
0.40	0.0881	0.4145	0.8463	—0.9028
0.60	0.1867	0.5663	0.6752	—0.8054
0.80	0.3124	0.6859	0.5251	—0.6935
1.00	0.4592	0.7779	0.3980	—0.5777
1.20	0.6220	0.8467	0.2938	—0.4659
1.40	0.7967	0.8968	0.2110	—0.3638
1.60	0.9798	0.9323	0.1474	—0.2751
1.80	1.1689	0.9568	0.0999	—0.2013
2.00	1.3619	0.9732	0.0658	—0.1425
2.20	1.5578	0.9839	0.0420	—0.0975
2.40	1.7553	0.9905	0.0260	—0.0645
2.60	1.9538	0.9946	0.0156	—0.0412
2.80	2.1529	0.9970	0.0090	—0.0254
3.00	2.3525	0.9984	0.0051	—0.0151
3.20	2.5523	0.9992	0.0028	—0.0087
3.40	2.7522	0.9996	0.0014	—0.0048
3.60	2.9521	0.9998	0.0007	—0.0025
3.80	3.1521	0.9999	0.0004	—0.0013
4.00	3.3521	1.0000	0.0002	—0.0006
		$n = 0.9$		
0.00	0.0000	0 0000	1 2415	—1.0786
0.20	0.0234	0.2269	1.0299	—1.0283
0.40	0.0881	0.4130	0.8333	—0.9318
0.60	0.1861	0.5618	0.6588	—0.8105
0.80	0.3106	0.6782	0 5096	—0.6809
1 00	0.4556	0.7673	0.3862	—0 5546
1.20	0.6161	0.8343	0.2870	—0.4393
1.40	0.7881	0.8836	0.2095	—0.3391
1.60	0.9686	0.9193	0.1503	—0.2557
1.80	1.1551	0.9447	0.1061	—0.1886
2.00	1.3459	0.9625	0.0738	—0.1364
2.20	1.5398	0.9749	0.0507	—0.0968
2 40	1.7356	0.9833	0.0344	—0.0676
2.60	1.9329	0.9889	0.0231	—0.0466
2.80	2.1311	0.9927	0.0154	—0.0316
3.00	2.3299	0.9953	0.0101	—0.0212
3.20	2.5291	0.9969	0.0067	—0.0141
3.40	2.7286	0.9980	0.0043	—0.0093
3.60	2.9283	0.9987	0.0028	—0.0061
3.80	3.1281	0 9992	0.0018	—0.0040
4.00	3.3279	0.9995	0 0012	—0.0026
4.20	3.5279	0.9997	0.0008	—0.0017
4.40	3.7278	0.9998	0.0005	—0 0011
4.60	3.9278	0.9999	0.0003	—0.0007
4.80	4.1278	0.9999	0.0002	—0.0004
5.00	4.3278	0.9999	0 0001	—0.0003
5.20	4.5277	1.0000	0.0000	—0.0002

TABLE 3 (continued)

η	F	F'	F''	F'''
		$n = 0.8$		
0.00	0.0000	0.0000	1.2559	—1.1775
0.20	0.0236	0.2281	0.1027	—0.1097
0.40	0.0883	0.4124	0.8205	—0.9671
0.60	0.1859	0.5582	0.6419	—0.8180
0.80	0.3094	0.6712	0.4934	—0.6692
1.00	0.4527	0.7574	0.3734	—0.5326
1.20	0.6109	0.8223	0.2790	—0.4143
1.40	0.7805	0.8705	0.2063	—0.3162
1.60	0.9583	0.9059	0.1512	—0.2375
1.80	1.1422	0.9319	0.1101	—0.1761
2.00	1.3305	0.9507	0.0798	—0.1293
2.20	1 5221	0.9643	0.0576	—0.0941
2.40	1.7160	0.9742	0.0415	—0.0681
2.60	1.9116	0.9813	0.0299	—0.0491
2.80	2.1084	0.9864	0.0216	—0.0353
3.00	2.3061	0.9900	0.0156	—0.0253
3.20	2.5044	0.9927	0.0113	—0.0182
3.40	2.7031	0.9946	0.0082	—0.0130
3.60	2.9022	0.9960	0.0059	—0.0094
3.80	3.1015	0.9971	0.0043	—0.0068
4.00	3.3009	0.9978	0.0032	—0.0049
4.20	3.5006	0.9984	0.0024	—0.0036
4.40	3.7003	0 9988	0.0017	—0.0026
4.60	3.9001	0.9991	0.0013	—0.0019
4.80	4.0999	0.9993	0.0009	—0.0014
5.00	4.2998	0.9995	0.0007	—0.0010
5.20	4.4997	0.9996	0.0005	—0.0008
5.40	4.6997	0.9997	0.0004	—0.0006
5.60	4.8996	0.9998	0.0003	—0.0004
5.80	5.0995	0.9998	0.0002	—0.0003
6.00	5.2995	0.9999	0.0002	—0.0002
6.20	5.4995	0.9999	0.0001	—0.0002
6.40	5.6995	0.9999	0 0001	—0.0001
6.60	5.8995	0.9999	0.0000	—0.0001
6.80	6.0994	1.0000	0.0000	—0.0000
		$n = 0.7$		
0.00	0.0000	0.0000	1.2790	—1.3073
0.50	0.1342	0.4894	0.7119	—0.9202
1.00	0.4512	0.7487	0.3593	—0.5118
1.50	0.8612	0.8767	0.1739	—0.2550
2.00	1.316	0.9382	0.0837	—0.1214
2.50	1.794	0.9681	0.0410	—0.0574
3.00	2.282	0.9829	0.0207	—0.0276
3.50	2.776	0.9904	0.0108	—0.0136
4.00	3.272	0.9944	0.0058	—0.0070
4.50	3.770	0.9967	0.0033	—0.0037
5.00	4.269	0.9979	0.0019	—0.0020
5.50	4.768	0.9987	0.0011	—0.0011
6.00	5.267	0.9991	0.0007	—0.0007

TABLE 3 (continued)

η	F	F'	F''	F'''
6.50	5.767	0.9994	0.0004	—0.0004
7.00	6.267	0.9996	0.0003	—0.0002
7.50	6.767	0.9997	0.0002	—0.0002
8.00	7.267	0.9998	0.0001	—0.0001
8.50	7.766	0 9999	0.0001	—0.0001
9.00	8.766	0.9999	0.0000	—1.0000
9.50	9.766	1.0000	0.0000	—0.0000
		$n = 0.6$		
0.00	0.0000	0.0000	1.316	—1.488
0.50	0.1359	0.4917	0.6964	—0.9566
1 00	0.4516	0.7420	0.3434	—0.4920
1.50	0.8570	0.8647	0.1688	—0.2361
2.00	1.306	0.9257	0.0854	—0 1130
2.50	1.778	0.9572	0.0451	—0 0555
3.00	2.261	0.9741	0.0249	—0.0284
3.50	2.751	0.9837	0.0144	—0.0152
4.00	3.244	0.9893	0.0087	—0.0085
4.50	3.740	0.9928	0.0054	—0.0049
5.00	4.236	0.9949	0.0035	—0.0029
5.50	4 734	0.9963	0 0023	—0.0018
6.00	5 233	0.9973	0.0016	—0.0012
6.50	5.732	0.9980	0.0011	—0.0008
7.00	6.231	0.9985	0.0008	—0.0005
7.50	6.730	0 9988	0.0006	—0.0004
8.00	7.229	0 9991	0.0004	—0.0003
8.50	7.729	0.9993	0.0003	—0.0002
9.00	8.229	0.9994	0.0003	—0.0001
9.50	8.729	0.9995	0 0002	—0.0001
10.00	9.229	0.9996	0.0002	—0.0001
10 50	9.728	0.9997	0.0001	—0.0001
11.00	10.23	0.9997	0.0001	—0.0000
11.50	10.73	0.9998	0.0001	—0.0000
12.00	11.23	0.9998	0.0001	—0.0000
12.50	11.73	0.9998	0.0001	—0.0000
13.00	12.23	0.9999	0.0000	—0.0000
13.50	12.73	0.9999	0.0000	—0.0000
14.50	13.73	0.9999	0.0000	—0.0000
15.50	14.73	0.9999	0.0000	—0.0000
16.00	15.23	1.0000	0.0000	—0.0000
		$n = 0.5$		
0.00	0.0000	0.0000	1.377	—1.760
0.50	0.391	0.4984	0.6810	—1.008
1.00	0.456	0.7389	0.3252	—0.4729
1.50	0.8578	0.8552	0.1611	—0.2172
2.00	1.302	0.9143	0.0847	—0.1037
2.50	1.768	0.9462	0.0473	—0.0523
3.00	2.245	0.9645	0.0279	—0.0280
3.50	2.731	0.9756	0.0173	—0.0158
4.00	3 221	0.9826	0.0112	—0.0093

TABLE 3 (continued)

η	F	F'	F''	F'''
		$n = 0.5$		
4.50	3.713	0.9872	0.0075	—0.0057
5.00	4.207	0.9903	0.0052	—0.0037
5.50	4.703	0.9926	0.0037	—0.0024
6.00	5.200	0.9942	0.0027	—0.0017
6.50	5.697	0.9953	0.0020	—0.0012
7.00	6.195	0.9962	0.0015	—0.0008
7.50	6.693	0.9969	0.0013	—0 0006
8.00	7.192	0.9974	0.0009	—0.0004
8.50	7.691	0.9979	0.0007	—0.0003
9.00	8.190	0.9982	0.0006	—0.0003
9.50	8.689	0.9984	0.0005	—0.0002
10.00	9.188	0.9987	0.0004	—0.0002
10.50	9.688	0.9988	0.0003	—0.0001
11.00	10.19	0.9990	0.0003	—0.0001
11.50	10.69	0.9991	0.0002	—0.0001
12.00	11.19	0.9992	0.0002	—0.0001
12.50	11.69	0.9993	0.0002	—0.0001
13.00	12.19	0.9994	0.0001	—0.0000
13.50	12.69	0.9995	0.0001	—0.0000
14.00	13.19	0.9995	0.0001	—0.0000
14.50	13.68	0.9996	0.0001	—0.0000
15.00	14.18	0.9996	0.0001	—0.0000
15.50	14.68	0.9997	0.0001	—0.0000
16.00	15.18	0.9997	0.0001	—0.0000
16.50	15.68	0.9997	0.0001	—0.0000
17.00	16.18	0.9998	0.0001	—0 0000
17.50	16.68	0.9998	0.0000	—0.0000
18.00	17.18	0.9998	0.0000	—0.0000
19.00	18.18	0.9999	0.0000	—0.0000
20.00	19.18	0.9999	0.0000	—0.0000
21 00	20.18	0.9999	0.0000	—0.0000
22.00	21.18	0.9999	0 0000	—0.0000
23.00	22.18	1 0000	0.0000	—0.0000

$$\eta = yx^{\frac{1-n}{1+n}}\left[\frac{2\rho}{k(1+n)}\,c^{2-n}\right]^{\frac{1}{1+n}}. \tag{15}$$

By substituting (14) and (15) in (12) and (13) we obtain an ordinary differential equation

$$|F''|^{n-1}F''' + FF'' + \frac{n+1}{2n}(1 - F'^2) = 0 \tag{16}$$

and the following boundary conditions:

$$F(0) = A,\quad F'(0) = 0,\quad \lim_{\eta\to\infty} F' = 1. \tag{17}$$

The numerical solution of the systems (16) and (17) was carried out by the "adjustment" method on the "Minsk-2" electronic computer. The solutions obtained at present for $A = 0$ and $0.5 \leqslant n \leqslant 1$ are shown in Table 3.

Let us derive expressions for the friction stress on the surface τ_0 and the dimensionless local resistance coefficient c_f:

$$\tau_0 = k\left|\frac{\partial u}{\partial y}\right|^n_{y=0} = [F''(0)]^n \left(\frac{2\rho}{k(1+n)} c^{2-n}\right)^{\frac{n}{1+n}} k c^n x^{\frac{2n}{1+n}}, \tag{18}$$

$$c_f = \frac{\tau_0}{1/2\,\rho U^2} = 2\left(\frac{2}{1+n}\right)^{\frac{n}{1+n}} [F''(0)]^n R_x^{-\frac{1}{1+n}},$$

$$R_x = \rho \frac{U^{2-n}x^n}{k} = \rho \frac{c^{2-n}x^2}{k}. \tag{19}$$

Using (15), we write an expression for the boundary-layer thickness conditions

$$\delta \sim x^{\frac{n-1}{n+1}}\left[\frac{k}{2\rho}(1+n)c^{n-2}\right]^{\frac{1}{1+n}} = \left(\frac{n+1}{2}\right)^{\frac{1}{1+n}} x R_x^{-\frac{1}{1+n}}. \tag{20}$$

Equation (20) shows that the value $n = 1$ (Newtonian liquid) is the limiting condition between the boundary layer with a thickness increasing in the direction of flow (dilatant fluids $n > 1$) and the motion of a boundary layer with a thickness decreasing in the direction of flow (pseudoplastic fluids $n < 1$).

We shall prove that the dimensionless function of the current on the surface $F(0)$ serves as a natural parameter for the mass transfer:

$$F(0) = -\frac{v_0}{U} R_x^{\frac{1}{1+n}} n^{-\frac{2+n}{1+n}} \frac{1+n}{2}. \tag{21}$$

Bibliography

1. Wilkinson, W.L. Non-Newtonian Liquids. [Russian translation. 1964.]
2. Serrin, I. — J. Math. and Mech., Vol. 8, No. 4. 1959.
3. Metzner, A.B. Handbook of Fluid Dynamics. Flow of Non-Newtonian Fluids. — McGraw-Hill, New York. 1961.
4. Tomita, Y. — Bull. Japan Soc. Mech. Engrs., Vol. 4, p. 77. 1961.
5. Berkovskii, B.M. — DAN BSSR, No. 1. 1965.
6. Acrivos, A., M.J. Shah, and E.E. Petersen. — A. I. Ch. E. Journ., Vol. 6, p. 312. 1960.
7. Kapur, J.N. — Journ. Phys. Soc. Japan, Vol. 17: 1303. 1962; Vol. 18: 144, 578. 1963.
8. Shah, M.J., E.E. Petersen, and A. Acrivos. — A. I. Ch. E. Journ., Vol. 8: 542. 1962.